AD-A066 610 ROCKWELL INTERNATIONAL ANAHEIM CA AUTONETICS STRATEG--ETC F/G 17/7
RING LASER GYRO MIRROR SUBSTRATE INVESTIGATION.(U)
MAY 78 R D HENRY, D MEDELLIN, J H LIAW F33615-77-C-1091

UNCLASSIFIED C77-492/201 AFAL-TR-78-52 NL

1 OF
AD
A066610

END
DATE FILMED
5-79
DDC

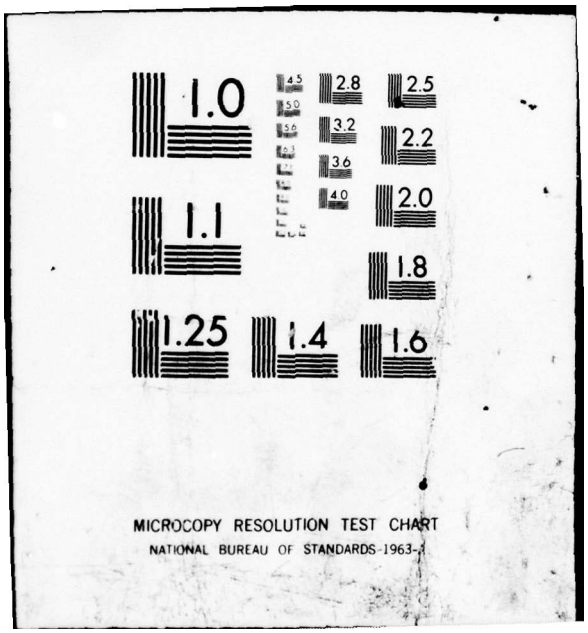
1.0
1.1
1.25
1.4
1.6
1.8
2.0
2.2
2.5
2.8
3.2
3.6
4.0
MICROCOPY RESOLUTION TEST CHART
NATIONAL BUREAU OF STANDARDS-1963-A

LEVEL II

AFAL-TR-78-52

RING LASER GYRO MIRROR SUBSTRATE INVESTIGATION

Autonetics Strategic Systems Division
Rockwell International
Anaheim, CA 92803

May 1978

Final Technical Report AFAL-TR-78-52
28 April 1977 to 28 January 1978

Approved for public release; distribution unlimited.

Prepared for

Air Force Avionics Laboratory
Air Force Wright Aeronautical Laboratories
Air Force Systems Command
Wright-Patterson, Air Force Base
Ohio 45433

NOTICE

When Government drawings, specifications, or other data are used for any purpose other than in connection with a definitely related Government procurement operation, the United States Government thereby incurs no responsibility nor any obligation whatsoever; and the fact that the government may have formulated, furnished, or in any way supplied the said drawings, specifications, or other data, is not to be regarded by implication or otherwise as in any manner licensing the holder or any other person or corporation, or conveying any rights or permission to manufacture, use, or sell any patented invention that may in any way be related thereto.

This report has been reviewed by the Information Office (OI) and is releasable to the National Technical Information Service (NTIS). At NTIS, it will be available to the general public, including foreign nations.

This technical report has been reviewed and is approved for publication.

David W. Pleva

DAVID W. PLEVA
Project Engineer

Robert E. Witters

ROBERT E. WITTERS
Acting Group Leader
Reference Systems Technology Group

FOR THE COMMANDER

George H Raroha

GEORGE H. RAROHA, Maj, USAF
Deputy Chief, Reference Systems Branch
Reconnaissance & Weapon Delivery Division

"If your address has changed, if you wish to be removed from our mailing list, or if the addressee is no longer employed by your organization please notify AFAL/TSR *,W-PAFB, OH 45433 to help us maintain a current mailing list".*

Copies of this report should not be returned unless return is required by security considerations, contractual obligations, or notice on a specific document.

AIR FORCE/56780/1 March 1979 — 65

UNCLASSIFIED

SECURITY CLASSIFICATION OF THIS PAGE (When Data Entered)

REPORT DOCUMENTATION PAGE	READ INSTRUCTIONS BEFORE COMPLETING FORM
1. REPORT NUMBER: AFAL-TR-78-52	2. GOVT ACCESSION NO. / 3. RECIPIENT'S CATALOG NUMBER
4. TITLE (and Subtitle): RING LASER GYRO MIRROR SUBSTRATE INVESTIGATION	5. TYPE OF REPORT & PERIOD COVERED: Final Report for 28 Apr 77 - 28 Jan 78
	6. PERFORMING ORG. REPORT NUMBER: C77-492/201
7. AUTHOR(s): R. D. Henry, D. Medellin and J. H. W. Liaw	8. CONTRACT OR GRANT NUMBER(s): F33615-77-C-1091
9. PERFORMING ORGANIZATION NAME AND ADDRESS: Rockwell International, Autonetics Strategic Systems Division, 3370 Miraloma Avenue, Anaheim, California 92803	10. PROGRAM ELEMENT, PROJECT, TASK AREA & WORK UNIT NUMBERS: 62204F, 6095-11-03
11. CONTROLLING OFFICE NAME AND ADDRESS: Air Force Avionics Laboratory, Air Force Wright Aeronautical Laboratories, AFSC, Wright-Patterson AFB, OH 45433	12. REPORT DATE: May 78 / 13. NUMBER OF PAGES: 95
14. MONITORING AGENCY NAME & ADDRESS (if different from Controlling Office)	15. SECURITY CLASS. (of this report): UNCLASSIFIED / 15a. DECLASSIFICATION/DOWNGRADING SCHEDULE

16. DISTRIBUTION STATEMENT (of this Report)

Approved for public release; distribution unlimited

17. DISTRIBUTION STATEMENT (of the abstract entered in Block 20, if different from Report)

18. SUPPLEMENTARY NOTES

19. KEY WORDS (Continue on reverse side if necessary and identify by block number)

Ring Laser Gyro, Mirrors, Substrates, Polishing

20. ABSTRACT (Continue on reverse side if necessary and identify by block number)

This report discusses methods used by Rockwell International for the fabrication and characterization of multilayer dielectric mirrors using single crystal garnet substrates. This work was performed under Contract No. F33615-77-C-1091. Polishing of garnet substrates to the required flatness for laser mirrors is described. The results of adhesion testing of SiO_2/TiO_2 multilayer dielectric high reflectance coatings on garnets are discussed. Lastly, the results of characterization of the mirrors by scattering measurements and lock-band measurements are described as well as correlation of these two evaluation tools with regard to prediction of mirror performance in a ring laser. Emphasis is on the experimental aspects of the work.

DD FORM 1 JAN 73 1473 EDITION OF 1 NOV 65 IS OBSOLETE

UNCLASSIFIED

SECURITY CLASSIFICATION OF THIS PAGE (When Data Entered)

391 827

JOB

FOREWORD

This report was prepared under Air Force Contract F33615-77-C-1091 sponsored by the Air Force Avionics Laboratory and covers work performed by the Electronics Research Center and the Strategic Systems Division of Rockwell International. The purpose of this contract was to conduct exploratory development into the use of Galolinium Gallium Garnet for ring laser gyro mirror substrates.

This program was conducted from April 1, 1977 through December 21, 1977. It was directed by H. J. Engebretson, Program Manager and M. J. Rupert Project Engineer of the Strategic Systems Division. Dr. R. D. Henry of the Electronics Research Center acted as principal investigator for this effort, providing the overall technical guidance for the program and for this report.

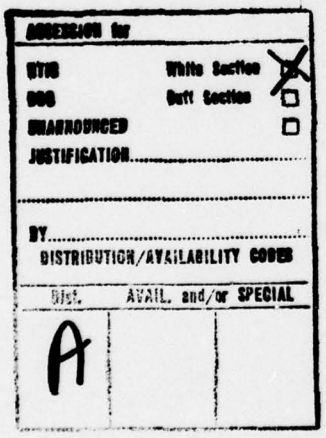

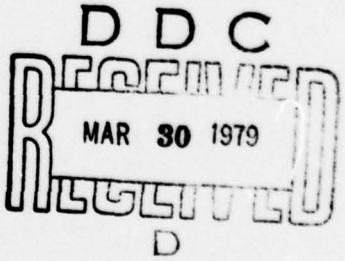

CONTENTS

ILLUSTRATIONS

TABLES

SECTION I

INTRODUCTION

1.1 BACKGROUND

The use of the ring laser as an inertial gyro is an idea that has been pursued for nearly 15 years by various laboratories (Ref 1). The basic idea is quite simple, which probably accounts for the persistence exhibited in pursuing the use of the ring laser gyro for such a long period. The simplest ideal ring laser contains a He/Ne plasma tube, three mirrors, and electronics for detection of the counter-rotating beams. The cavity path length difference (Δp) between the clockwise and counter-clockwise beams will vary as

$$\Delta p = \pm 2\Omega A/c \tag{1}$$

where A is the projected area of the optical ring orthogonal to the angular velocity vector (Ω) and c is the speed of light in vacuum. Since the fractional frequency shift ($\Delta\nu/\nu$) of the resonant modes of the laser equals the fractional path length change ($\Delta p/p$), the frequency difference of the counter-rotating beams is given by

$$\Delta\nu = \frac{4A}{L\lambda}\,\Omega \tag{2}$$

where L is the cavity length and λ the wavelength. Simply by measuring $\Delta\nu$, one obtains the angular velocity Ω.

The most serious problem encountered in attempting to use a ring laser as a gyrocompass is that for low rotation rates (or small mode splittings) the two counter-rotating beams have no frequency difference in a real ring laser. Back-scattered radiation causes these two oscillators to become synchronous and they are pulled to a common frequency of oscillation (Ref 2). This is not a surprising result and the effect will always be present since one cannot hope to completely remove scattering from a structure that confines the beams to some geometrical pattern. Unfortunately, in present state-of-the-art ring lasers, this phase-locking of the counter-rotating beams occurs for rotation rates below a few hundred deg/hr. This is approximately 5000 times too large to make the instrument useful as a gyrocompass and biasing techniques must be used to make the ring laser useful in measuring rotation rates. Several biasing techniques have been used such as the mechanical dither (Ref 3), Faraday cells (Ref 4, 5), the transverse Kerr effect (Ref 6) and the four beam

1. W. M. Macek and D. T. M. Davis Jr., Appl Phys Letter 2, 67 (1963).
2. Frederick Aronowitz, Laser Applications, Vol I, edited by Monte Ross, Pub Academic Press, NY (1971).
3. A. F. H. Thomson and P. G. R. King, Electron Lett 2, 382 (1966).
4. P. H. Lee and J. G. Atwood, IEEE J. Quantum Electronics 2, 235 (1966).
5. R. D. Henry et al, Electro Optics/Laser 77 Conference, Oct 1977, Anaheim, CA.
6. U. S. Patent No. 3,927,946, Dated December 23, 1975. Ring Laser Frequency Biasing Mechanism. Inventor: R. E. McClure, Sperry Rand Corp.

differential laser gyro (Ref 7). All of these deviations from the simple ideal ring exist to overcome the problems associated with the phase-locking. Recently, the rather extreme approach of using a passive cavity ring (Ref 8) has been demonstrated and the main object of this approach is to eliminate the phase-locking problem.

One would like to avoid the complication of biasing the ring laser, but this seems a rather remote possibility since the value of scattering loss needed would be in the parts per billion category for aircraft grade (0.01 deg/hr) instruments. But more importantly, even for biased ring lasers the error sources are related to the inherent unbiased value of the lock-band for modulated operation. The main reason for this is that if one alternates the bias from positive to negative one must pass through this locked region and this will introduce errors in one form or another, the form depending on how one chooses to traverse this region. So even for biased ring lasers, one would like to reduce the back-scattering and presumably the lock-band to as low a value as possible in order to decrease the error sources of the ring laser gyro.

The main source of scattering in a ring laser arises from the reflections at the path defining mirrors. This is where the largest refractive index differences occur and hence where the scattering can be largest. Indeed, if one views an operating ring laser, the scattering is quite apparent and the main sources are easily identified by the large bright red spots seen on the corner mirrors. For a "perfect" mirror, one would not be able to see these spots. The investigation of some of the sources of this scattered radiation is one of the main goals of this program with the unstated but obviously final goal being the reduction of the ring laser lock-band.

The investigation of all sources of scattering for mirrors is beyond the scope of this effort so that one specific source of scattering was investigated since it was believed to be the main source. In an in-house investigation prior to the start of this program, experiments were performed which indicated that mirror substrate preparation was probably the most important problem in ring laser mirror scattering. The net result of these experiments was that it appears that polishing techniques for fused silica substrates are inadequate. Surface strains left in the fused silica mirror substrates can cause both physical thickness and refractive index variations to occur in the subsequently deposited multilayer dielectric films and this will lead to scattering of the reflected beams. In addition to preparing and evaluating mirrors made with fused silica substrates, the same dielectric coatings were deposited onto polished single crystal wafers of Gadolinium Gallium Garnet (GGG). This is the material used as a substrate for the growth of bubble domain materials (Ref 9) and is known for its ability to retain large stresses without relief through dislocation formation in the single crystal form. Typical dislocation densities for present GGG are less than two per square centimeter with zero over large central areas of a boule being more the rule than the exception.

7. D. Grant et al, Proc. IEEE Natl Aerospace and Electronics Conf, 1028 (1977).
8. S. R. Balsamo and S. Ezekial, Proc. IEEE National Aerospace and Electronics Conference, 1062 (1977).
9. A. H. Bobeck and E. Della Torre, Selected Topics in Solid State Physics, Vol XIV, edited by E. P. Wohlfarth, North-Holland Publishing Co., Amsterdam, 1975.

The results of evaluation of the coatings on the GGG wafers looked very promising. Both the physical and optical inhomogneities of the deposited multilayer dielectric layers were dramatically decreased. For this reason, it was decided to investigate the use of gadolinium gallium garnet as a mirror substrate material for use in ring lasers in this program.

Since this is the first reported use of garnets in mirror substrates, there were several problems to be investigated and overcome before one could hope to use GGG as a mirror substrate. Firstly, the improved surface quality of GGG substrates over fused silica is believed to arise from the type of polishing used for the GGG. The GGG substrates initially investigated were commercially purchased and had received what is now a standard chemical-mechanical polish using a Syton (Ref 10) slurry. Since these initial wafers were intended for use as bubble domain substrates, the flatness was very poor and usually one finds that the surface is saddled rather than spherical with radii of curvature of less than 50 cm for wafers of GGG polished for bubble domain applications. Furthermore, the garnet substrates are typically prepared to be less than 0.4 mm in thickness. Thus, the first part of this program was to adapt the chemical-mechanical polishing technique to the preparation of flat and relatively thick mirror substrate configurations while retaining the strain-free final surface.

The second problem to be addressed was the coating adherence of standard SiO_2/TiO_2 multilayer dielectric films to the GGG substrate over temperature cycling from $-55^{o}C$ to $+71^{o}C$. Finally, the quality of the mirrors must be evaluated to decide if the use of garnet single crystal mirror substrates really help in reducing the lock-band. For this we chose to measure the majority of the mirrors by inserting each into an active ring laser and determining the lock-band of the instrument with the specific mirror as part of the resonant structure. This technique is not as easily accomplished as scatter evaluation, but since reduction of the lock-band is the real concern we decided to measure it as directly as possible rather than relying on a theoretical connection between scattering and lock-band. As will be seen in Para 6.2.3, this was a fortuitous choice since our data indicate that there does not appear to be any simple connection between lock-band and mirror scattering for scattering above 0.05 percent.

1.2 PROGRAM ORGANIZATION

This program is being carried out as a joint effort by the Electronics Research Center and the Autonetics Strategic Systems Division of Rockwell International. The Electronics Research Center is a part of the Electronic Devices Division and the Strategic Systems Division is a part of the Electronic Systems Group, all of which are a part of the Electronics Operations of Rockwell International. Since the program is a joint effort between two rather separated (organizationally but not spatially) groups, the functional organization responsible for this project is shown in Figure 1. The Autonetics Strategic Systems Division Ring Laser Gyro Group, under Mr. S. G. Shutt, has been involved with research and development of ring laser gyros since 1964. The Solid State Materials Research Branch of the Electronics Research Center,

10. HT30 Syton; a product of Monsanto Corp.

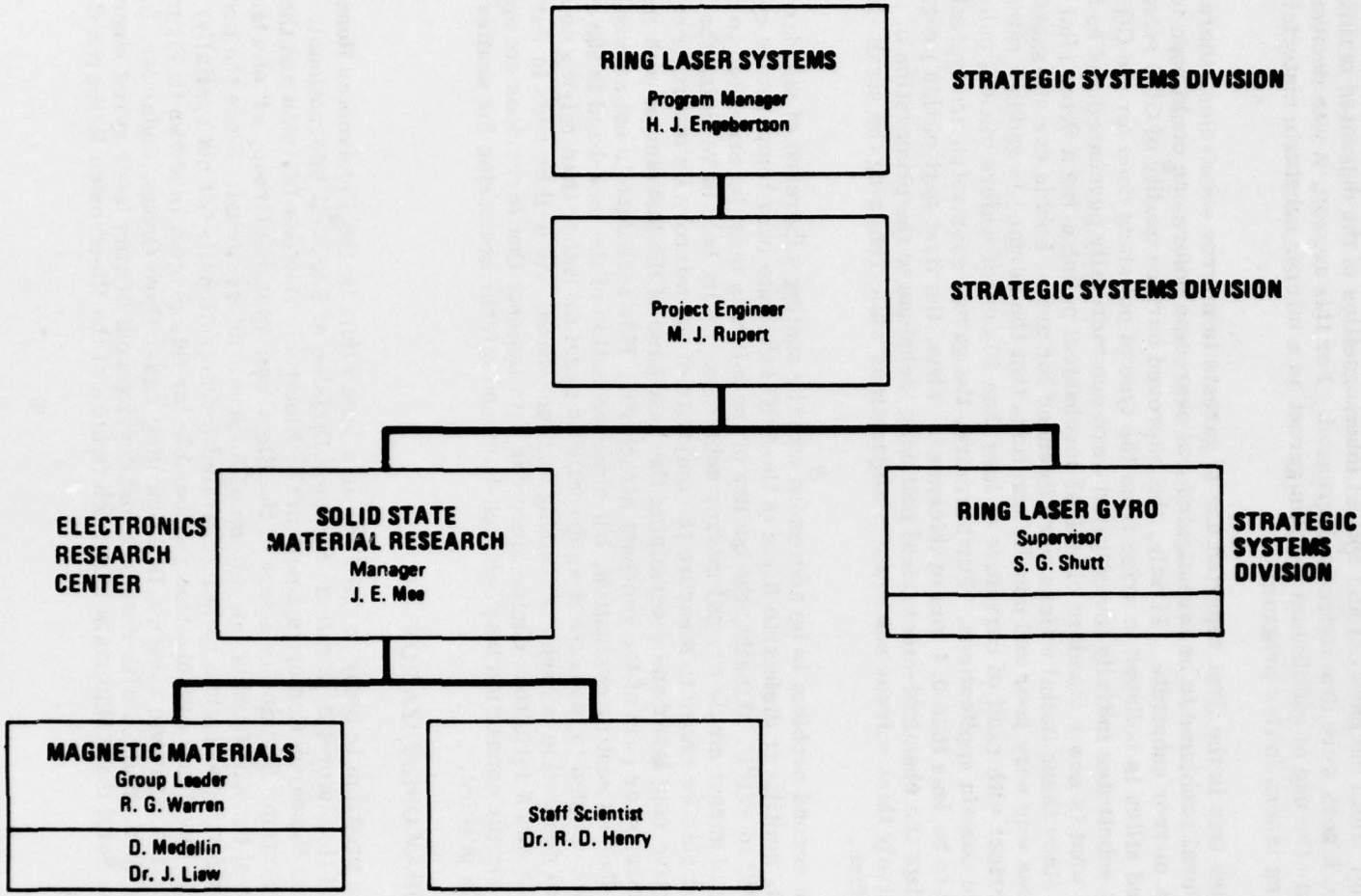

Figure 1. Functional Project Organization

under Dr. J. E. Mee, has an extensive background in processing gadolinium gallium garnet materials for bubble domain memory usage as well as in processing many materials for optical applications and has been actively co-operating with the Autonetics Strategic Systems Division in support of ring laser work for over two years.

The program management functions were handled by Strategic Systems Division and the technical direction by Electronics Research Center personnel. A general outline of the program is given below for orientation purposes in reading the remainder of this report.

1. Garnet polishing
2. MLD coating
3. Coating adherence testing
4. Mirror evaluation

Dr. R. D. Henry of the Electronics Research Center acted as principal investigator for this effort, providing the overall technical guidance for the program and for this report. The authors would also like to acknowledge valuable contributions by Dr. F. Vescial, Mr. S. G. Shutt and Mr. T. Otis of the Strategic Systems Division during the course of this work.

SECTION II

GARNET MIRROR SUBSTRATE PREPARATION

Sawn wafers of gadolinium gallium garnet for use in this effort were purchased from Union Carbide Corporation in 5.1 cm diameter form having nominal thicknesses of 2 mm and 8 mm for use in fabricating 7.75 mm and 11.9 mm diameter mirrors. The smaller diameter was chosen to conform structurally with one of the standard Spectra-Physics product lines and the larger diameter was chosen to conform with the structure used on one of the Rockwell ring laser gyros presently being fabricated (Table 1). In the case of the smaller mirror, one change was made in the nominal dimensions. The mirror thickness was decreased from the standard 4 mm to 2 mm in an effort to reduce the material costs. Since the Young's modulus of GGG is three times that of fused silica, this increase in aspect ratio of the substrate still yields a mirror with higher structural resistance to bending than that of the standard fused silica part.

Since the polishing of GGG is done on relatively soft surfaces, it was decided to first polish the 5.1 cm diameter wafers to obtain flatness and finally to core drill and edge these polished 5.1 cm wafers to obtain the required size mirror substrates for this program. Sizing first and polishing last might have presented some problems in obtaining mirrors with flatness better than 20 meters radius of curvature as required for this effort.

Gadolinium Gallium Garnet ($Gd_3Ga_5O_{12}$) known as GGG was the substrate material selected for this effort, for a number of reasons that will be pointed out later. GGG is a standard substrate material used for epitaxial growth of single crystal iron garnet films in the magnetic bubble domain technology in which Rockwell is heavily involved. This near-perfect material has a complex cubic garnet structure, with a melting point of 1720°C. Its chemical and mechanical stability is excellent, and it can be grown by the Czochralski growth method, the most widely used technique for the production of high quality oxide single crystals. Large diameter single crystals of sapphire, spinel, lithium niobate, silicon, etc, are typically grown using the Czochralski process.

The hardness of the <111> surfaces of GGG is 7.5 on the Moh scale and 1098 on the Knoop microhardness scale. Since this material is relatively low in hardness it is possible to use colloidal SiO_2 slurries to polish the surfaces directly from a fine ground finish without the need for intermediate polishing steps. The harder single crystal materials such as sapphire and spinel require that diamond be used for the slicing, grinding, and polishing steps. Comparison hardness values of various materials are given in Table 1.

To obtain flat and "damage-free" surfaces especially on thin crystals, the damage induced during the slicing process must be removed. We have found that by chemically etching the crystals we are able to prevent propagation of both thermal and mechanical induced damage. Chemical etching of such crystals will also prevent subsequent warping and/or bowing after the lapping and final polishing procedures.

Table 1. Comparison of Hardness Values of Various Materials of MOH and Knoop Scales

Substance	Formula	MOH Value	Knoop Value
Fluorite	CaF_2	4	163
Glass (soda lime)	--	--	530
Fused Silica	--	5.5-6	500
Quartz	SiO_2	7	820
Garnet	$Gd_3Ga_5O_{12}$	7.5	1098
Spinel	$MgO \cdot Al_2O_3$	8	1300
Alumina	Al_2O_3	9	1600-2200
Diamond	C	10	7000

Phosphoric acid, when used at 280°C is fairly rapid (12 μm/min) etchant and also produces a polished surface on as-sawn GGG wafers. Individual crystals were etched with the above solution using the beaker etching technique. Each crystal was first pre-heated for 20 min above the acid solution and under a watch glass to avoid thermal shocking. The crystal was immersed for a 2 minute etch-polish and post-heated for 4 minute above the acid solution.

The single-side lapping method was utilized during this investigation. The as-sawn or chemically polished wafers are wax mounted onto a flat plate and lapped with a 60.0 cm Lapmaster, as shown in Figure 2. This machine has the capability of providing lapped surfaces which are within 1 fringe of flatness over a 12 cm diameter for a properly conditioned lapping plate.

The purpose of lapping is to remove all surface damage incurred during sawing, size to desired thickness, and establish a flat surface prior to polishing. The lapping steps will vary depending upon the severity of saw damage and/or initial wedging of the wafers.

For the polishing, we used a standard Strasbaugh Model R6UR optical polisher. as shown in Figure 3. This machine has a variable rotation rate polishing table on which the polishing pad is attached. The polishing block rotates about a pivot point of an oscillating arm. The arm throw and oscillation frequency are also adjustable. Figure 4 shows a diagram of the machine polishing action.

A polishing plate which rotates about its center will not produce flatness of wafers distributed across its surface. Obviously the material toward the edges travels a greater distance across the polishing pad. Some correction for this condition can be accomplished by the random motion of the arm as shown in Figure 4. However, the greatest correction can be obtained by controlling the dwell time of the outer wafers on the polishing pad itself. Figure 5 is a diagram showing the configuration used for this work in which the arm motion controlling the position of the polishing

Figure 2. Twenty-four Inch Lapmaster

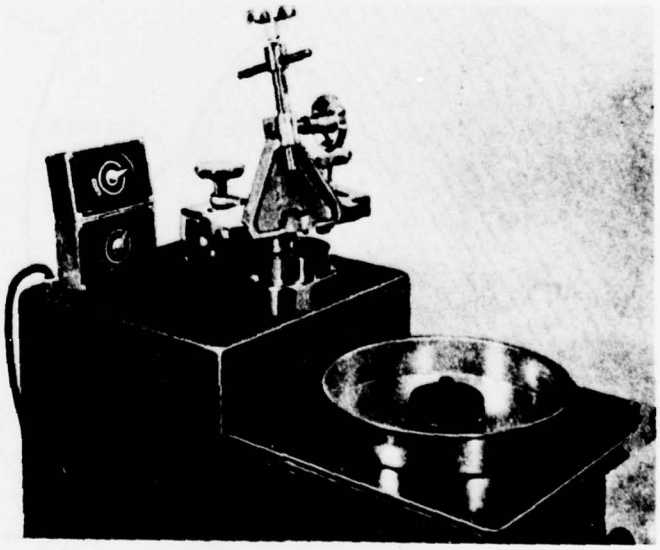

Figure 3. Strasbaugh Model R6UR Optical Polisher

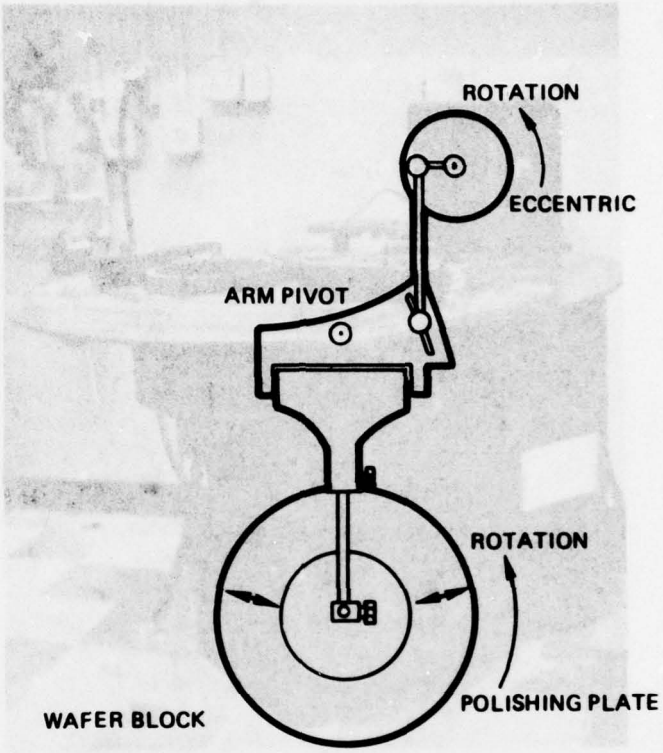

Figure 4. Strasbaugh Optical Polishing Machine Action

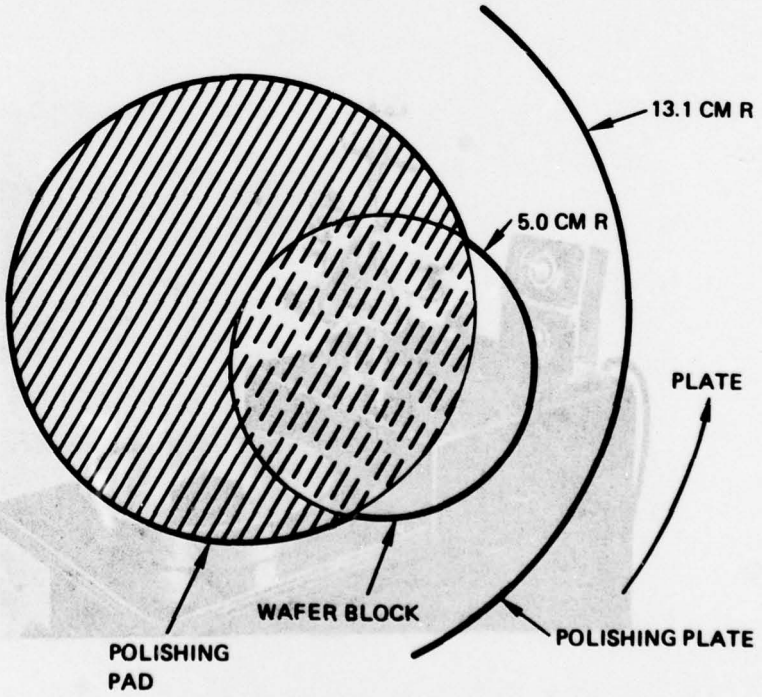

Figure 5. Polishing Plate - Pad - Block Configuration for Maximum Outward Swing of the Block

block is such that the outer wafers are off the edge of the pad for a portion of the rotation cycle. Therefore, for a specific wafer arrangement on the block, polishing pad diameter and machine throw arm adjustment, flatness of the wafers across the polishing block can be obtained.

Our laboratory has for years specialized in chemical-mechanical polishing techniques of single crystalline, polycrystalline, and amorphous materials for electronic and optical use. Although little has been published about the polishing mechanisms, we have found that the chemical-mechanical polishing media composition must have the proper ratio of mechanical to chemical material removal for flat smooth damage-free surfaces. This process when properly implemented has been found to produce damage-free surfaces. The mechanical polishing process always results in extensive surface damage that is made visible by etching the final surface.

Other polishing variables to be considered in order to produce flat damage-free surfaces are as follows:

1. The polishing pad for the machine must have sufficient "hardness" to minimize wafer edge rolloff and development of convex surfaces. The wear characteristics of the pad are also important so that the overall process is kept constant. We use Pellon Pan-W (Ref 11) pads for the processing of flat GGG wafers.

2. Wafer loading (i.e., grams/cm^2) must be such that the proper ratio of chemical to mechanical material removal is maintained.

The polishing fixture, as shown in Figure 6, used for this work has three adjustable feet with sapphire ($A\ell_2O_3$) pads which help maintain proper parallelism and flatness during the lapping and polishing process. The surface of the polishing fixture is flat and highly polished to afford a good reference surface for the mirrors and to minimize the quantity of low temperature wax required for mounting.

For this work the GGG wafers were wax mounted on the polishing fixture, and $A\ell_2O_3$ feet roughly adjusted to the same plane as the wafer using a Starrett height gauge. A tenth wave optical flat was then placed on top of the $A\ell_2O_3$ feet. Under a monochromatic light source the feet were readjusted until a symmetric fringe pattern was obtained. Before lapping the feet are lowered (below wafer surface) by .25 in. using a height gauge. The samples were then lapped on the first side to a 3 to 5 μm surface finish. A brief polish was then initiated on the wafer surfaces so that reflections can be observed using the monochromatic light source of the Model D305 Davidson non-contact interferometer. Both wafer flatness and reference to the polished plate can be observed by this method. After the planarity of this first side of the samples is established the wafers are turned over and the process repeated. During the lapping or polishing of this second side a change in the center of mass of the wafer holding fixture can be used to correct a non-parallel condition.

The first group of three 5.1 cm x 2 mm thick as-sawn GGG substrates were wax mounted equally-spaced around the periphery of a 13.4 cm stainless steel polishing fixture, as shown in Figure 7.

11. A product of Pellon Corp., Lowell, Mass.

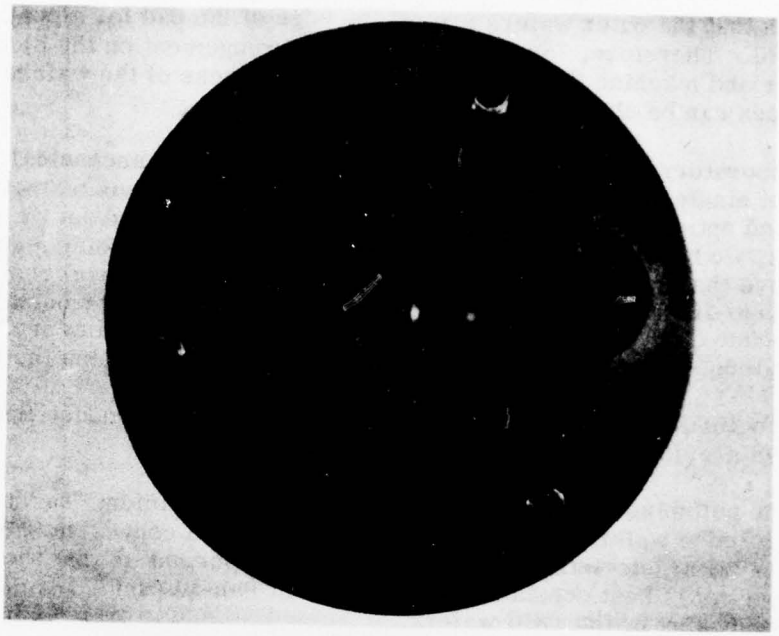

Figure 6. Polishing Fixture with Sapphire Pads

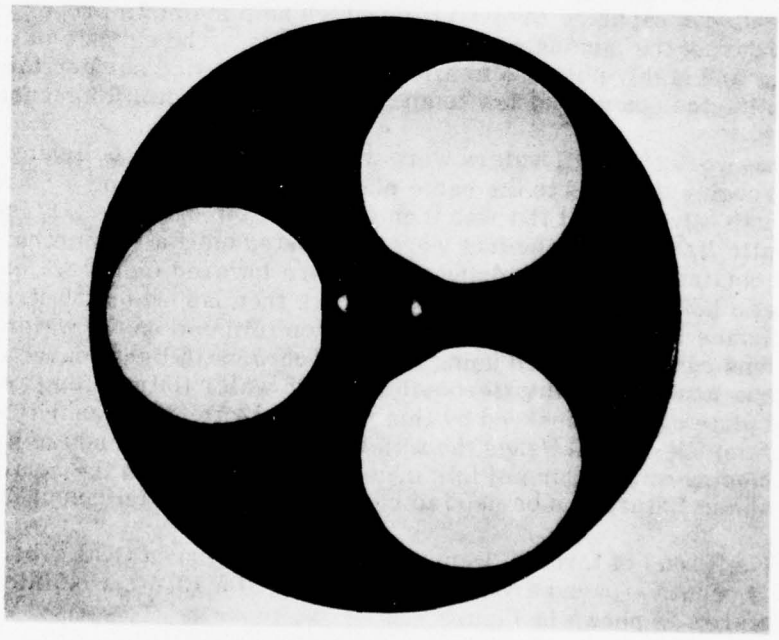

Figure 7. Polishing Fixture with Three GGG Substrates

The set was selected on the basis of having the deepest saw damage as well as the most wedging (51 μm) from side-to-side for our experiment. It became necessary to start the initial lapping with 20 μm $A\ell_2O_3$, progressing through 12 μm $A\ell_2O_3$, and finally to a 5 μm $A\ell_2O_3$ abrasive slurry.

A total of 102 μm of material was removed by the lapping process as can be seen in Table 2. Table 2 allows one to quickly see the different processing treatments given each group. For example, groups I and II were lapped from the as-cut condition, while groups III and IV were H_3PO_4 etched first and then lapped starting with 12 μm $A\ell_2O_3$.

For the polishing, a slurry of Nalco 1060 SiO_2 and 0.25 μm diamond was tried. After polishing for 12 hr, and intermittently replacing the pad, only 25 μm of material was removed. Faint shallow surface scratches were easily detected at 110X, using the Nomarski technique. A slurry of 1060 SiO_2 and H_2O was then tried for 15 hr and final polish with Syton SiO_2 and H_2O for another hour. The last 16 hr of polishing removed an additional 25 μm of material. Processing of the second side was done in the same manner as the first side. Final results achieved after processing both sides exceeded those required by the contract work statement. However, it is understandable that the time spent to produce these flat damage-free surfaces is too costly.

Group II was processed slightly different than the first group. The three GGG wafers used in this group were sliced better and did not exhibit any bowing or tapering. Initial lapping was done with 12 μm $A\ell_2O_3$ and then with the 5 μm $A\ell_2O_3$ to remove 75 μm of material. Polishing of the first side of this group was the same as Group I, with the exception of the final hour using Syton SiO_2. For the final hour, the Ph of the Syton slurry was dropped to 1. In processing the second side, as can be seen in Table 2, we did not use the 1060 SiO_2 and 0.25 μm diamond polishing mixture. We used 1060/H_2O, and dropped the pH to 1. Material removal rates turned out to be even greater than with the 1060/diamond mixture. Additionally, the surface finish is superior to the above mixture.

For group III, it was decided to H_3PO_4 acid etch-polish the GGG blanks before further processing. The crystals were etched for 2 minutes in phosphoric acid at 280°C removing 25 μm of material from each side. These crystals were etched because of some noticeable minor warpage and/or strain in the GGG material, even though these slices were thick. Etching of crystals will also prevent micro edge chipping during the lapping and polishing sequences.

On this group, we were able to lap with an even finer (3 μm $A\ell_2O_3$) abrasive than the previous groups, due to etching of the crystals. The total material removed in lapping was reduced to 50 μm versus 75 μm and 100 μm on the previous two groups. Besides etching of crystals and the 3 μm $A\ell_2O_3$ lapping steps, the rest of the process remained the same as Group II, side 2.

The fourth group consisted of 7.9 mm thick GGG crystals. This group was processed the same way as the previous one; however, a more detailed explanation will be given to best understand the so-far established procedure. Each crystal was H_3PO_4 etched for 2 min in the same manner as explained previously, removing 50 μm of material from each side. The etching produced a smooth surface finish even where the saw marks were evident from the slicing. The lapping was started

Table 2. Mirror Substrate Preparation

	H_3PO_4 Etch	(By Etching) Mat. Rem.	Lapping 20μm	12μm	5μm	3μm	(By Lapping) Total Mat. Rem.	1060/ 1/4μm	1060/ H_2O	1060/ H_2O/ H_3PO_4	Syton/ H_2O	Syton/ H_2O/ H_3PO_4	(By Polishing) Total Mat. Rem.
Group No. 1													
1st Side	–	–	X	X	X	–	100μm	X	X	–	X	–	100μm
2nd Side	–	–	X	X	X	–	100μm	X	X	–	X	–	100μm
Group No. 2													
1st Side	–	–	–	X	X	–	75μm	X	X	–	–	X	100μm
2nd Side	–	–	–	X	X	–	75μm	–	–	X	–	X	100μm
Group No. 3													
1st Side	X	25μm	–	X	X	X	50μm	–	–	X	–	X	100μm
2nd Side	X	25μm	–	X	X	X	50μm	–	–	X	–	X	100μm
Group No. 4													
1st Side	X	25μm	–	X	X	X	50μm	–	–	X	–	X	100μm
2nd Side	X	25μm	–	X	X	X	50μm	–	–	X	–	X	100μm

using 12 μm $A\ell_2O_3$, and progressing in steps to the 3 μm $A\ell_2O_3$ abrasive. A total of 50 μm of material was removed in lapping in ~6 hr being careful to have the proper height adjustment on the feet to maintain parallelism.

Adjustments on the optical polishing machine were kept constant throughout the processing of the four groups. A 26 cm diameter base plate to which the Pellon Pad was attached, was used. In order to maintain the bullseye (fringe pattern) in the center of each GGG blank, the pad diameter was either increased or decreased in size, periodically. Optical techniques generally call for machine adjustments to control the test (fringe) pattern on the part being polished. This method works well for optical parts since microscratches normally do not create any problems. In our work we find that we create a semi-scratchy surface when we make a major machine adjustment.

After the 5 cm wafers were polished using these techniques, the mirror substrate shapes were obtained by diamond core drilling and diamond edging to the required diameters. This procedure left the cylinder edges in a rough ground state and as will be seen later, this caused severe problems in obtaining good mirrors and for the most part, completely prevented obtaining good mirrors for the smaller diameter mirrors. As is usually the case where one is investigating a new area, this seemingly disastrous result was actually fortuitous since it provided mirrors with a wide range of scattering for comparison with lock-band measurements.

The description of the cleaning procedure will be delayed for now and will be covered in Section IV since each coating batch received different treatments.

SECTION III

MULTI-LAYER DIELECTRIC COATING DEPOSITION

A total of 74 mirror substrates received multi-layer dielectric coatings during the duration of this program, six of which were fused silica and the remainder being garnet mirror substrates which were prepared as previously described. Twenty-four large garnet mirrors were prepared and 50 small garnet mirrors were prepared. Now this is six more of the larger garnet mirror substrates than were actually prepared. In the case of the larger size, this was accomplished by repolishing the mirrors after they had been previously coated.

Four separate batches of mirror substrates were coated for this program by three different sources. The coatings were all made for p-polarized light and an angle of incidence of 30 deg. It was necessary to choose the p-wave rather than the s-wave because Brewster angle prisms were used instead of mirrors on two corners of the ring laser that was used for mirror lock-band evaluation. Typically, this means our measured lock-bands will be higher than would have been obtained if the s-wave had been chosen (Ref 12). But the convenience of having only one mirror in the ring was judged to out-weigh this inconvenience. The main thing one needs to keep in mind is that one must be careful in comparing our values to those obtained by other workers if the s-wave were used for the other measurements. For instance, a mirror which has a lock-band contribution of 100 deg/hr for the p-wave might only have a contribution of 30 deg/hr for the s-wave depending upon the source of the contribution.

The various coating batches are designated in Table 3 along with the pertinent information describing the coating parameters. The important thing to note for evaluation purposes is that only the mirrors provided by Optical Coating Laboratories, Inc. (OCLI) were evaluated using scatterometer techniques. These are batches III and IV. Batch II was the only group coated for 1.15 μm and none of these mirrors could be evaluated with the test-bed ring laser. For these mirrors, magnesium fluoride was used instead of silicon dioxide. Although several quarter-waves of MgF_2 can be safely deposited on garnet, it was found that more than four quarter-waves caused fracturing of the MLD coating. All 12 of the 1.15 μm mirrors exhibited severe fracturing and so only Batches I, III and IV were evaluated for this program. Most of the substrates from Batch II were repolished and used for obtaining large mirror substrates for Batch IV.

The cleaning procedure used for the substrates prior to MLD coatings for Batch I was simply a careful wiping of the surface with lens paper wetted with spectrophotometric grade acetone and a flushing of the surface with dry nitrogen just prior to loading into the vacuum chamber. The same procedure was used for Batch II.

The cleaning procedure used for Batch III is not known in detail since it involved some OCLI proprietary procedures. The garnet substrates were initially immersed in boiling acetic acid, then boiling 10 percent nitric acid, water rinsed and then cleaned in the normal OCLI procedure used for degreasing fused silica mirror substrates.

---

12. M. L. Scott and J. M. Elson, to be published.

Table 3. MLD Coatings Performed for This Program

Coating Batch	Vendor	Wavelength	Incidence Angle (deg)	Transmission (p-wave) (Percent)	Scatter Measurement	No. of Mirrors
I	Spectra Physics	633	30	0.2	No	18
II	Rockwell	1152	30	1.5	No	12
III	OCLI	633	30	0.2	Yes	22
IV	OCLI	633	30	0.2	Yes	22

The cleaning procedure for Batch IV is known in detail and it consisted of adapting our standard bubble domain materials cleaning procedures to the two different mirror substrate shapes. A standard photoresist spinner was changed to accommodate the mirror substrates by using a small O-ring to vacuum seal and mount the mirror substrates as shown in Figure 8. The spinner is operated at 2000 rpm while the top mirror substrate surface is physically scrubbed with polyurethane and various liquids. The order of the cleaning fluids used are trichloroethane, an alkanox-NaOH solution, deionized water and isoproyl alcohol. The times used were 30 sec, 30 sec, 60 sec and 30 sec respectively and it is important that the surface is not allowed to dry until the final isopropyl rinse. This procedure has consistently produced bubble memory devices with less than two defects per square centimeter and microscopic examination of mirror substrates cleaned in this fashion verified that very low particle densities were obtained for these substrates also.

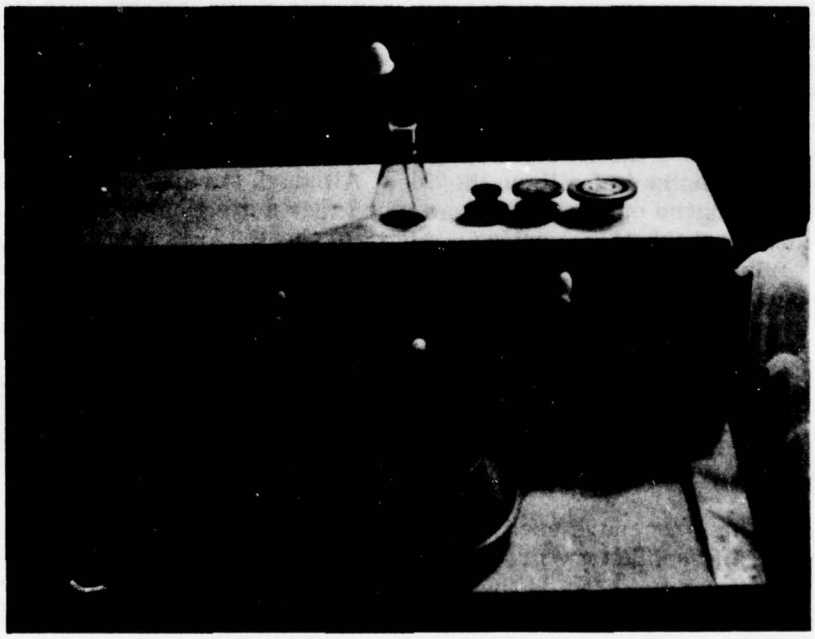

Figure 8. Photoresist Spinner Used for Cleaning Mirror Substrates

SECTION IV

MIRROR COATING ADHERENCE TESTING

The MLD coatings used in the preparation of the garnet substrate mirrors is the same as is used for coating fused silica substrates. The exact details of the structures are not known and presumably vary from one coating vendor to another, but in all cases the materials used were SiO_2 and TiO_2. The most important property of the MLD coatings is that they contain alternate quarterwave stacks of these materials, with a few layers presumably being nonquarterwave to suppress 3.39 μm lasing of the ring. The adherence of these MLD coatings have never been evaluated when deposited on garnet surfaces and so it was necessary to test the coating adherence in this program.

The test decided upon is in no way comprehensive and meets no military specification to the author's knowledge. Rather, it represents the minimum adherence requirement for a mirror coating for use in a ring laser gyro in the opinion of the program investigators. This minimum requirement is that no appreciable deformation of the coating occur after several temperature cycles over the range of -55°C to +75°C.

The first set of eighteen 7.75 x 2 mm mirror substrates were coated by Spectra-Physics. Nine of these coated mirrors underwent the coating adherence tests. The temperature cycling was provided by a Stratham temperature chamber in conjunction with a Stratham Rate Programmer PR-11. The test involved five temperature cycles of 25°C to -55°C to 65°C to 25°C at a rate of 5°C/min. The first two temperature cycles did not result in any observable changes in the mirror coatings, but after three cycles the coatings started to peel at the edges of the mirrors. The Nomarski photographs for samples 1, 2, 3, 8 through 13 are shown in Figures 9 through 17, respectively.

After five temperature cycles no further degradation was observed. These are shown in Figures 18 through 26. Figures 18 through 21 show the same areas as Figures 9 through 12, respectively. The general appearance of the edges of sample 9, 10, 11, 12 and 13 are more or less the same, therefore, Figures 22 through 26 are just the general appearance of the edges of these mirrors after five temperature cycles and are not necessarily the same spots as Figures 13 through 17, respectively.

The peeling of the coatings only occurred near the edges of the mirrors and did not propagate more than 100 μm from this edge. Therefore, we feel that the MLD coatings of SiO_2/TiO_2 on garnet substrates can be considered to have passed the minimum adhesion test requirements as set forth in this program.

Figure 9. Sample No. 1 - After 4 Cycles

Figure 10. Sample No. 2 - After 3 Cycles

Figure 11. Sample No. 3 - After 3 Cycles

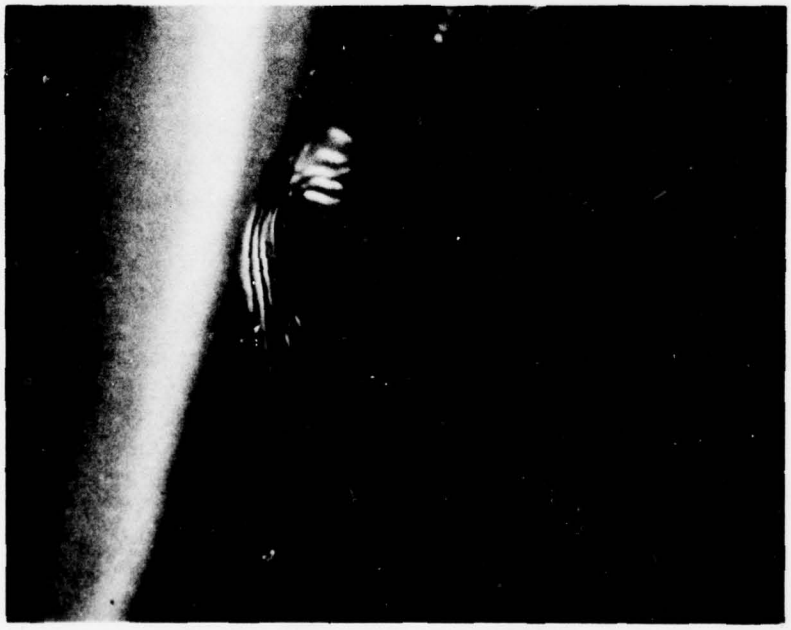

Figure 12. Sample No. 8 - After 3 Cycles

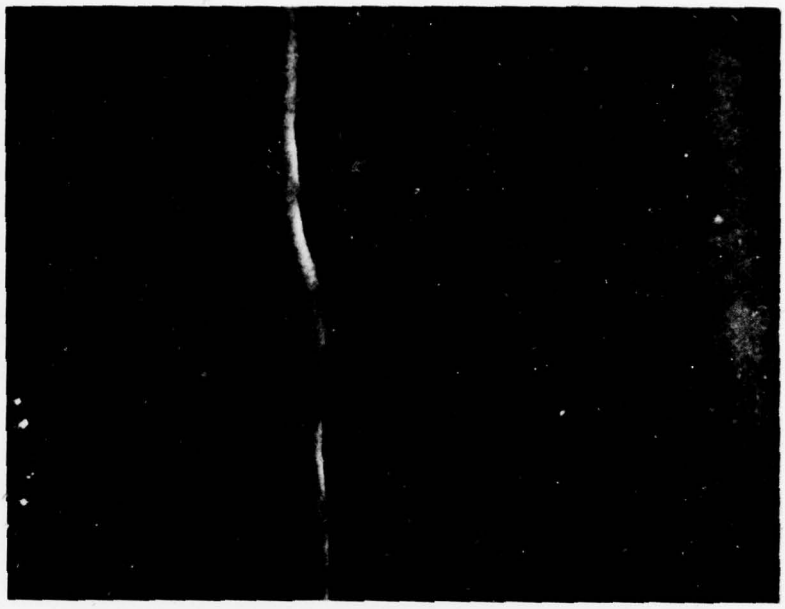

Figure 13. Sample No. 9 - After 3 Cycles

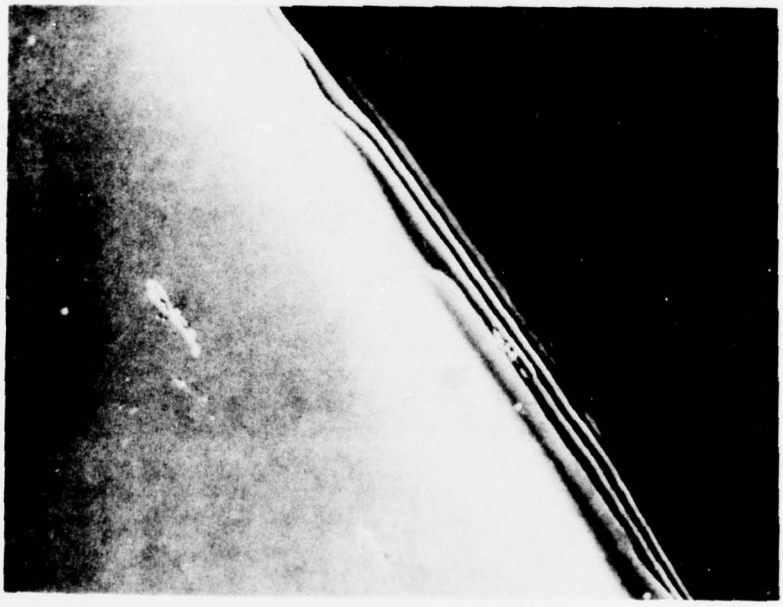

Figure 14. Sample No. 10 - After 3 Cycles

Figure 15. Sample No. 11 - After 3 Cycles

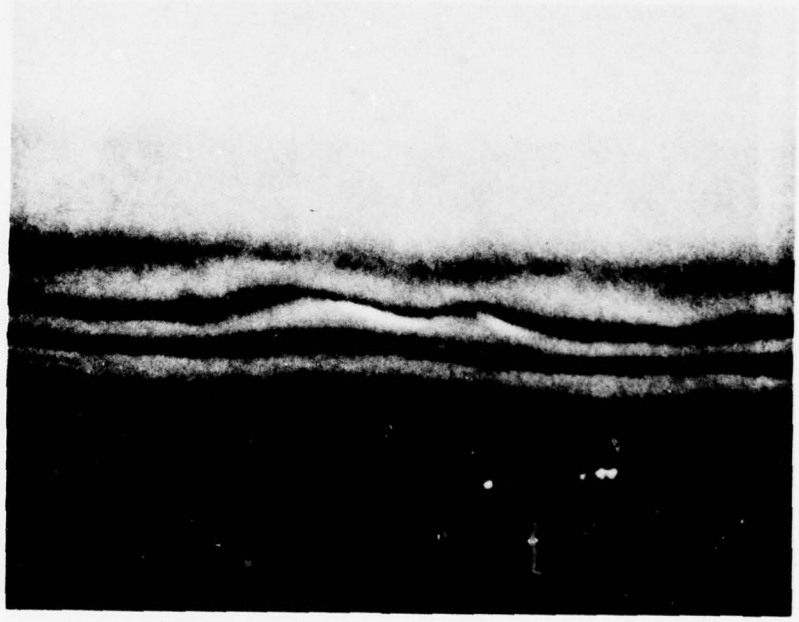

Figure 16. Sample No. 12 - After 3 Cycles

Figure 17. Sample No. 13 - After 3 Cycles

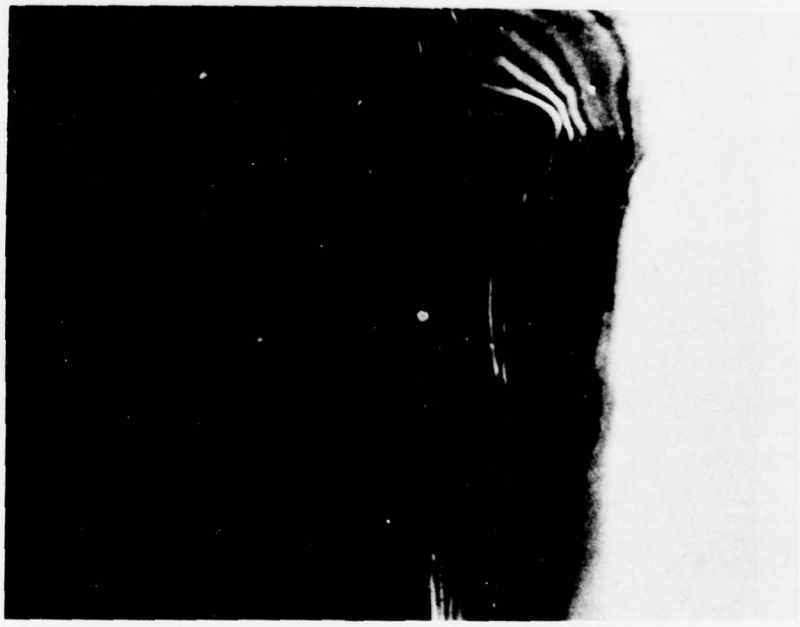

Figure 18. Sample No. 1 - After 6 Cycles

Figure 19. Sample No. 2 - After 5 Cycles

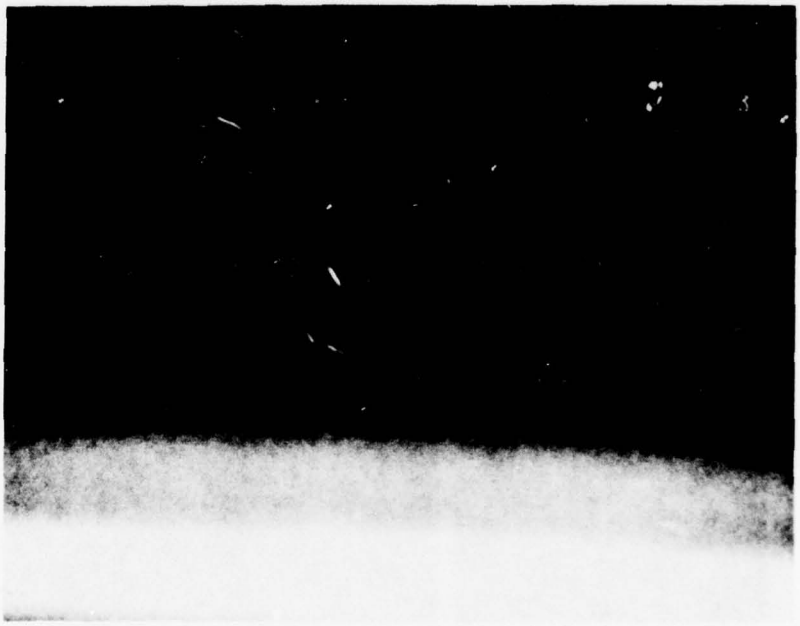

Figure 20. Sample No. 3 - After 5 Cycles

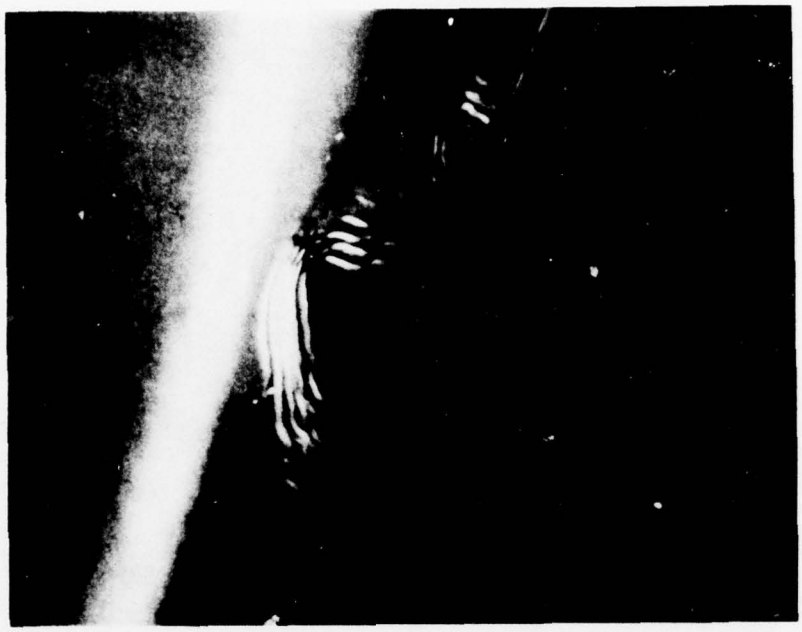

Figure 21. Sample No. 8 - After 5 Cycles

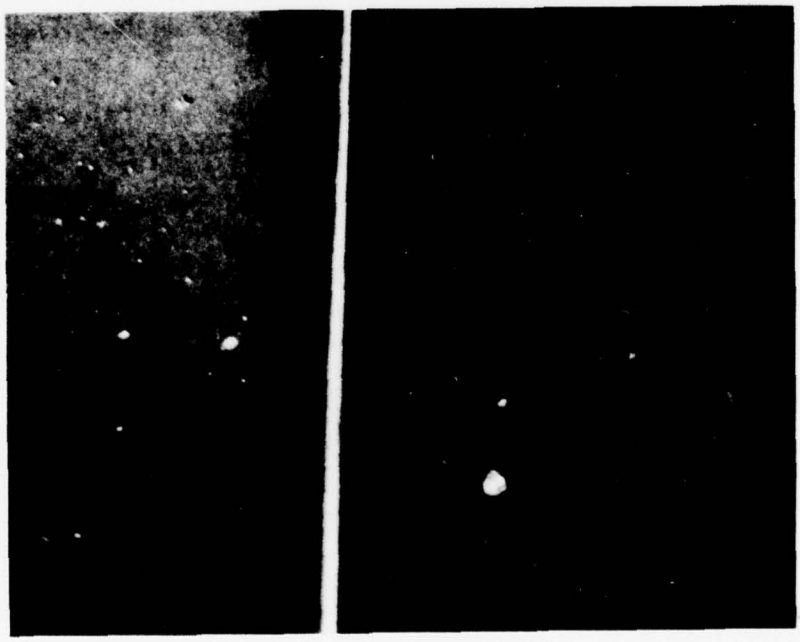

Figure 22. Sample No. 9 - After 5 Cycles

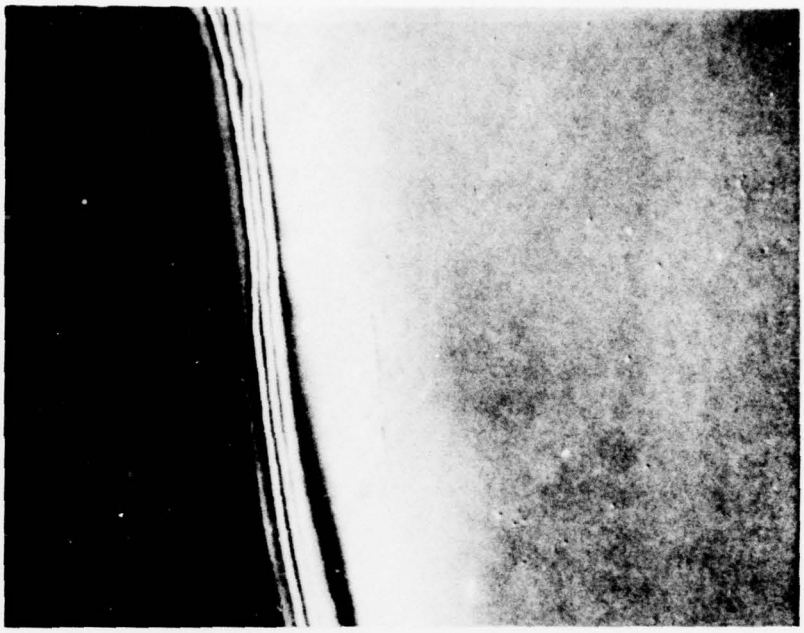

Figure 23. Sample No. 10 - After 5 Cycles

Figure 24. Sample No. 11 - After 5 Cycles

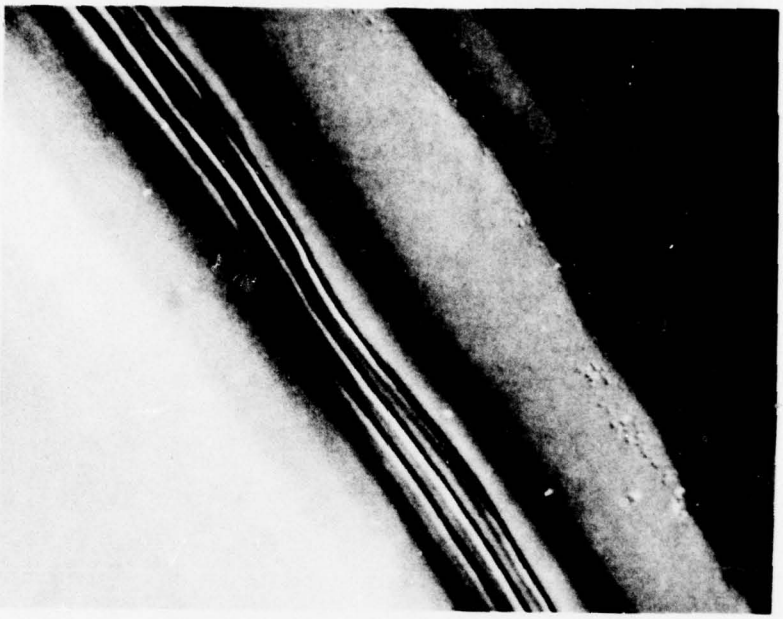

Figure 25. Sample No. 12 - After 5 Cycles

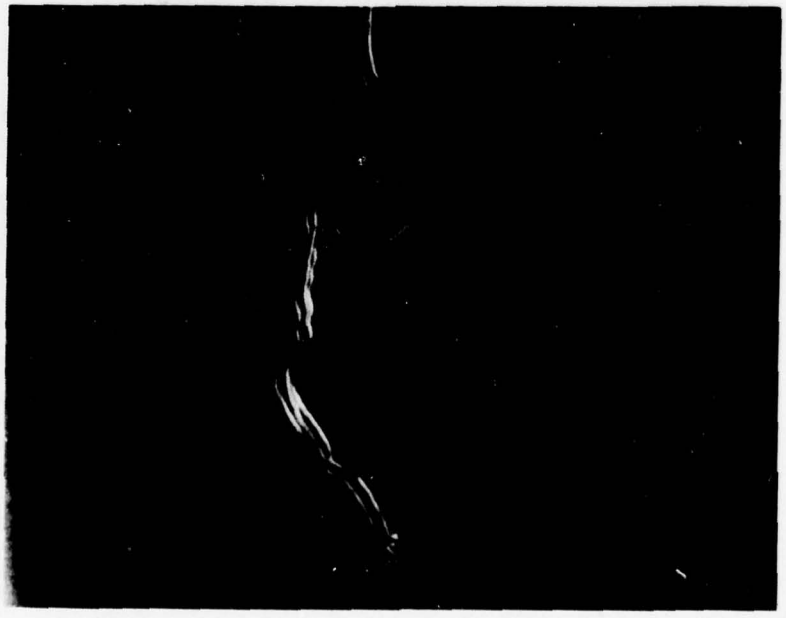

Figure 26. Sample No. 13 - After 5 Cycles

SECTION V

MIRROR EVALUATION

The evaluation of the mirror coatings on the fused silica and garnet substrates was performed using microscopy, scattering measurements and measurements of the lock-band of a test-bed ring laser containing the specific mirror. After a brief description of each technique, the results obtained on some of the mirrors are presented in the following sections of this report.

5.1 MICROSCOPY

The MLD coatings were evaluated using Nomarski interference microscopy and scanning electron microscopy (SEM). The latter is used to evaluate the general surface roughness, ignoring any obvious large particle contribution to the surface roughness. In a sense, it represents the type of surface that one could obtain if all the cleaning problems could be overcome. The Nomarski interference microscopy reveals the optical roughness while the SEM reveals physical roughness only.

The Nomarski technique is based upon reflecting light from the sample surface and mixing this light with that from the same source. Relative phase shifts are translated into intensity variations via the mixing and the image obtained has a three dimensional appearance with shading occurring as though one were viewing the object with side lighting. Either refractive index variations or physical thickness variations will appear as recessed or raised areas. It is an excellent and rapid non-destructive method for viewing optical roughness on the 1-30 μm scale.

The surfaces of two mirrors from Batch I are shown in Figure 27 and 28. These mirrors have, respectively, been fabricated using a garnet mirror substrate and a fused silica substrate. Note the improvement in the optical roughness that was obtained by using the garnet mirror substrate. Several of the garnet substrates were examined from all mirror coating batches and Figure 27 represents the typical result. Of the three fused silica substrates from Batch I, all showed the generally mottled surface as depicted in Figure 28. However, for the three fused silica substrates used in Batch III, none of these mirrors exhibited this mottled appearance. Presumably, this difference is from the difference in vendor coatings, since all six fused silica substrates were purchased from the same vendor at the same time.

Only two MLD coatings were investigated using SEM techniques. Since all the materials involved in the laser mirrors used for this program are dielectric insulators, it is necessary to evaporate approximately 200A of gold onto the surface being investigated. This can be considered a destructive test since it is never really clear that one can remove the gold without damaging the MLD coating. One fused silica and one garnet mirror from Batch I were evaluated using the SEM technique. The results of this limited study were in agreement with the more comprehensive study done prior to the start of this program. The general surface features of the fused silica and garnet mirror are shown in Figure 29 and 30 respectively. As before, a decrease in surface roughness is quite apparent for the garnet substrate.

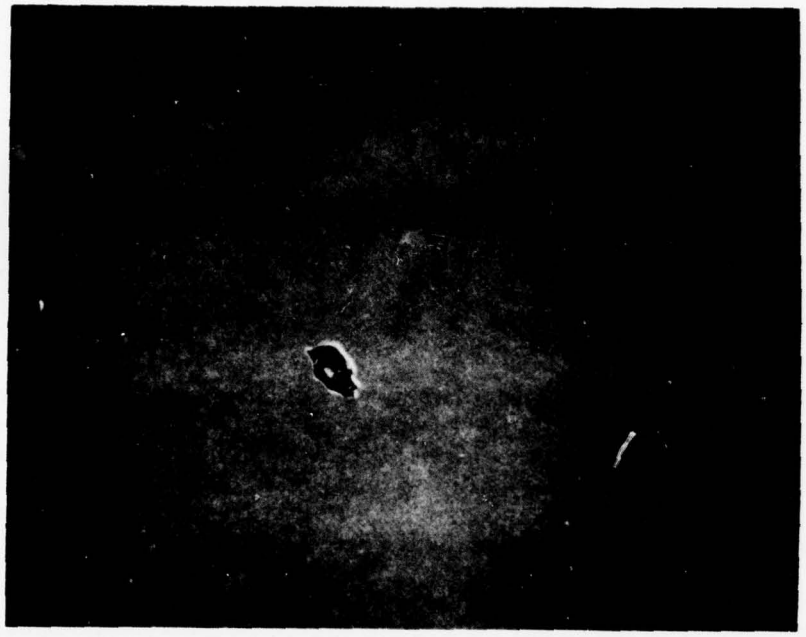

Figure 27. Nomarski Photograph of a Garnet Mirror

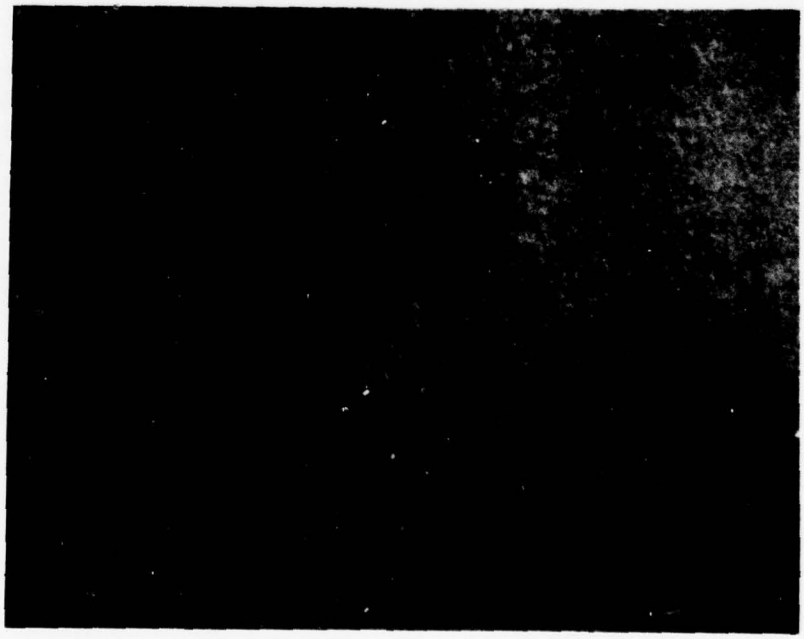

Figure 28. Nomarski Photograph of a Fused Silica Mirror

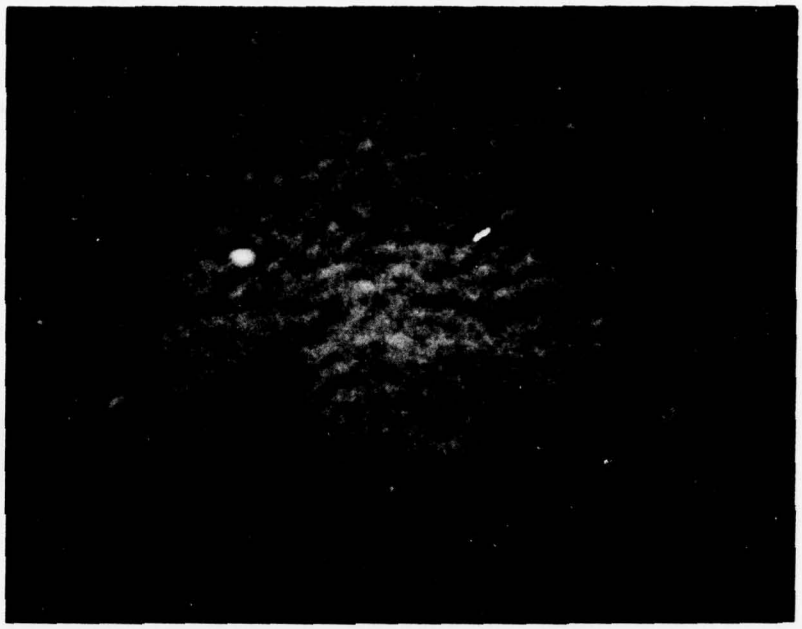

Figure 29. SEM Photograph at 25,000 X of a Fused Silica Mirror

Figure 30. SEM Photograph at 25,000 X of a Garnet Mirror

5.2 MIRROR SCATTERING MEASUREMENTS

The main source of scattering in a ring laser arises from the three or more path defining mirrors. The ideal mirror would have no scattering but this is not the case for present state of the art MLD laser mirrors. The scattering contribution is usually between 0.01-0.3 percent for .633 μm coatings and this phenomenon is believed responsible for the large phase-locking region observed in ring laser gyros. One can understand qualitatively how this phase locking is related to the amount of back-scattered radiation by considering the effect of injecting a small signal into the phase-locked loop of any oscillator. For a large enough injected signal, the oscillator will become synchronous with the injected signal. At what point this occurs depends on the amplitude of the injected signal and the gain of the oscillating loop. A somewhat more useful semi-quantitative picture of the relationship between back-scattered radiation and the phase locking that occurs in a ring laser can be seen by following the simple uncoupled approach of Aronowitz (Ref 2).

For no backscattering, the relationship between the instantaneous phase difference of the counter rotating beams and rotation rate is given by

$$\dot{\psi}_c = \frac{8\pi A\Omega}{\lambda L} \tag{3}$$

For the simple case of scattering of only one beam into the direction of the other, the phases of the counter rotating beams can be represented as depicted in Figure 31. The coordinate system rotates with the phase of the electric field E_1, E_1 and E_2 represent the amplitudes of the two beams. r_2E_2 represents the amplitude scattered

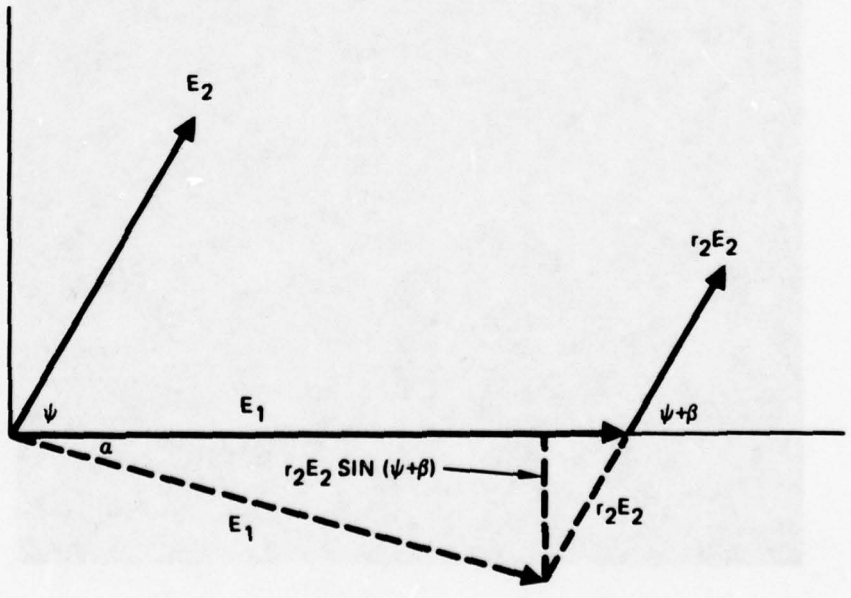

Figure 31. Phase Diagram for Frequency Pulling

along the direction E_1. ψ is the instantaneous phase difference and β is a phase shift arising from the scattering. The change in phase of E_1 per pass is just α and since the frequency must change to keep a resonant standing wave in the cavity this frequency shift is just

$$\Delta\varphi = -\alpha\ t_p = -\frac{r_2 E_2}{E_1} \sin(\psi + \beta)\ \frac{c}{L} \tag{4}$$

where t_p (= c/L) is the time per pass. Equation 3 must be changed then to

$$\psi = \frac{\ell \pi A}{\lambda L}\left[(\Omega - \Omega_L \sin(\psi + \beta)\right] \tag{5}$$

with $\Omega_L = \dfrac{r_2 E_2 c}{E_1 L}$.

The quantity Ω_L is what is referred to as the lock-band and as can be seen it depends very slowly on the value of the scattered intensity (r_2^2). For some representative values of beam diameter of 0.05 cm, path length of 60 cm, wavelength of 633 μm, total uniformly scattered intensity of 0.01 percent and assuming a diffraction limited solid angle as effective in beam coupling one obtains an estimate of Ω_L of 222 deg/hr. Since this is the right order of magnitude, it seems to justify the statement that lock band is caused by scattering. For later purposes, the only important point to note is that there should be a linear relationship between Ω_L and $\sqrt{r_s^2}$ where r_s^2 is the scattered intensity.

Measurement of this scattered intensity is obviously an important parameter to the final lock-band that a ring laser gyro will have and one of the vendors (OCLI) used for obtaining MLD coatings for this program routinely provides such measurements for mirror coatings fabricated for use in ring laser gyros. Since coating Batches III and IV were obtained from this vendor, scattering measurements are available for each mirror which can be used in conjunction with lock-band measurements to investigate the relation between r_s and Ω_L. Again, the exact details of the scattering measurements are considered proprietary by the vendor but a general description of the scattering measurements can be given.

For our mirrors, a p-polarized 633 nm He/Ne laser beam of diameter 0.1 cm is reflected from the surface of the mirror and scattered light is collected at an angle of 17 deg greater than the direct reflection. This intensity is then converted using a proprietary relation between this intensity and that of the total scattering. The validity of this procedure is unknown and the numbers provided were simply taken at face value. Nevertheless, it seems reasonable that the backscattered radiation will be somehow linearly connected to this quoted value and since we are only concerned with relative values of scattering, it is reasonable to use these measurements.

The scattered radiation is measured in the mirror center and in four positions which are located approximately 0.13 cm from the center and spaced by 90 deg rotation. For each spot, the mirror is rotated through 450 deg in the mirror plane. The scatterometer recordings for the mirrors of coating Batches III and IV are included in Appendices A and B respectively. An example of such a recording is given in Figure 32. The trace labeled (A) is for the center of the mirror and the recordings labeled (B), (C),

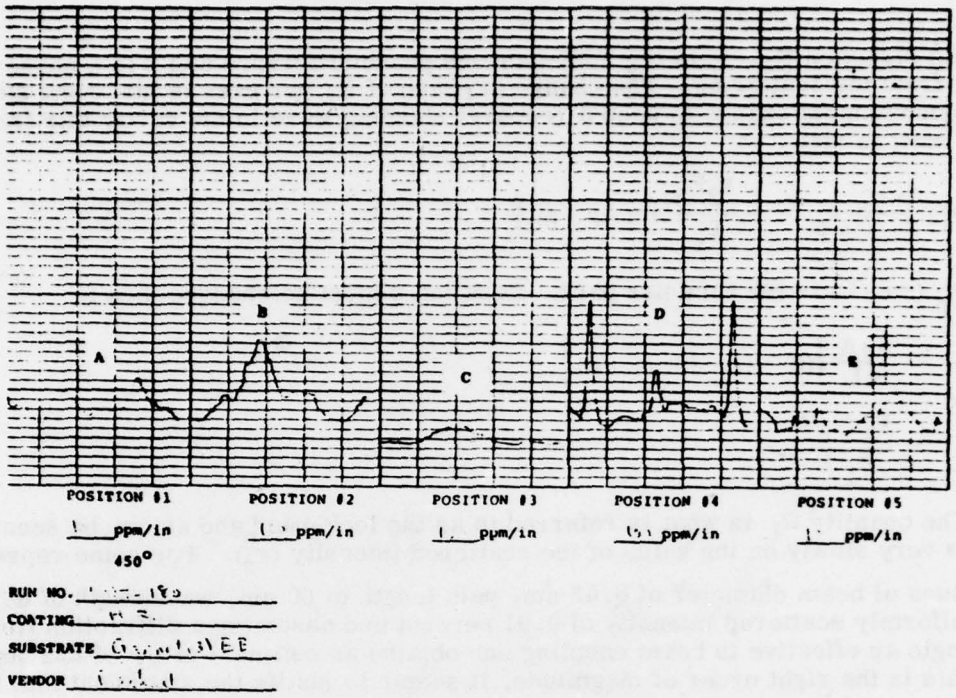

Figure 32. Scattering Traces for Mirror BB

(D) and (E) are for the other four positions. The vertical axis represents the scattered intensity and the horizontal axis represents incremental rotation in the mirror plane. All scattering measurements are made in this order so that the first trace always represents the mirror center.

5.3 TESTBED RING LASER

It was decided at the onset of this work that the only reliable test for judging that mirror improvement was being made was to measure the contribution of each mirror to the ring laser lock-band. The mirror of interest would be incorporated into an operating ring laser and the lock-band of the ring laser measured by some means. Originally, it was thought that the simplest solution would be to have a paramagnetic Faraday cell in the ring and modulate the bias to observe the residual biases and lock-band. However, later it was decided to use a mechanical dithering to extract the lock-band. The advantage of the mechanical dither over the Faraday cell is that one will always have a smaller total instrument lock-band for the mechanical dither since it is a clear aperture technique.

There are disadvantages to using a lock-band measurement to evaluate mirrors. The most important one is that the measurement gives no insight into why one mirror is better than another. Furthermore, it is not an easily implemented technique since it involves mounting the mirror, tuning the ring laser and attempting to make the measurements in as short a time as possible to reduce the effects of dirt accumulation after cleaning of the mirror. Nevertheless, it appears from the results of this investigation that the choice was a good one, mainly because these results seem to indicate that no present evaluation technique is clearly related to lock-band.

The ring laser used for these measurements is shown in Figure 33. The instrument was built by this laboratory for the testing of garnet Faraday cells and was easily adapted to handle this mirror evaluation. The instrument contains a plasma tube sealed by two Brewster angle prisms, one of which has a 200 cm radius of curvature surface. The bore size is 0.2 cm and the instrument lases at either 633 nm or 1152 nm. For this project, only 633 nm operation was used since the mirrors made for 1152 nm had fractured coatings. The plasma gain section is 15.24 cm in length, having a split cathode to reduce residual bias. For this work, the plasma current was nominally 3.5 mA. For the 633 nm line, the beam at the spherical surface is approximately circular with a diameter of 0.079 cm. The gain section was filled to 4 torr with a 13 to 1 He^3-Neon mixture with the Ne^{20} to Ne^{22} ratio being 52 to 48.

The third corner of this p-polarized ring laser is occupied by the mirror that is to be evaluated. The only path length control is located at this corner. Four controls are provided for moving the mirror - translation along the gain tube length, translation orthogonal to the gain tube length and the standard two mirror tilt directions. No vertical adjustment of the mirror was provided.

Mode control was provided for by inclusion of a variable aperture. In practice, this aperture was not used. It was found that one could select single mode operation through mirror movement and only with single mode operation could one observe the beats used to measure the lock-band. If one could make the measurement one was assured of single mode operation. Undoubtedly, the oversized bore was responsible for this mode selection ability of the instrument. Of course, it is not clear that it was the TEM_{00} that was excited but it really doesn't matter that much to this investigation which mode was being used. It is mainly a comparison test between mirrors that is of interest.

5.3.1 Dither Table

Two different techniques were used with the ring laser in attempting to extract the lock-band of the instrument with the various mirrors. One was the direct technique of mounting the ring laser on a rate table and measuring the rotation needed to unlock the ring. This is described in Para 5.3.2. The other technique to be described here was the application of a sinusoidal mechanical rotation via a piezoelectric driver flexure. The analysis of this type of data is not really straightforward even in the ideal case. The equation describing the phase difference of the two counter rotating beams is

$$\dot{\psi} = \frac{8\pi A}{\lambda L} \left[\Omega + \Omega_o \sin(2\pi ft) - \Omega_L \sin(\psi + \beta)\right] \qquad (6)$$

where Ω_o is the peak drive rotation, f is the frequency of oscillation and all other parameters are as previously defined. The ring will go in and out of lock in a very non-linear fashion depending on the value of both Ω_o and Ω_L and one must simultaneously extract both parameters from the time variation of ψ. This was attempted, but numerical solutions of Eq 6 indicated the logical situation as shown in Figure 34. One expects the waveform to invert on the negative half cycle but the actual variation of the beam intensity (of either beam) is shown in Figure 35. Although the waveforms of the two beams were inverted, the beams did not show waveform inversion on the negative half cycle and hence using these signals to obtain quantitative results is quite suspect.

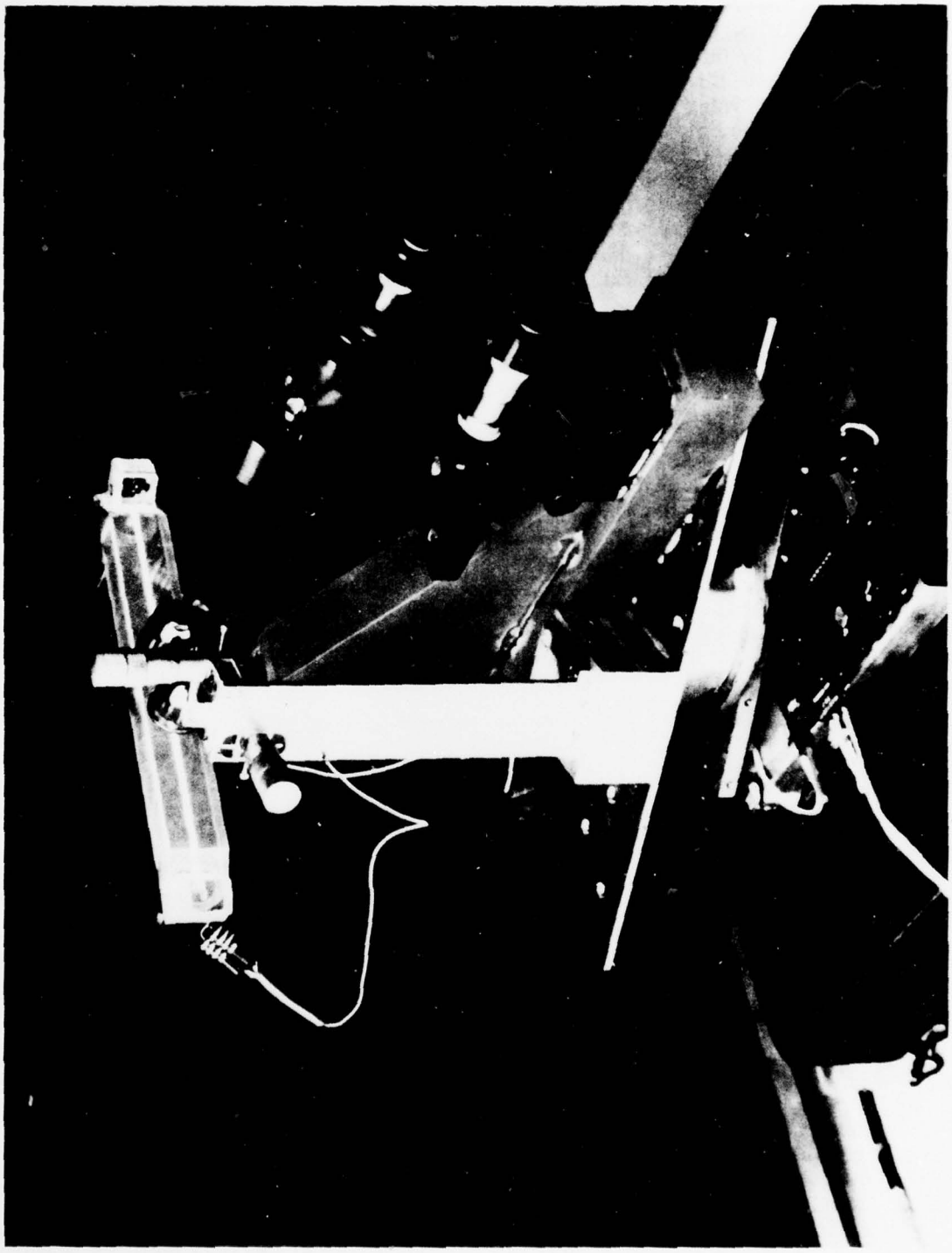

Figure 33. Ring Laser

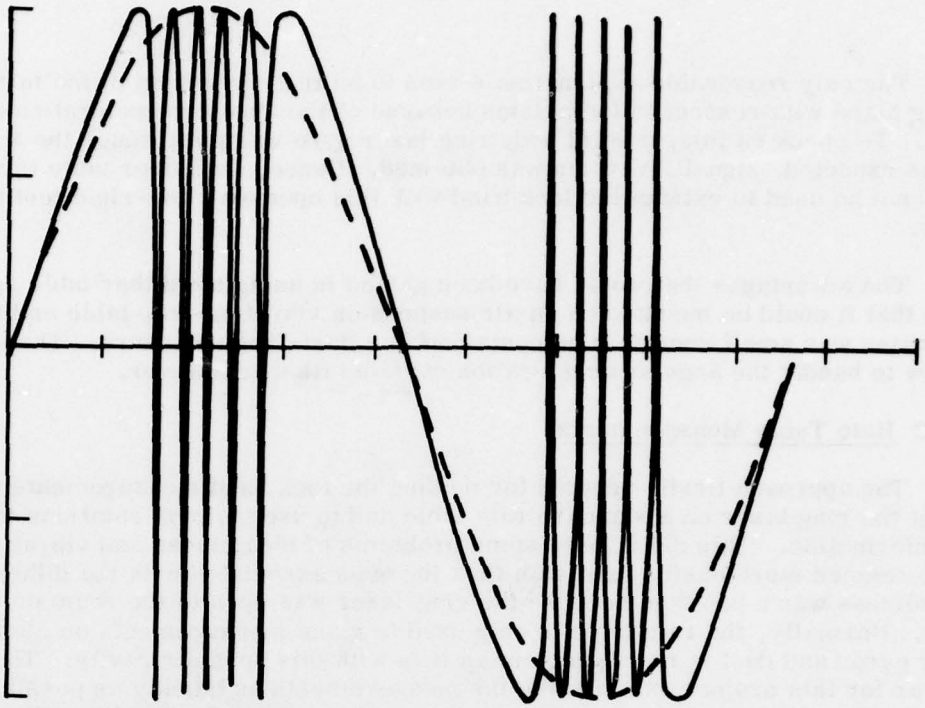

Figure 34. Calculated Intensity (Vertical Axis) vs Time (Horizontal Axis) Using Eq 6

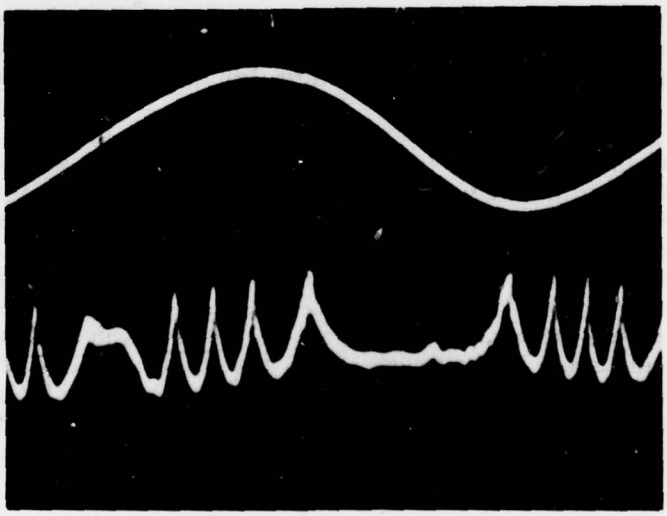

Figure 35. Upper Curve is Relative Rotation Angle vs Time and Lower Curve is Beam Intensity vs Time

The only reasonable explanation seems to be that movement of the mirror is taking place with respect to the prisms because of the angular accelerations of the table. To check on this, a solid body ring laser gyro was put through the same tests and as expected, signal inversion was obtained. Hence, the dither table technique could not be used to extract the lock band with this open air, non-rigid test bed ring laser.

The advantages that would have been gained in using the dither table approach were that it could be mounted on an air suspension vibration-free table and the entire apparatus was small enough to be contained in a dust-free enclosure. The question of how to handle the angular acceleration obviated its use however.

5.3.2 Rate Table Measurements

The approach finally adopted for making the lock band measurements was to mount the ring laser on a standard rate table and to use uniform rotations to extract the information. This did impose some problems of cleanliness and vibration, but these seemed more easily dealt with than the ones associated with the dither table. Cleanliness was a problem because the ring laser was open to the room on the rate table. Normally, the rate table is only used to make measurements on closed ring laser gyros and dust is not a problem as it is with this open air cavity. The only answer for this project was to make the measurements as quickly as possible after cleaning the mirror surfaces to prevent accumulation of dust. Additionally, the prism surfaces were cleaned after six mirror measurements. The time needed for making the measurement after cleaning the mirror was only about 10 min, with the majority of this being spent in mounting the mirror and aligning the laser.

The second problem encountered was that a high level of vibration exists on this rate table. It was high enough to unlock the ring laser if the ring laser was clamped to the table. To isolate the ring laser, approximated 0.5 cm of polyurethane foam rubber was used between the table and the ring laser. This reduced the vibration level by a factor of 20, but one still had to allow for the vibration in the measurements.

The measurement procedure adopted was to clean the mirror, mount it and align the laser with the table rotating to maximize the beats on the single beam intensity. Then the minimum rotation needed in both directions for unlocking the laser was measured. Additionally, the maximum rotation needed in both directions to keep the noise from locking the ring laser was measured. The difference between the minima and maxima is taken to be the rotational noise and the lock band is assumed to be located half way between these two values. This may be an overestimate of the lock-band, but again we stress that we are more interested in comparison values, rather than in quoting some best number. The results should at least allow comparison of mirrors although the value of the lock-band may be wrong by some multiplicative number. It should be noted that with the noise measured this multiplicative constant would only be 20-30 percent different from unity, so our values are not grossly in error.

5.3.3 Test Results

Mirrors from coating Batches I, III and IV were evaluated using the testbed ring laser in conjunction with the rate table measurement technique discussed in Para 5.3.2. For the mirrors from Batch I, no scattering measurements were provided by the

vendor so only the lock-band data are available. No comparison of mirror scatter with the measured lock-band is possible for these mirrors and so only the mirror designation and lock-band are listed in Table 4. The mirrors with a G or GS designation have a garnet substrate of dimensions 7.75 mm diameter by 2 mm thick and S-1 and SS-1 are fused silica substrates that were simultaneously coated. The dimensions of the fused silica substrates are 7.75 mm diameter by 4 mm thick.

The only utility of the data from coating Batch I is that it demonstrates that nothing was gained by using the garnet substrates. The average value of lock-band obtained for the fused silica mirrors is actually lower than the average for the garnet mirrors. But remember that for this first batch, we found with Nomarski microscopy and scanning electron microscopy that the overall surface texture was considerably better for the garnet mirrors (Para 5.1). What this means is that the scattering is from the particulate matter that was on the substrate prior to deposition of the MLD coating. It is the first indication that we have a cleaning problem in substrate preparation but as will be seen it is not, unfortunately, the last time we will see this.

Table 4. Batch I Mirrors

Mirror Designation	Total Lock-Band (deg/hr)
S-1	454
SS-1	652
GS-1	662
GS-7	580
G-1	587
G-6	464
G-8	587

For the mirrors from coating Batches III and IV scattering measurements were performed on most of the mirrors so that a comparison of the scattering values and lock-band measurements can be made. The substrate cleaning problems that occurred with the first coating batch continued and the net result is that only four mirrors of the smaller size had scattering values below 0.05 percent. For the larger mirrors, all except one had scattering less than 0.05 percent and the only exception was loaded with the wrong side toward the source. This seems to indicate that the cleaning problem arises from the close proximity of the edge of the mirror substrate. It now seems likely that it was the ground sides of the mirror that were responsible for the contamination of the substrate surface.

For this reason, we will discuss the results of the lock-band measurements according to the mirror size rather than just coating batch. As will be seen, this is roughly equivalent to dividing the mirrors according to scattering value, with the dividing value being 0.05 percent.

For the larger mirrors which were all on garnet substrates, the substrate dimensions were nominally 1.19 cm diameter by 0.79 cm thick. The results of the lock-band and scattering measurements are shown in Table 5. The scattering values in parts per million (ppm) are given for the averaged center trace and the plus and minus range values represent the possible extremes that could arise if one were

Table 5. Larger Garnet Mirrors Characterization Data

Mirror Designation	Lock-Band (deg/hr)	Scatter (r_s^2) (ppm)
1L	576	320^{-250}_{+0}
1L	540	120^{-60}_{+30}
3L	504	200^{-120}_{+0}
4L	504	1500^{-300}_{+500}
5L	684	250^{-0}_{+500}
6L	576	500^{-150}_{+300}
AA	540	300^{-130}_{+0}
BB	576	90^{-40}_{+10}
CC	576	300^{-70}_{+50}
DD	504	130^{-30}_{+40}
EE	540	150^{-40}_{+0}
FF	504	150^{-50}_{+20}
Three Prisms	612	–

using other than the center of the mirror for the lock-band measurement. These values of the extremes are arrived at by averaging the rotational values at the other positions. We have taken an average value of the scatter at each position because no indexing is provided for correlation of angle between the mirror and the scattering trace.

The value of lock-band for the ring laser obtained with three prisms (no mirror) is shown to be 612 deg/hr. This is a rather high value for a 60 cm ring laser and is believed to arise from the poor quality of the fused silica used in making the prisms. One can actually observe scattering of the beam throughout the prism volume, indicating a large index inhomogeniety. It was hoped that the scattering from these prisms would be much less than that of the test mirrors, but instead it seems to be comparable.

In Figure 36, the lock-band is plotted aginst the value of scattering. The dark circle represents the lock-band and average mirror center scattering and the various shapes represent the possible deviation from these values for that mirror. Except for the mirror with large scattering, the data indicate nearly a linear relationship between scattering (r_s^2) and lock-band. But recall that from Para 5.2 one expects instead for Ω_L to depend upon r_s^2 as

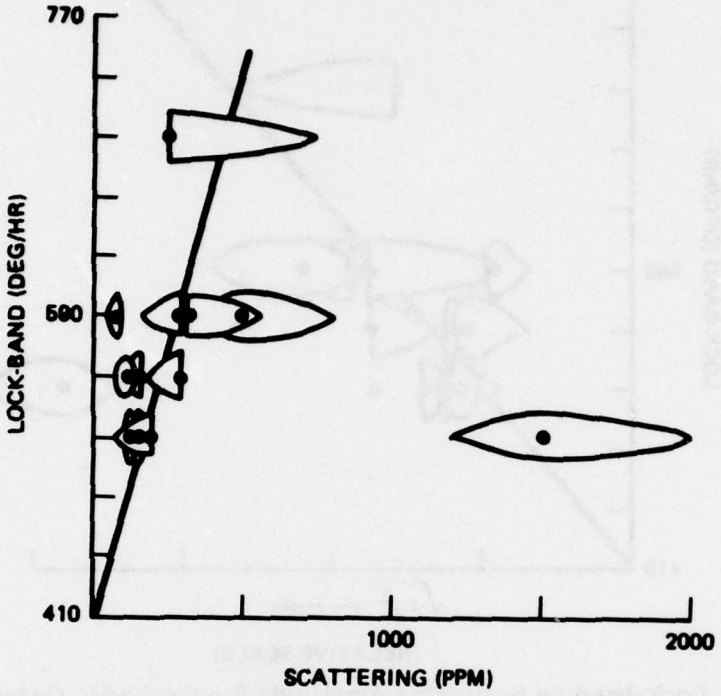

Figure 36. Lock-band Scattering Intensity for the Larger Garnet Mirror

$$\Omega_L \propto \sqrt{f_s^2}. \tag{7}$$

In Figure 37, the same data is plotted assuming Eq 7 above and as can be seen, the errors are sufficiently great that one cannot really say that the fit is any better. Really, about all that can be said is that the data indicate an increasing lock-band for increasing scatter, with perhaps a linear or square root dependence upon scattered intensity. This might seem like a rather weak statement, but as will be seen from the data on all mirrors, this is a relatively strong statement to make. Not even a weak correlation is observed for mirrors with scattering greater than 0.05 percent.

For the small mirrors, the scattering values were, generally greater than 0.05 percent and as will be seen, no correlation between measured lock-band and scattered intensity was found. The values of total lock-band and scattered intensity for the center of each mirror are given in Tables 6 and 7 for the small mirrors of Batches III and IV respectively. For Batch III (Table 7) the mirrors designated FS1 and FS2 are fused silicon substrates and as can be seen, the values of scattered intensity and lock-band are lower than for the average garnet substrate. This probably occurred because these two mirrors did not have ground sides and so were cleaner than the average garnet substrate prior to deposition of the MLD coating.

The important result is shown in Figure 38 in which total lock-band is plotted versus scattered intensity. The triangles represent the largest mirrors (AA, BB, CC, DD, EE and FF), the squares the fused silica mirrors and the circles the small garnet mirrors. It seems quite apparent from Figure 38 that no correlation exists between the measured lock-band and the value of measured scatter for the mirror.

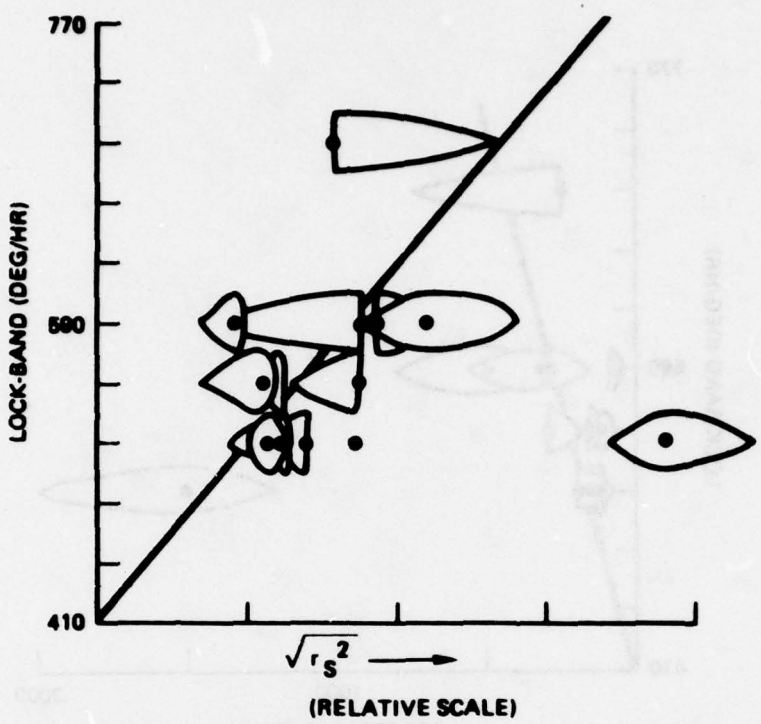

Figure 37. Lock-band vs Scattering Amplitude for the Large Garnet Mirrors

The line used in Figure 36 for the large mirrors is included in Figure 38 for comparison purposes. Rather the data seems completely random, with some of the mirrors with the highest values of scatter having the smallest lock-band. However, it is important to note that the repeatability of the measurement for the mirrors is much better than one needs to describe this random pattern of data. Measurement of 10 mirrors a second time yielded values of lock-band within ±60 deg/hr of the previously obtained values. One needs errors in repeatability of four times this to account for this problem.

The results of the lock-band and scatter measurements for the small garnet mirrors of coating Batch IV are shown in Table 6. No fused silica substrates were coated for Batch IV. This data is plotted in Figure 39. This data is a little more suggestive than that for Batch III. From Figure 39 one sees that for scatter less than 0.05 percent, there appears to be correlation between scattered intensity and lock-band and that for values of scattered intensity above 0.10 percent this correlation breaks down completely.

From this discussion, one might conclude that it must be the scattering measurement that is in error. But four mirrors were returned to the vendor out of coating Batch IV and the scattering measurements repeated. While the traces did not appear identical, the average features were the same as those of the previously run traces, so that the scattering measurement at least does not have repeatability errors. And, of course, scale factor errors in scattering are not really of interest here. Thus it would appear that neither measurement has errors large enough to account for the behavior seen in this program.

Table 6. Lock-Band and Scattering for Small Mirrors from Coating Batch III

Mirror Designation	Lock-Band (deg/hr)	Scatter (r_s^2) (ppm)
A	540	400^{-0}_{+250}
C	504	1100^{-600}_{+2900}
E	526	1000^{-300}_{+1000}
F	551	650^{-150}_{+50}
G	432	700^{-300}_{+0}
H	443	450^{-0}_{+250}
J	479	1400^{-200}_{+400}
L	479	600^{-50}_{+200}
M	515	500^{-100}_{+300}
O	526	1200^{-550}_{+1800}
P	490	900^{-250}_{+300}
FS1	453	200^{-0}_{+50}
FS2	490	250^{-50}_{+0}

Table 7. Lock-Band and Scattering for Small Mirrors from Coating Batch IV

Mirror Designation	Lock-Band (deg/hr)	Scatter (r_s^2) (ppm)
25	497	1700^{-0}_{+500}
35	620	600^{-300}_{+0}
45	418	2500^{-1500}_{+500}
55	536	3000^{-1000}_{+2000}
65	796	450^{-50}_{+150}
85	500	$330^{-70}_{+2\cdot}$
95	472	$2000^{-?}_{+?}$
105	634	3000^{-1800}_{+500}
125	921	3000^{-1200}_{+0}
145	598	1100^{-100}_{+900}
155	569	1800^{-0}_{+700}

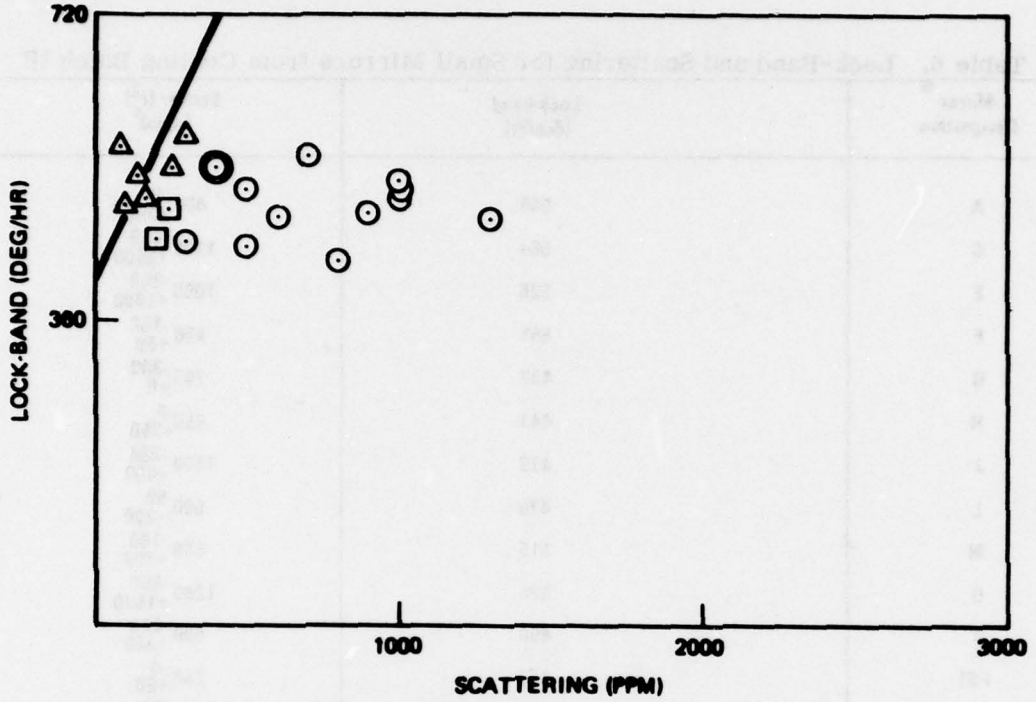

Figure 38. Lock-Band vs Scattering Intensity for Mirrors of Batch III
(△-large garnet; ⊙ -small garnet; ⊡ -fused silica)

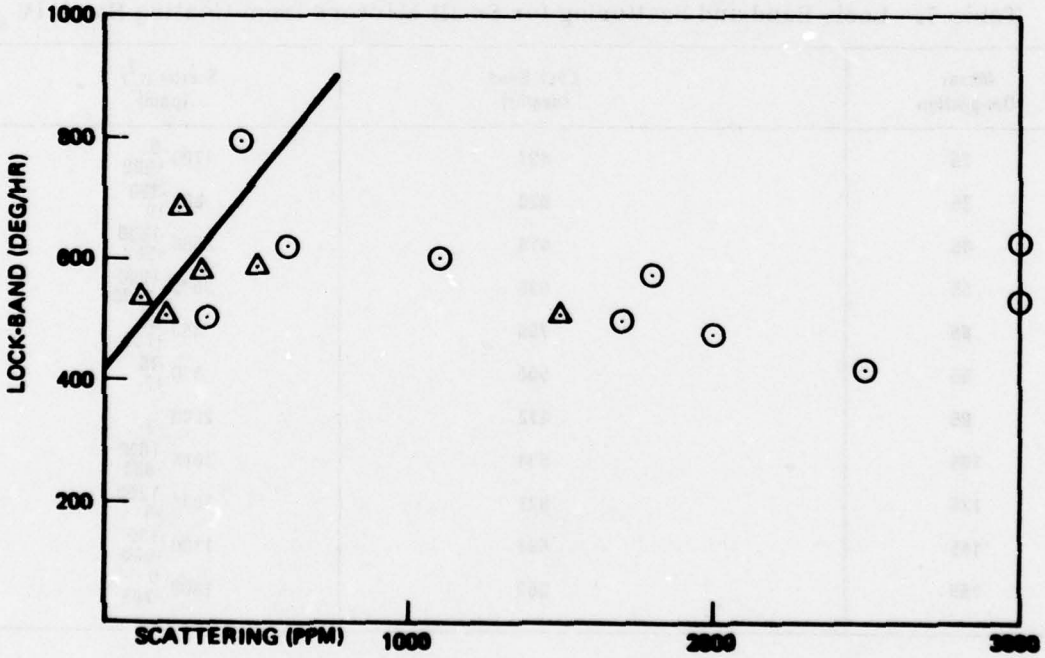

Figure 39. Lock-Band vs Scattering Intensity for Mirrors of Batch IV
(△-large garnet; ⊙ -small garnet)

SECTION VI

CONCLUSIONS

With the work performed on this program, it has been possible to convincingly answer some of the original questions regarding the use of garnet mirror substrates. Firstly, it has been demonstrated that one can adapt the chemical-mechanical polishing of garnets to obtain optically flat surfaces. Secondly, it has been shown that the same SiO_2/TiO_2 MLD coatings will adhere to the garnet substrates over several temperature cycles from -55°C to 75°C.

Whether or not garnet substrates will improve mirrors for ring laser gyros has only been partially answered. Certainly, if one takes the criteria of a good mirror as being one that has scatter less than 0.05 percent, then the larger mirrors indicate that a 100 percent yield can be obtained with garnets. The real question of whether the strain-free surface of the garnet will ultimately produce a better mirror was never really addressed properly. The contamination problems, which were probably caused by the ground surfaces on the mirror sides, overshadowed this effect and prevented its investigation. The scanning electron microscope results indicate that smaller scattering will be obtained with garnets if one overcomes the contamination problems. However, no dramatic reduction in scattering or lock-band was found with the garnet mirror substrates.

The results of trying to correlate the measured lock-band with the scattering measurements actually raise more questions than they answer. From the 37 mirrors tested, it appears that for less than 0.05 percent scattering there is a monotonic relation between lock-band and scattered intensity. But for values much above this, the correlation seems to completely disappear. A mirror with 0.2 percent scattering exhibited the smallest lock-band measured in this program. The data seem to indicate that scattering is related more to the possible variation of the measured lock-band than to its value. This is obviously an area that should be more thoroughly investigated.

REFERENCES

1. W. M. Macek and D. T. M. Davis, Jr., Appl. Phys. Letter 2, 67 (1963).

2. Frederick Aronowitz, Laser Applications, Vol. I, edited by Monte Ross, Pub. Academic Press, NY (1971).

3. A. F. H. Thomson and R. G. R. King, Electron Letter 2, 382 (1966).

4. P. H. Lee and J. G. Atwood, IEEE J. Quantum Electronics 2, 235 (1966).

5. R. D. Henry et al, Electro-Optics/Laser 77 Conference, Oct 1977, Anaheim, CA.

6. U.S. Patent #3,927,946, Dated December 23, 1975. Ring Laser Frequency Biasing Mechanism. Inventor: R. E. McClure, Sperry Rand Corp.

7. D. Grant et al, Proc. IEEE Nat'l Aerospace and Electronics Conf, 1028 (1977).

8. S. R. Balsamo and S. E. Ezekial, Proc. IEEE Nat'l Aerospace and Electronics Conf., 1062 (1977).

9. A. H. Bobeck and E. Della Torre, Selected Topics in Solid State Physics, Vol. XIV, edited by E. P. Wohlfarth, North-Holland Publishing Co., Amsterdam, 1975.

10. HT30 Syton; a product of Monsanto Corp.

11. A product of Pellon Corp., Lowell, Mass.

12. M. L. Scott and J. M. Elson, to be published.

APPENDIX A. MIRROR SCATTERING TRACES, BATCH III

These scattering traces for the mirrors of Batch III are included in this report for completeness. The traces were provided by Optical Coating Laboratories, Inc., using standard scattering measurement techniques developed by that laboratory for assessment of ring laser gyro mirror quality.

Of particular interest in this group of traces is the one for the larger garnet mirror BB. Not only is the value of scattering very low but more importantly the variations with rotation of the substrate are very low. This is to be contrasted with those for FS1, FS2 and FS3 (fused silica mirrors) of this batch. Although the average values of scattering are nearly as low for these three mirrors, there are very rapid variations in scattering as the mirror is rotated.

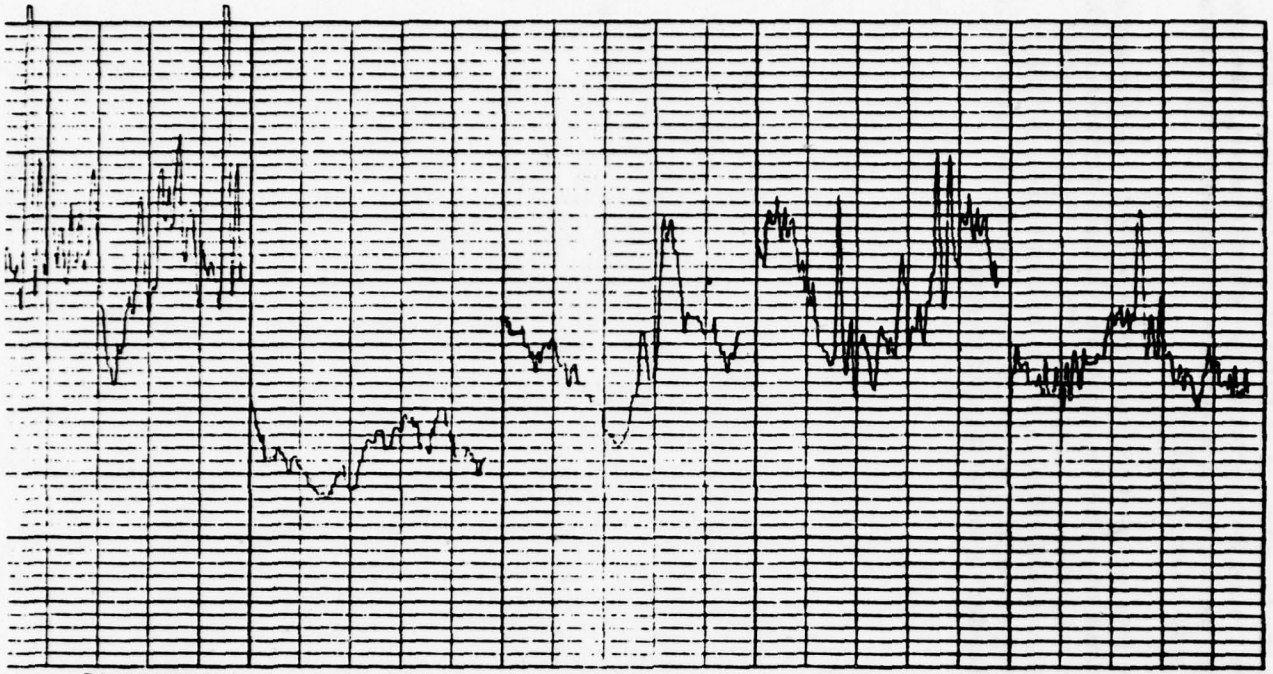

POSITION #1	POSITION #2	POSITION #3	POSITION #4	POSITION #5
(10) ppm/in	(5) ppm/in	( ) ppm/in	(5) ppm/in	(5) ppm/in

450°

RUN NO. 10.7-12

COATING H K

SUBSTRATE Garrett (1) Al

VENDOR Rockwell

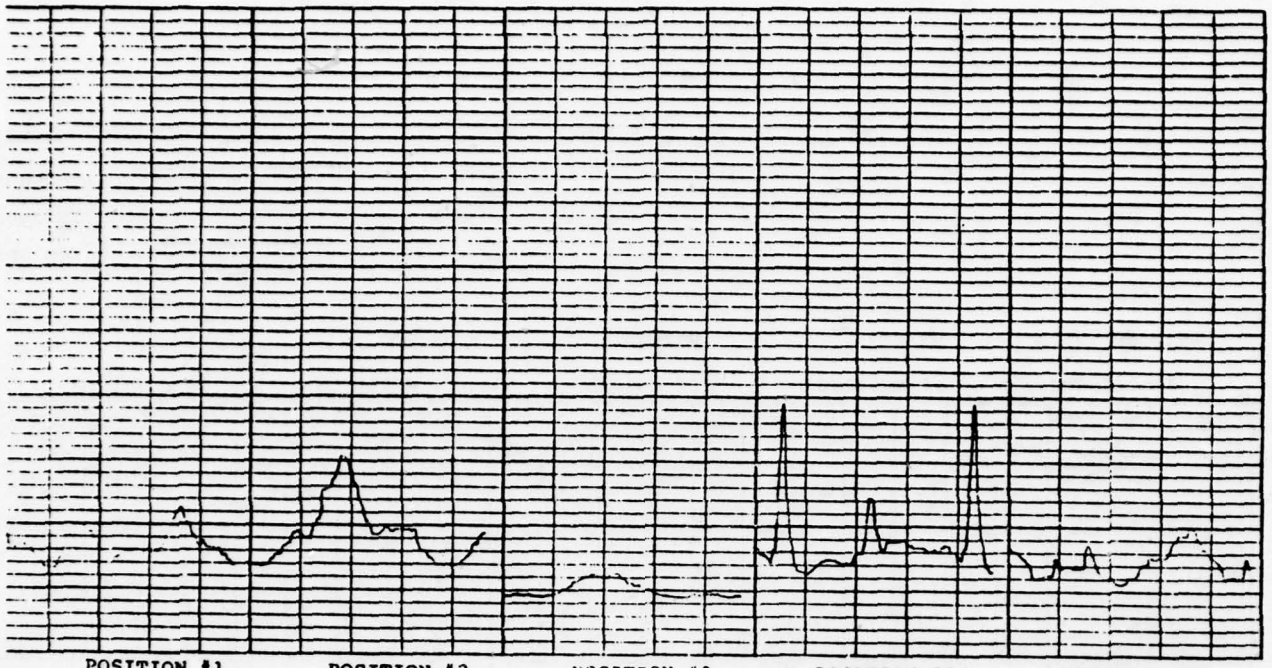

POSITION #1	POSITION #2	POSITION #3	POSITION #4	POSITION #5
1 ppm/in	10 ppm/in	1 ppm/in	10 ppm/in	1 ppm/in

450°

RUN NO. 157-180

COATING M S.

SUBSTRATE Grade (3) EE

VENDOR Poco

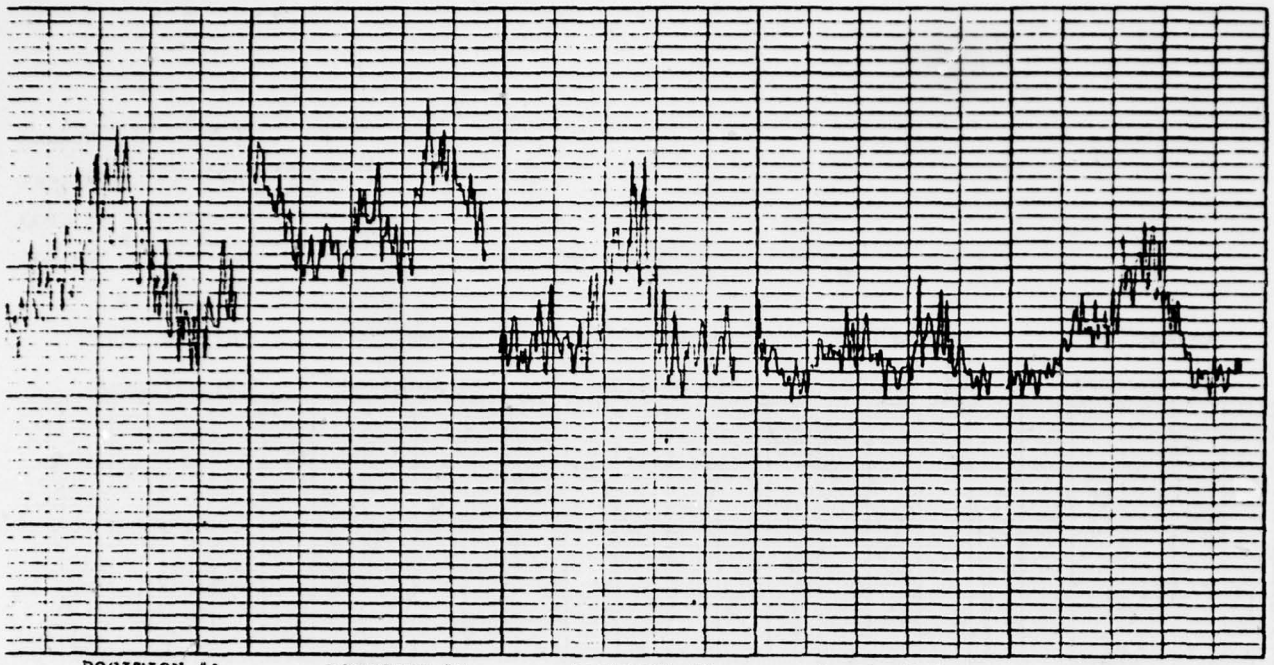

POSITION #1	POSITION #2	POSITION #3	POSITION #4	POSITION #5
[illegible] ppm/in	[illegible] ppm/in	[illegible] ppm/in	[illegible] ppm/in	[illegible] ppm/in

450°

RUN NO. [illegible]

COATING [illegible]

SUBSTRATE [illegible]

VENDOR [illegible]

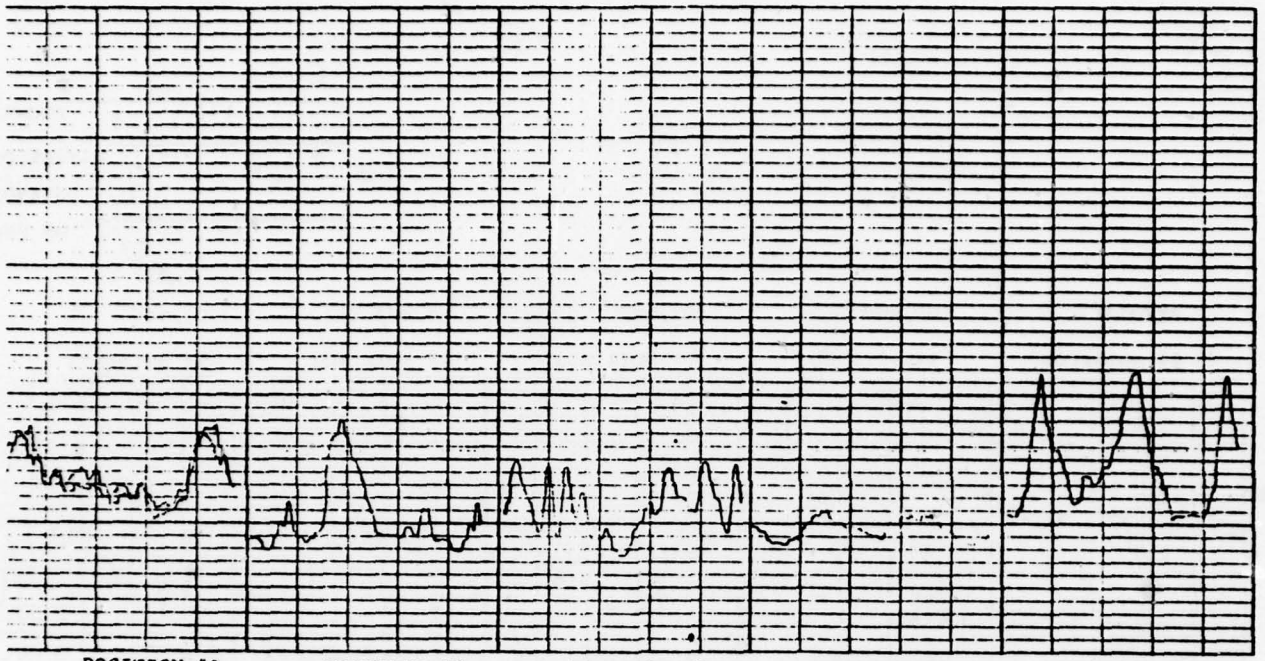

POSITION #1	POSITION #2	POSITION #3	POSITION #4	POSITION #5
[illegible] ppm/in	[illegible] ppm/in	[illegible] ppm/in	110 ppm/in	[illegible] ppm/in

450°

RUN NO. [illegible]

COATING HR

SUBSTRATE [illegible]

VENDOR [illegible]

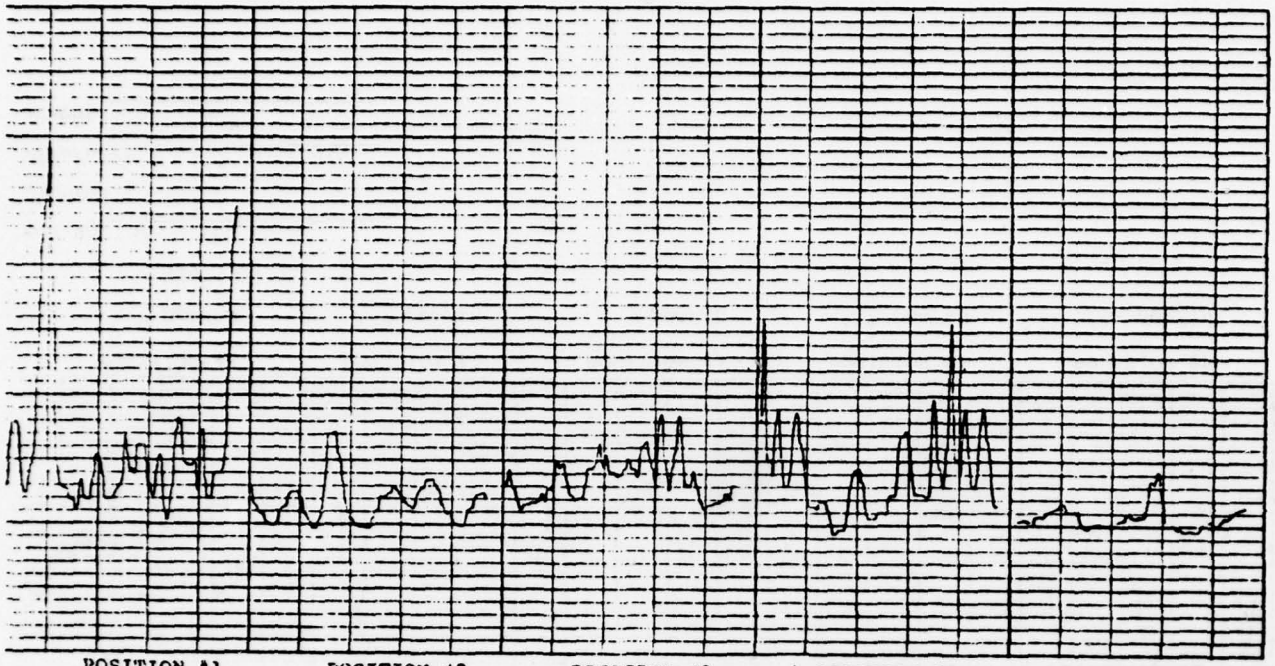

POSITION #1	POSITION #2	POSITION #3	POSITION #4	POSITION #5
( ) ppm/in	( ) ppm/in	( ) ppm/in	( ) ppm/in	( ) ppm/in

450°

RUN NO. [illegible]

COATING [illegible]

SUBSTRATE [illegible]

VENDOR [illegible]

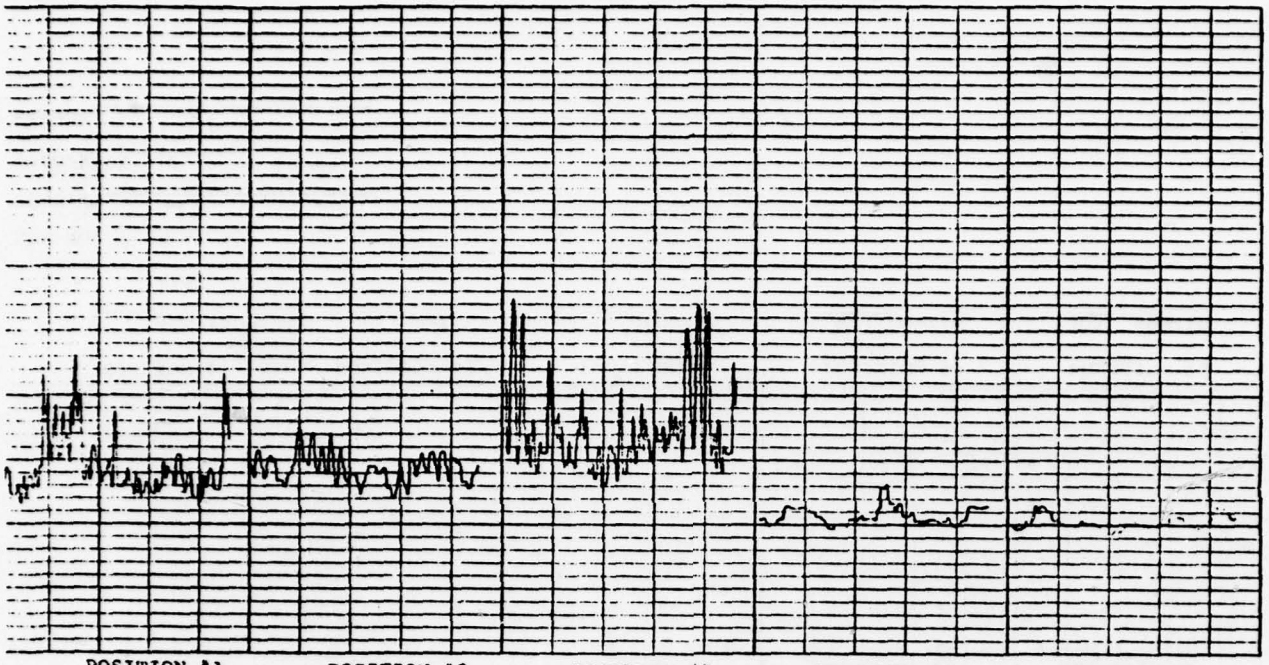

POSITION #1	POSITION #2	POSITION #3	POSITION #4	POSITION #5
ppm/in	ppm/in	ppm/in	ppm/in	ppm/in

450°

RUN NO.

COATING

SUBSTRATE

VENDOR

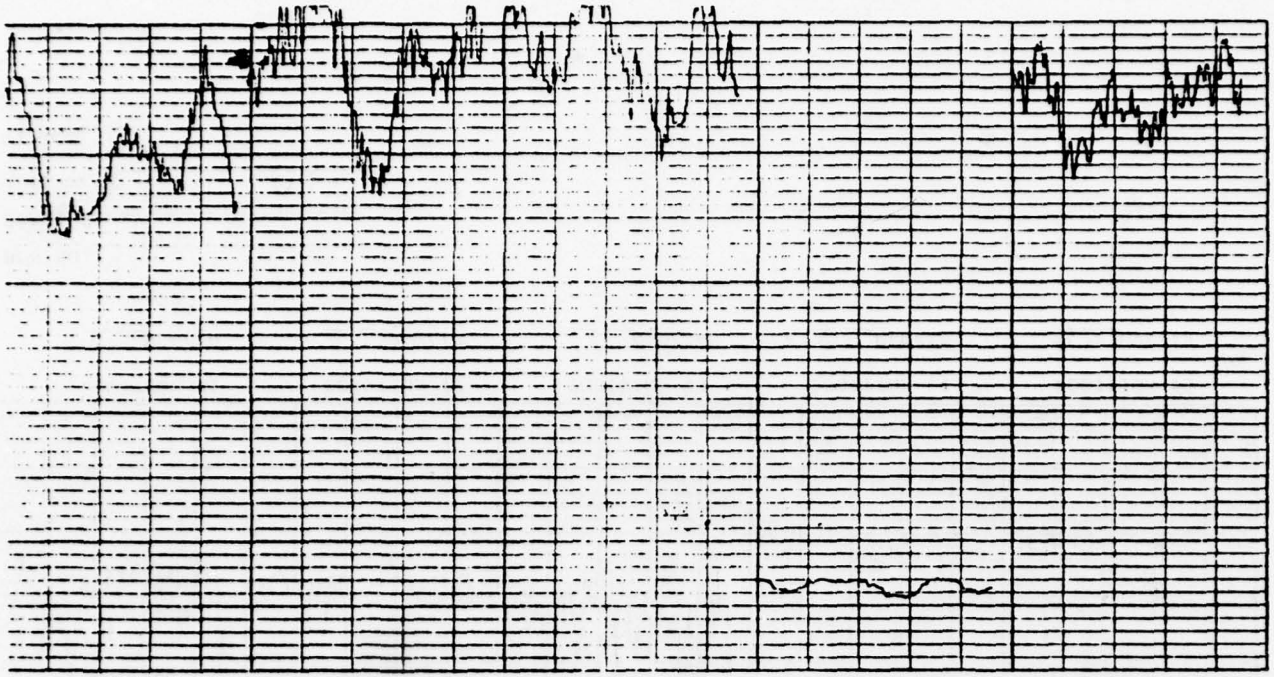

POSITION #1	POSITION #2	POSITION #3	POSITION #4	POSITION #5
10 ppm/in	100 ppm/in	[illegible] ppm/in	1000 ppm/in	10 ppm/in

450°

RUN NO. [illegible]

COATING H.E.

SUBSTRATE [illegible] (3) A

VENDOR [illegible]

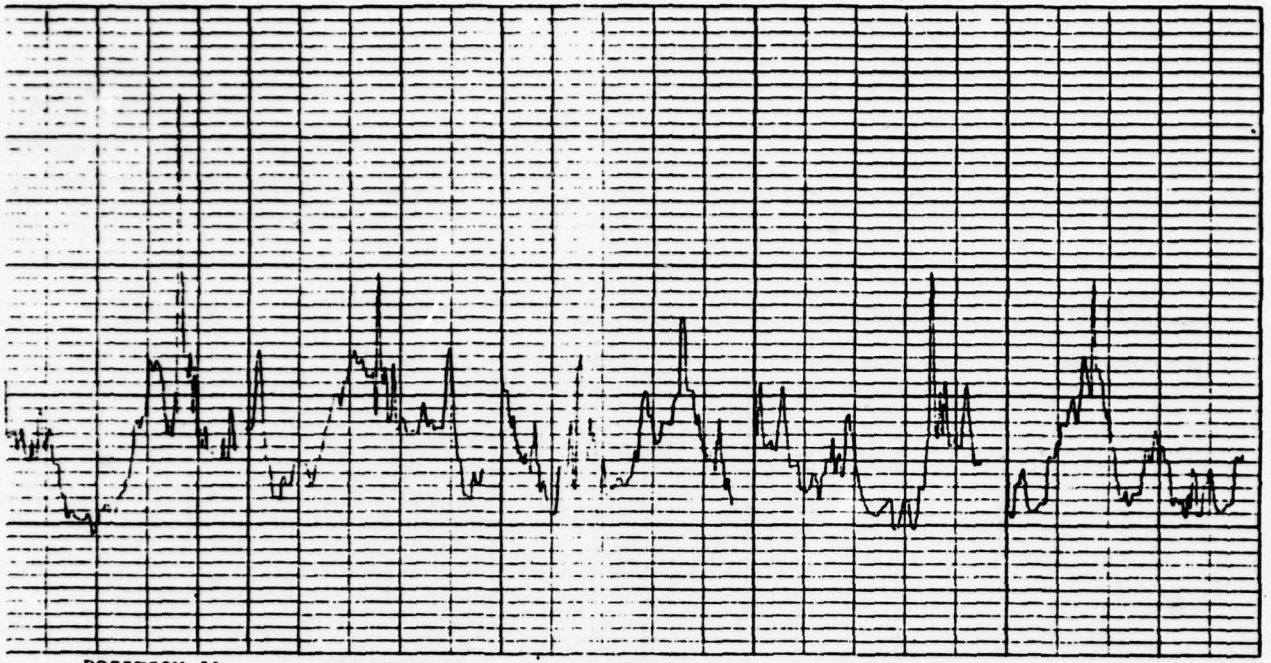

POSITION #1 POSITION #2 POSITION #3 POSITION #4 POSITION #5

[illegible] ppm/in [illegible] ppm/in [illegible] ppm/in [illegible] ppm/in [illegible] ppm/in

450°

RUN NO. [illegible]

COATING [illegible]

SUBSTRATE [illegible]

VENDOR [illegible]

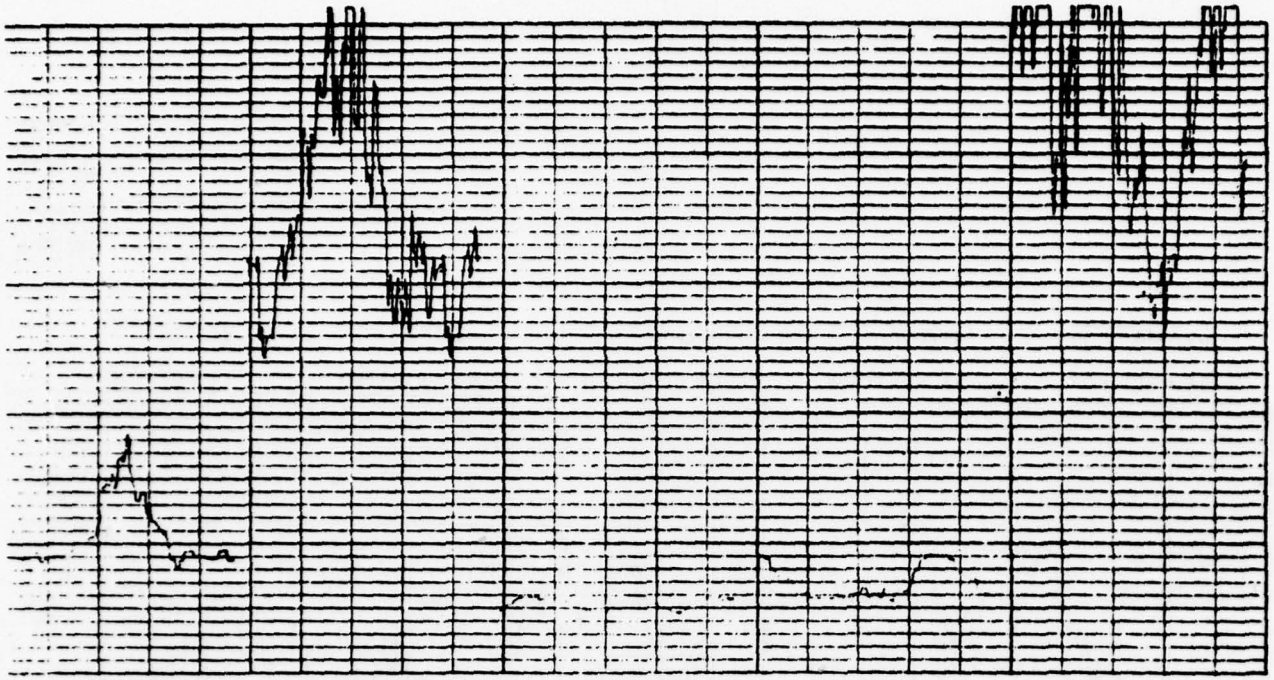

POSITION #1 | POSITION #2 | POSITION #3 | POSITION #4 | POSITION #5

[illegible] ppm/in | [illegible] ppm/in | [illegible] ppm/in | [illegible] ppm/in | [illegible] ppm/in

450°

RUN NO. [illegible]

COATING [illegible]

SUBSTRATE [illegible]

VENDOR [illegible]

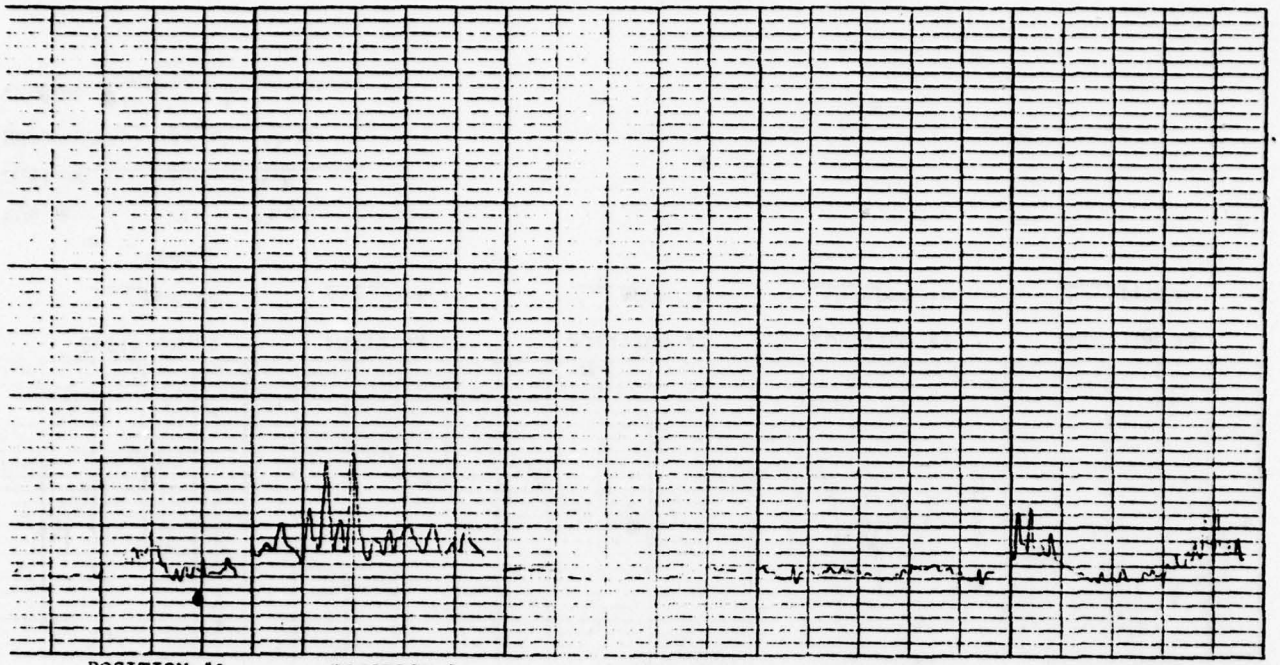

POSITION #1	POSITION #2	POSITION #3	POSITION #4	POSITION #5
[illegible] ppm/in	[illegible] ppm/in	[illegible] ppm/in	[illegible] ppm/in	[illegible] ppm/in

450°

RUN NO. [illegible]

COATING [illegible]

SUBSTRATE [illegible]

VENDOR [illegible]

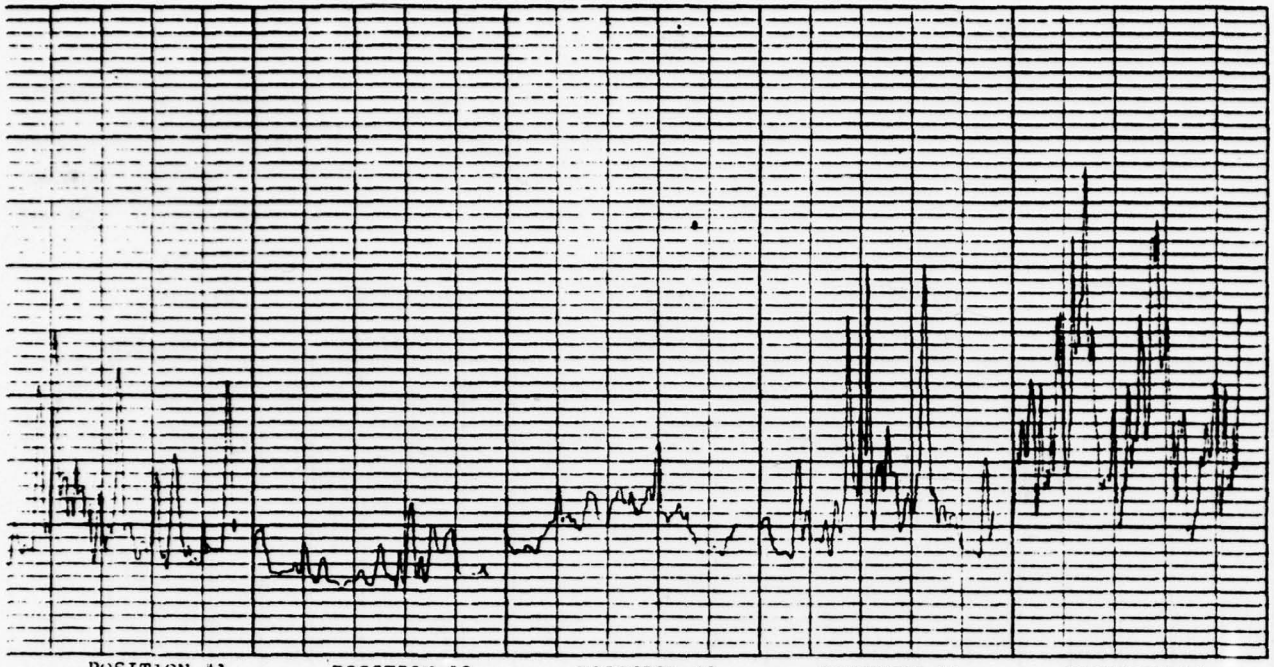

POSITION #1	POSITION #2	POSITION #3	POSITION #4	POSITION #5
ppm/in	ppm/in	ppm/in	ppm/in	ppm/in

450°

RUN NO.

COATING H.R

SUBSTRATE

VENDOR

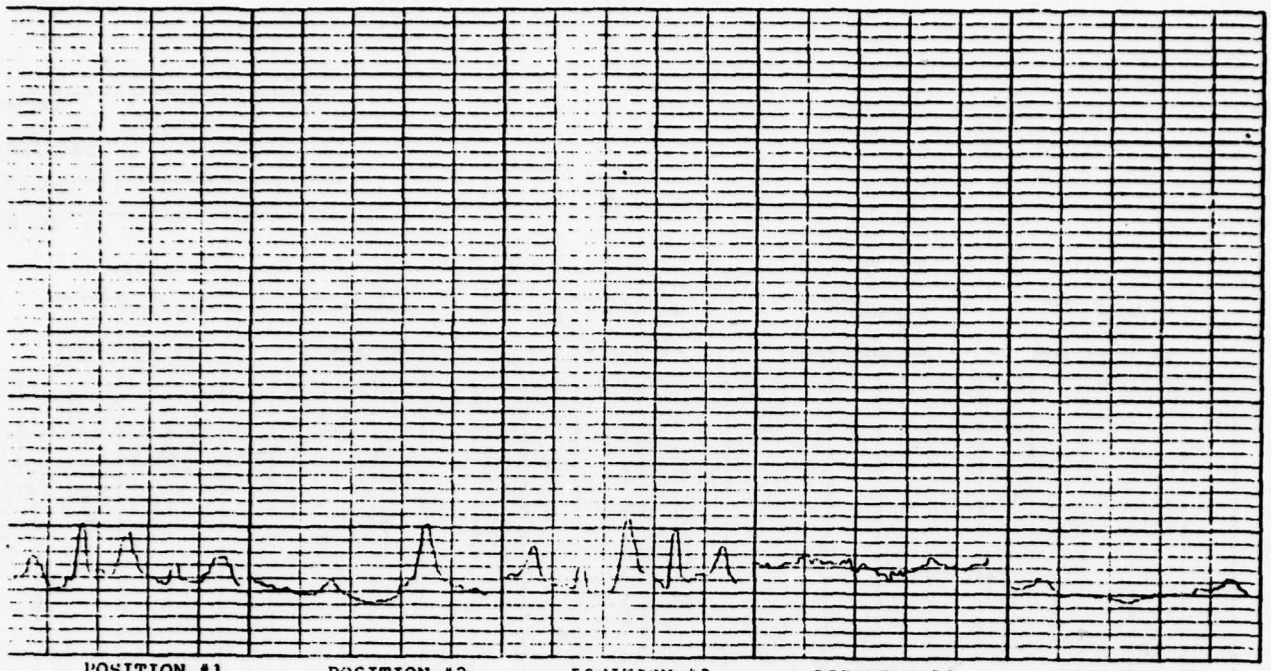

POSITION #1	POSITION #2	POSITION #3	POSITION #4	POSITION #5
ppm/in	ppm/in	ppm/in	1000 ppm/in	1000 ppm/in

450°

RUN NO.

COATING

SUBSTRATE

VENDOR Rohr

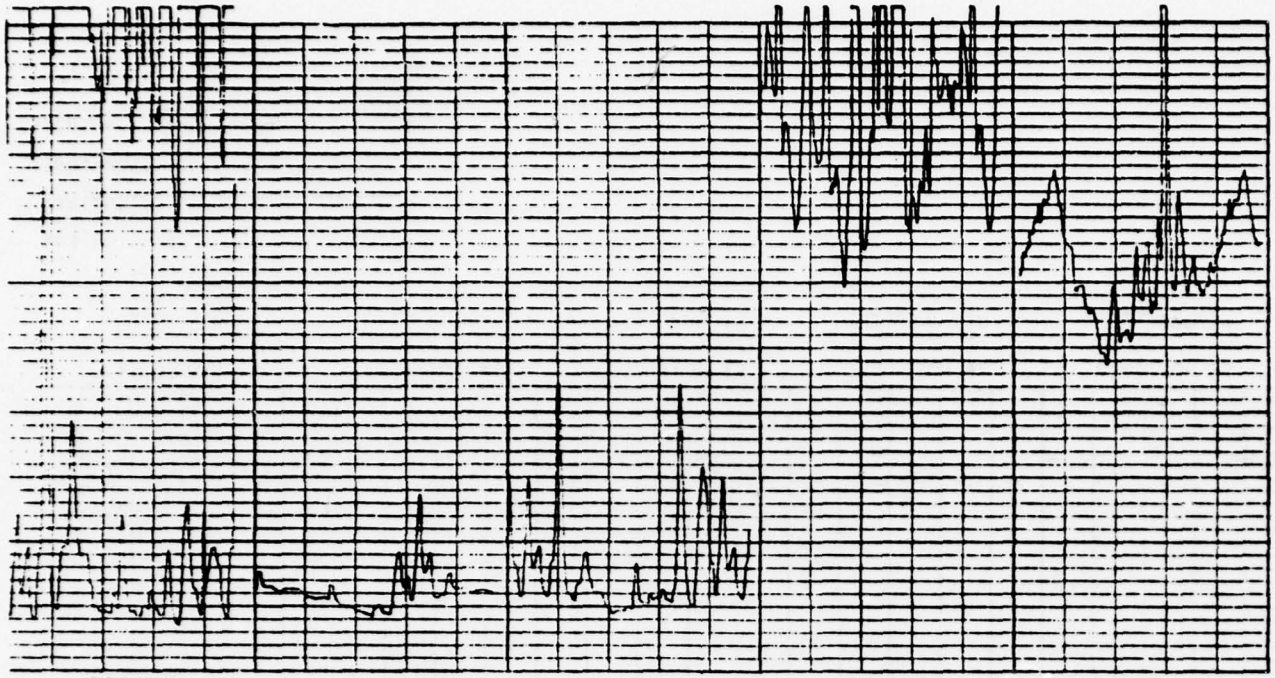

POSITION #1	POSITION #2	POSITION #3	POSITION #4	POSITION #5
ppm/in	ppm/in	ppm/in	ppm/in	ppm/in

450°

RUN NO.

COATING

SUBSTRATE

VENDOR

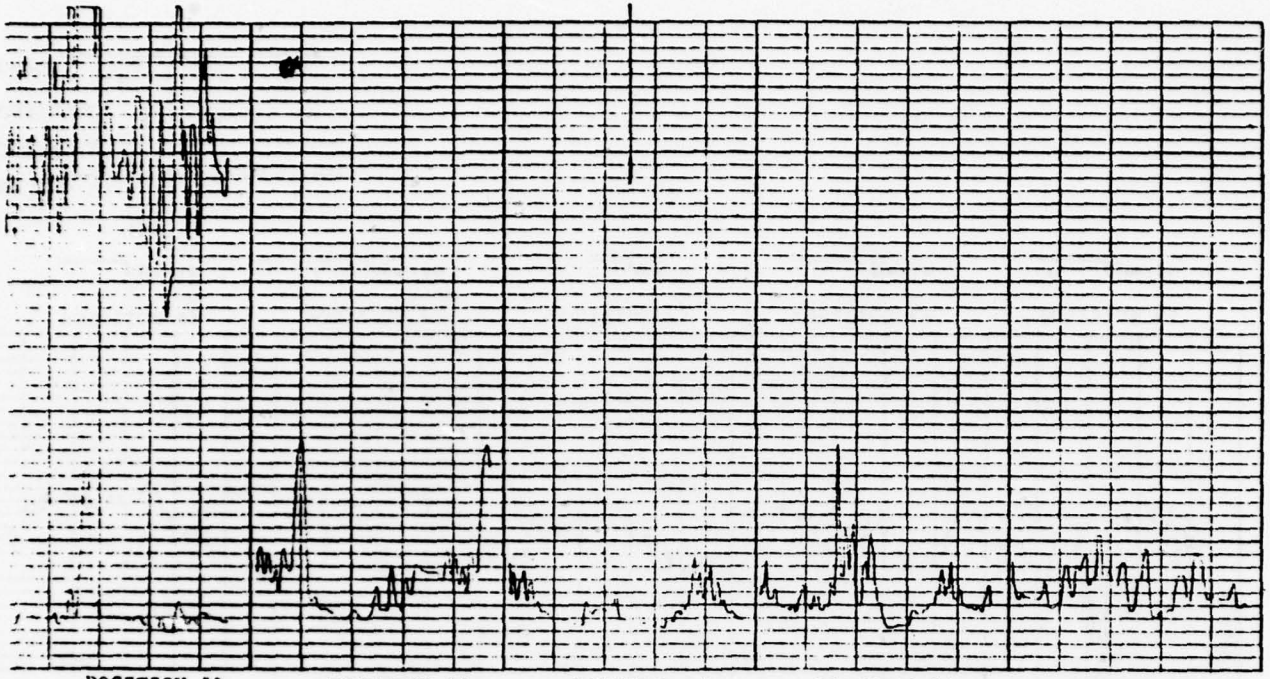

POSITION #1	POSITION #2	POSITION #3	POSITION #4	POSITION #5
____ppm/in	[illegible] ppm/in	[illegible] ppm/in	[illegible] ppm/in	[illegible] ppm/in

450°

RUN NO. [illegible]

COATING [illegible]

SUBSTRATE [illegible]

VENDOR [illegible]

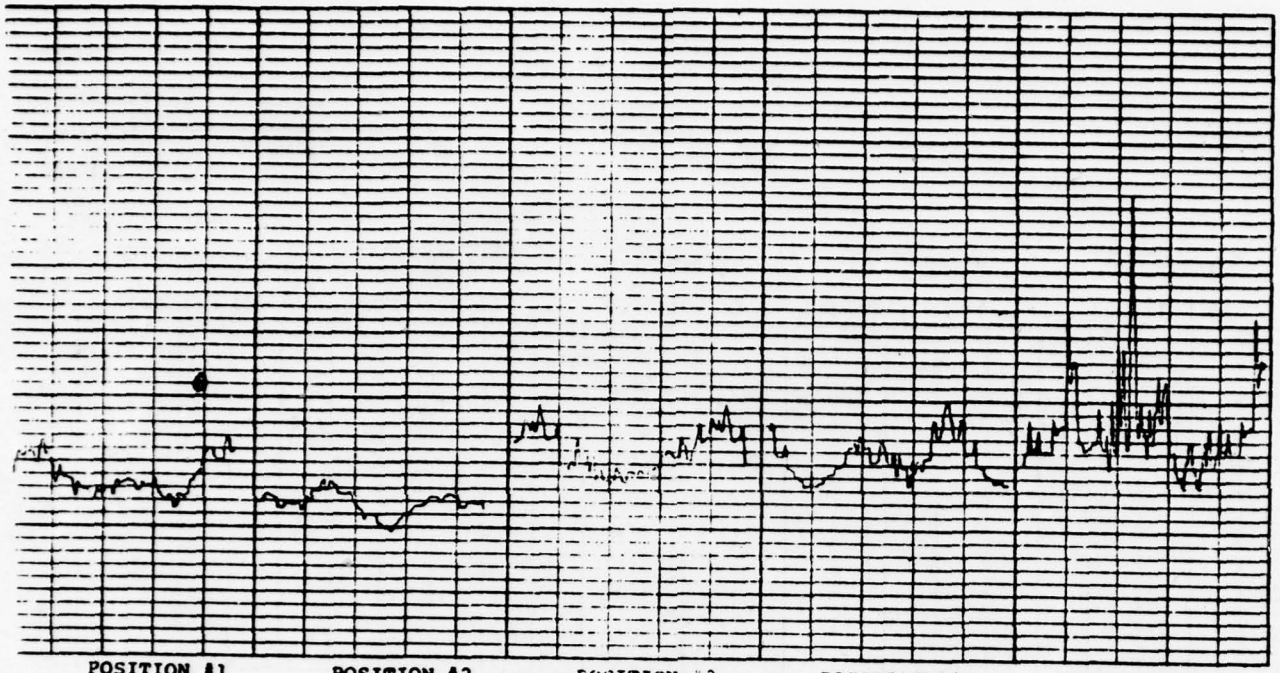

POSITION #1	POSITION #2	POSITION #3	POSITION #4	POSITION #5
ppm/in	ppm/in	ppm/in	ppm/in	ppm/in

450°

UN NO. [illegible]

OATING H R.

UBSTRATE Garnet Si [illegible]

ENDOR [illegible]

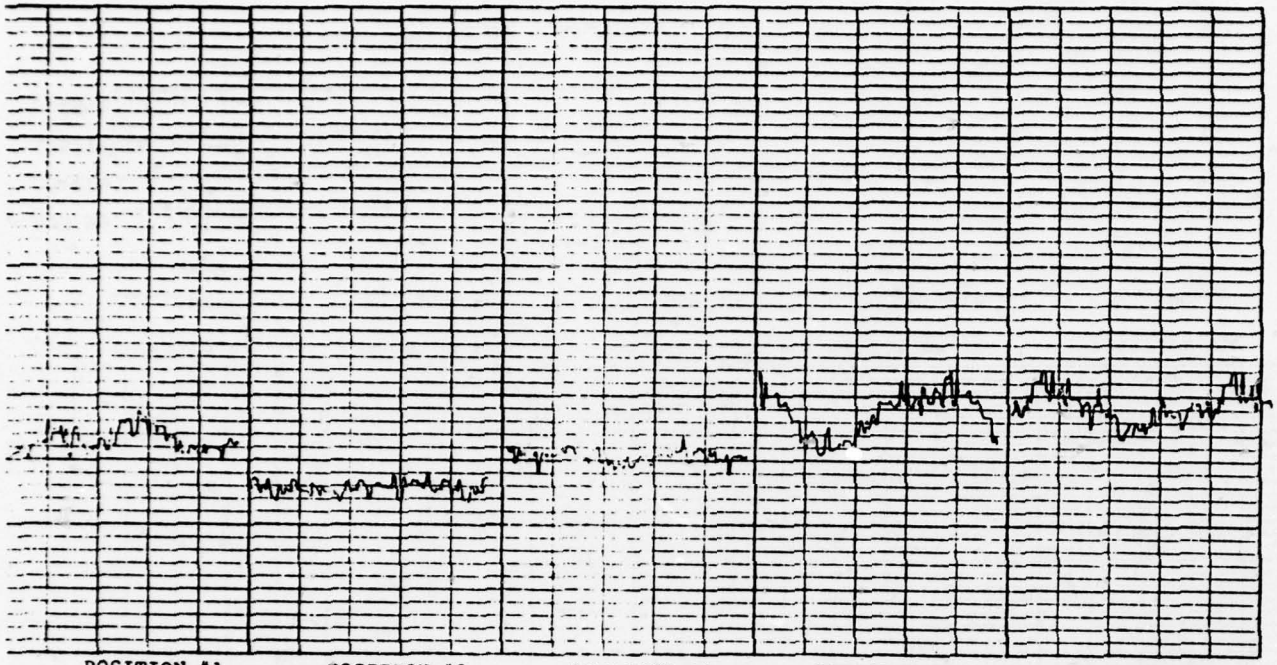

POSITION #1	POSITION #2	POSITION #3	POSITION #4	POSITION #5
[illegible] ppm/in	[illegible] ppm/in	[illegible] ppm/in	[illegible] ppm/in	[illegible] ppm/in

450°

RUN NO. [illegible]

COATING H.T.

SUBSTRATE [illegible]

VENDOR Rockwell

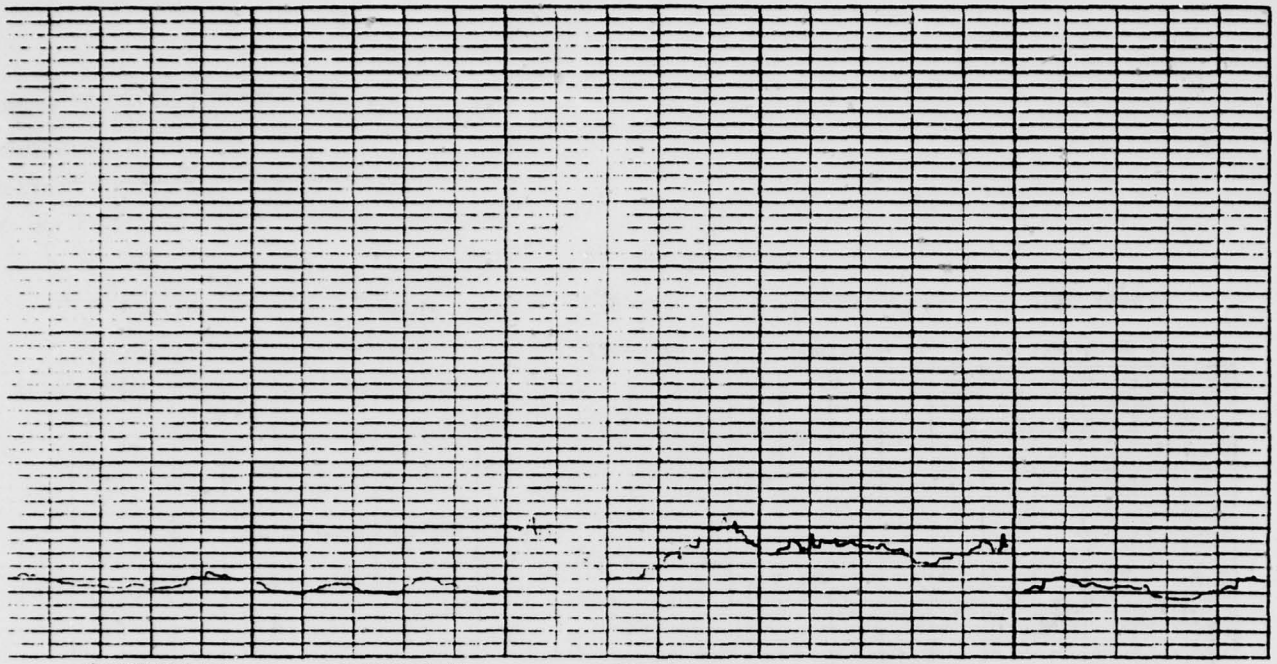

POSITION #1	POSITION #2	POSITION #3	POSITION #4	POSITION #5
[illegible] ppm/in	[illegible] ppm/in	[illegible] ppm/in	1000 ppm/in	[illegible] ppm/in

450°

RUN NO. [illegible]

COATING N.B.

SUBSTRATE [illegible]

VENDOR Rockwell

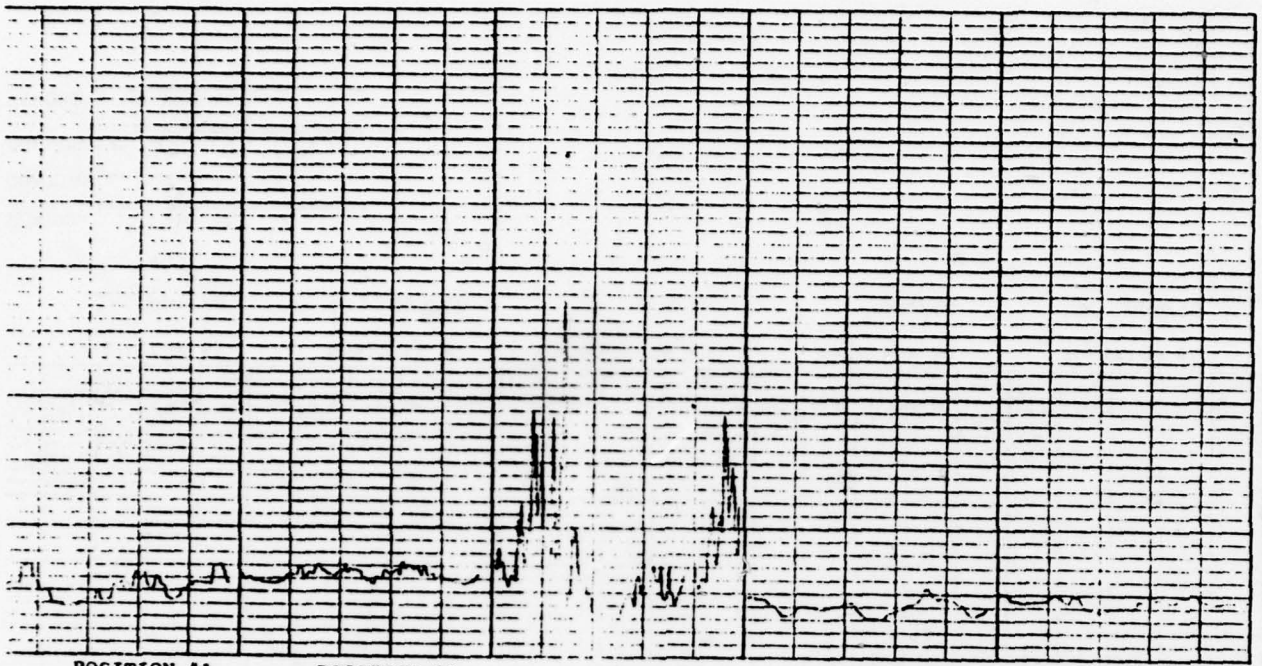

POSITION #1 ___ ppm/in

POSITION #2 ___ ppm/in

POSITION #3 ___ ppm/in

POSITION #4 ___ ppm/in

POSITION #5 ___ ppm/in

450°

UN NO. [illegible]

OATING [illegible]

UBSTRATE [illegible]

ENDOR [illegible]

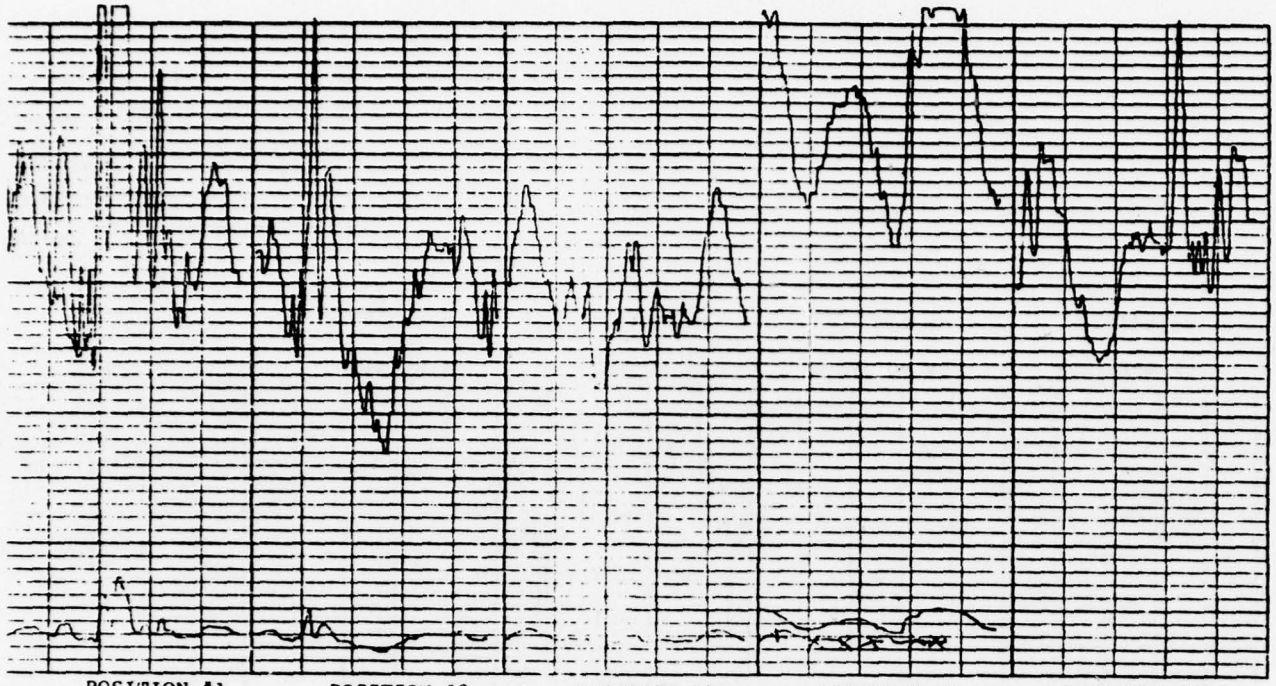

POSITION #1 ___ ppm/in

POSITION #2 100 ppm/in

POSITION #3 ___ ppm/in

POSITION #4 ___ ppm/in

POSITION #5 ___ ppm/in

450°

RUN NO. ___

COATING ___

SUBSTRATE ___

VENDOR ___

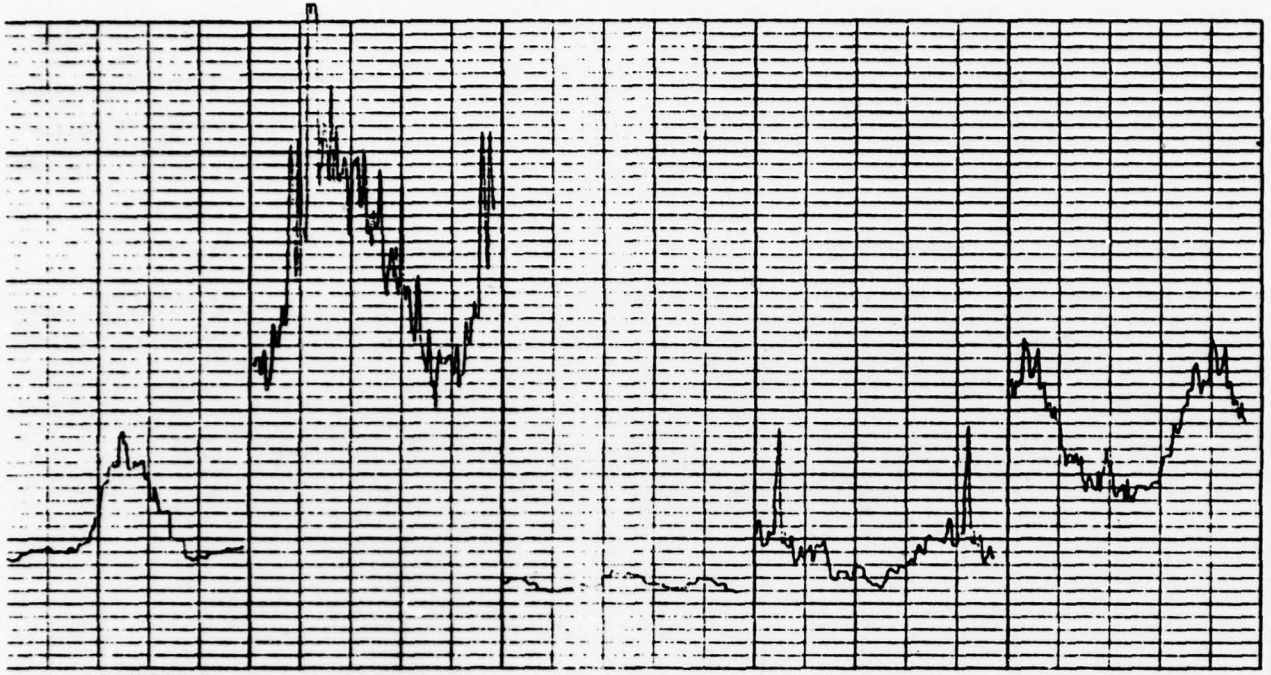

POSITION #1	POSITION #2	POSITION #3	POSITION #4	POSITION #5
[illegible] ppm/in	[illegible] ppm/in	[illegible] ppm/in	[illegible] ppm/in	[illegible] ppm/in

450°

RUN NO. [illegible]

COATING [illegible]

SUBSTRATE Garrett [illegible]

VENDOR Rockwell

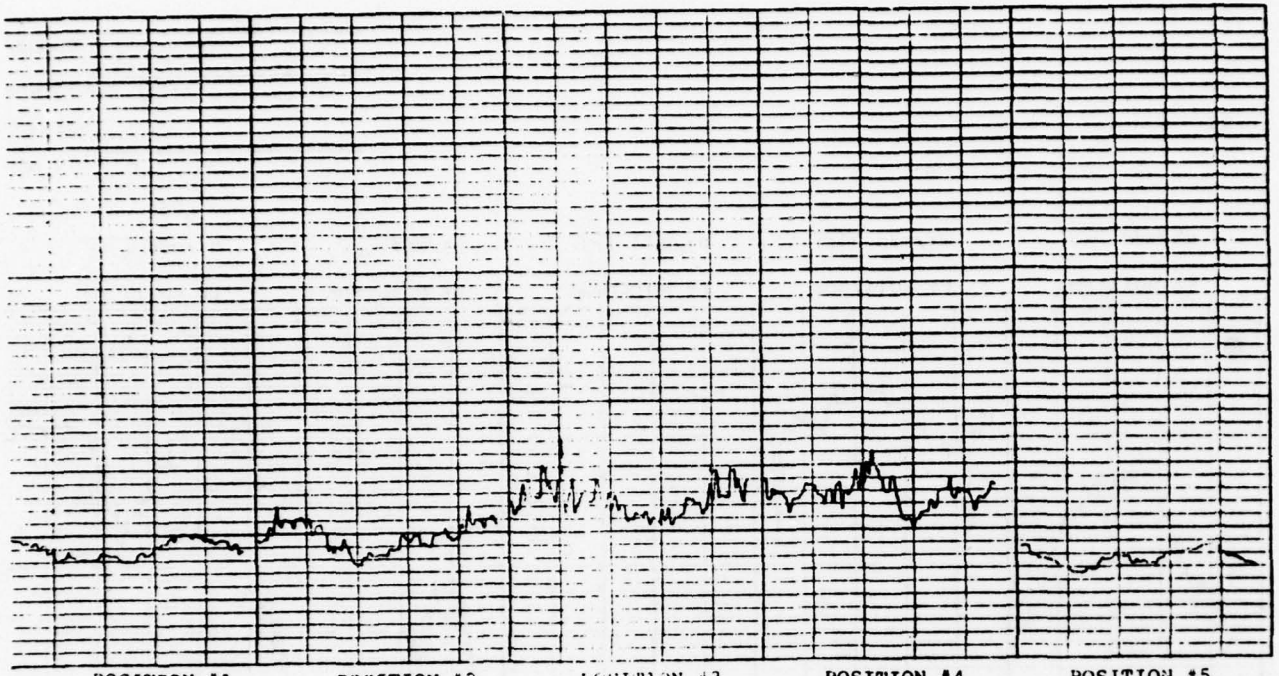

POSITION #1	POSITION #2	POSITION #3	POSITION #4	POSITION #5
ppm/in	ppm/in	ppm/in	ppm/in	ppm/in

450°

RUN NO.

COATING

SUBSTRATE

VENDOR

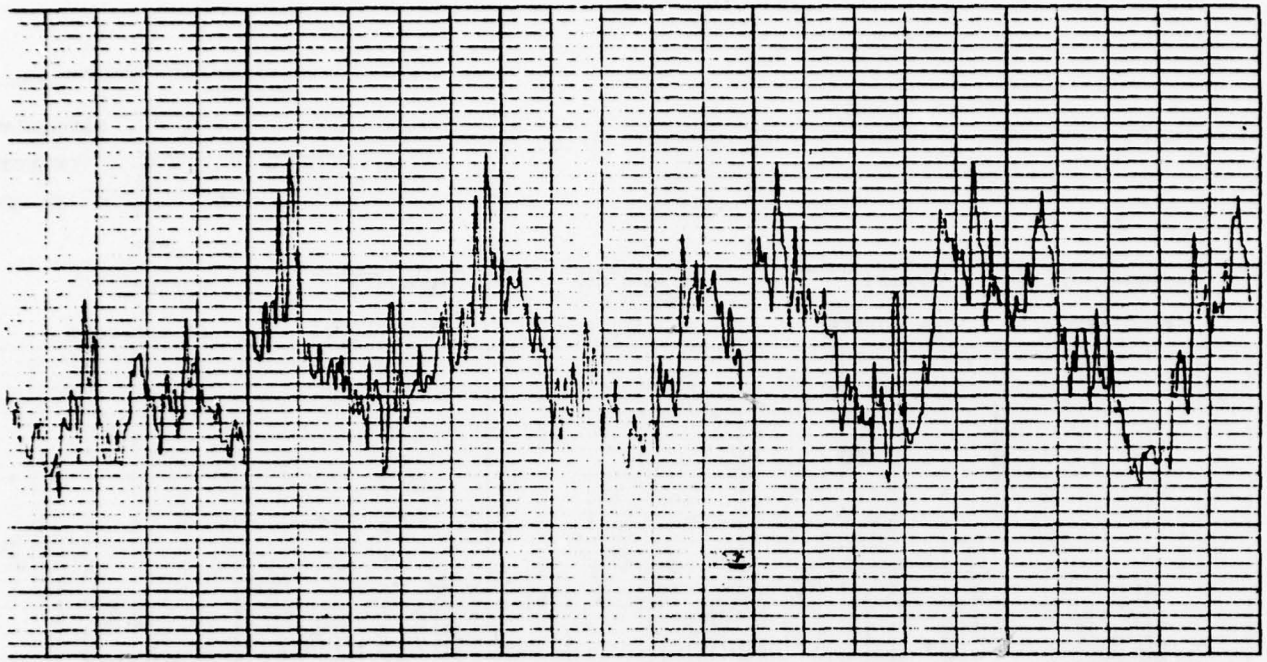

POSITION #1	POSITION #2	POSITION #3	POSITION #4	POSITION #5
[illegible] ppm/in	100 ppm/in	[illegible] ppm/in	100 ppm/in	100 ppm/in

450°

RUN NO. 1057-120

COATING T[illegible] H.E.

SUBSTRATE F.S. 41

VENDOR Pratt

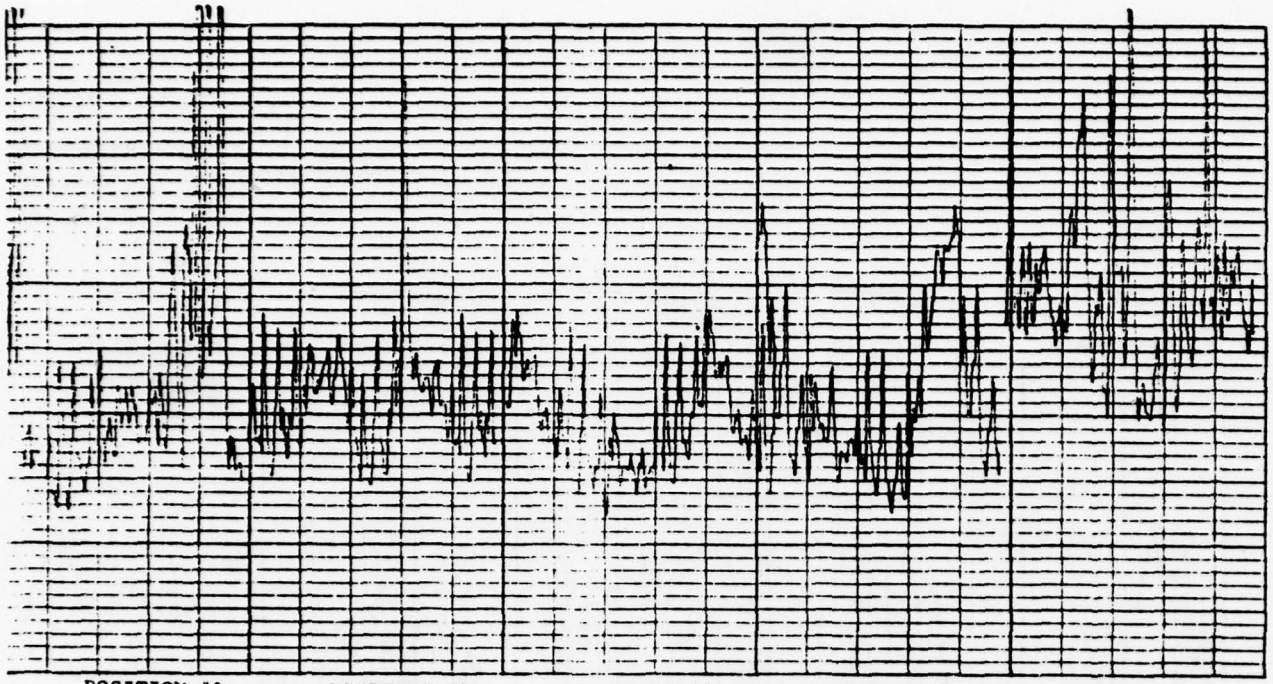

POSITION #1	POSITION #2	POSITION #3	POSITION #4	POSITION #5
[illegible] ppm/in	[illegible] ppm/in	[illegible] ppm/in	[illegible] ppm/in	[illegible] ppm/in

450°

RUN NO. [illegible]

COATING [illegible]

SUBSTRATE [illegible]

VENDOR [illegible]

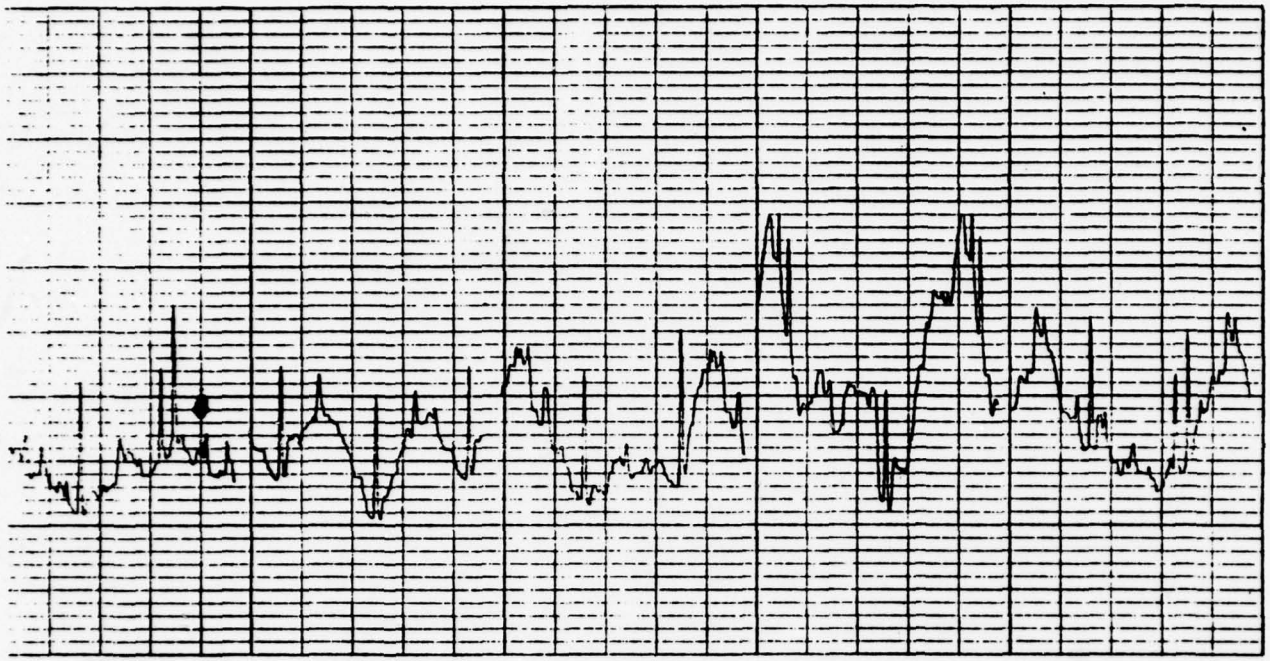

POSITION #1	POSITION #2	POSITION #3	POSITION #4	POSITION #5
ppm/in	(0) ppm/in	(0) ppm/in	(0) ppm/in	(0) ppm/in

450°

RUN NO. [illegible]

COATING Ta2-Si2 H.R.

SUBSTRATE [illegible]

VENDOR [illegible]

APPENDIX B. MIRROR SCATTERING TRACES, BATCH IV

These scattering traces for the mirrors of Batch IV are included in this report for completeness. The traces were provided by Optical Coating Laboratories, Inc., using standard scattering measurement techniques developed by that laboratory for assessment of ring laser gyro mirror quality.

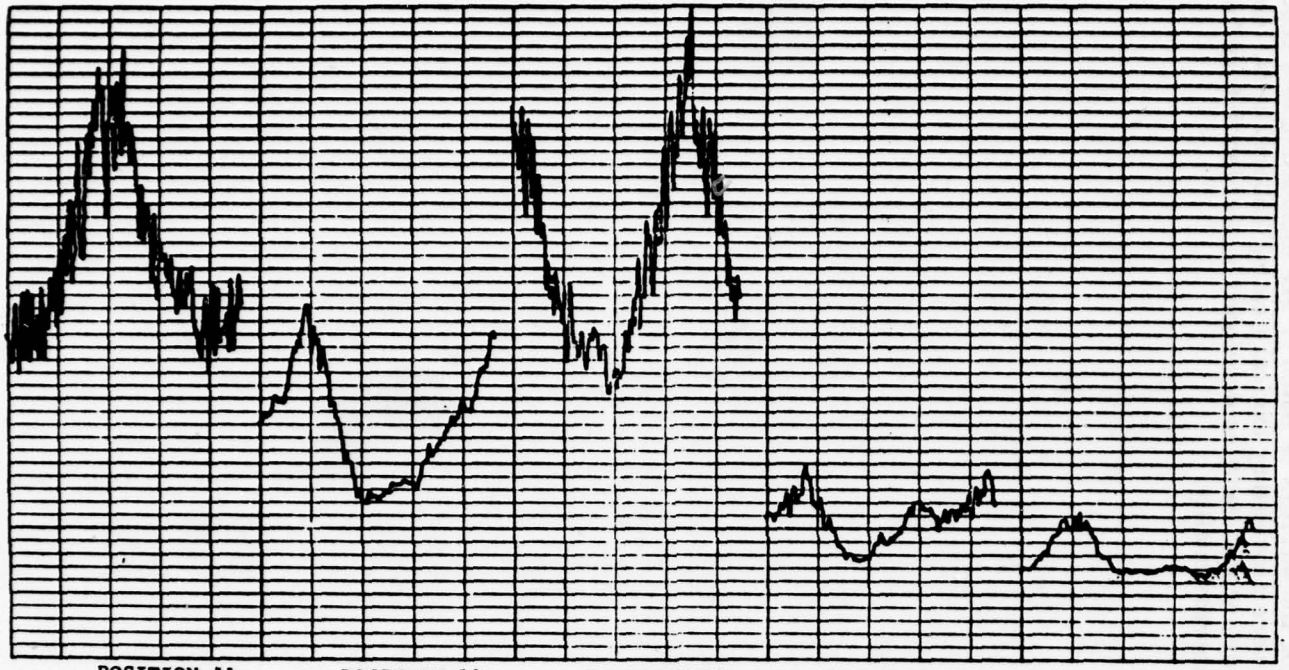

POSITION #1	POSITION #2	POSITION #3	POSITION #4	POSITION #5
100 ppm/in	100 ppm/in	100 ppm/in	100 ppm/in	100 ppm/in

450°

RUN NO. 1007-233

COATING T~.2% @ 30°

SUBSTRATE 1 L

VENDOR ROCKWELL

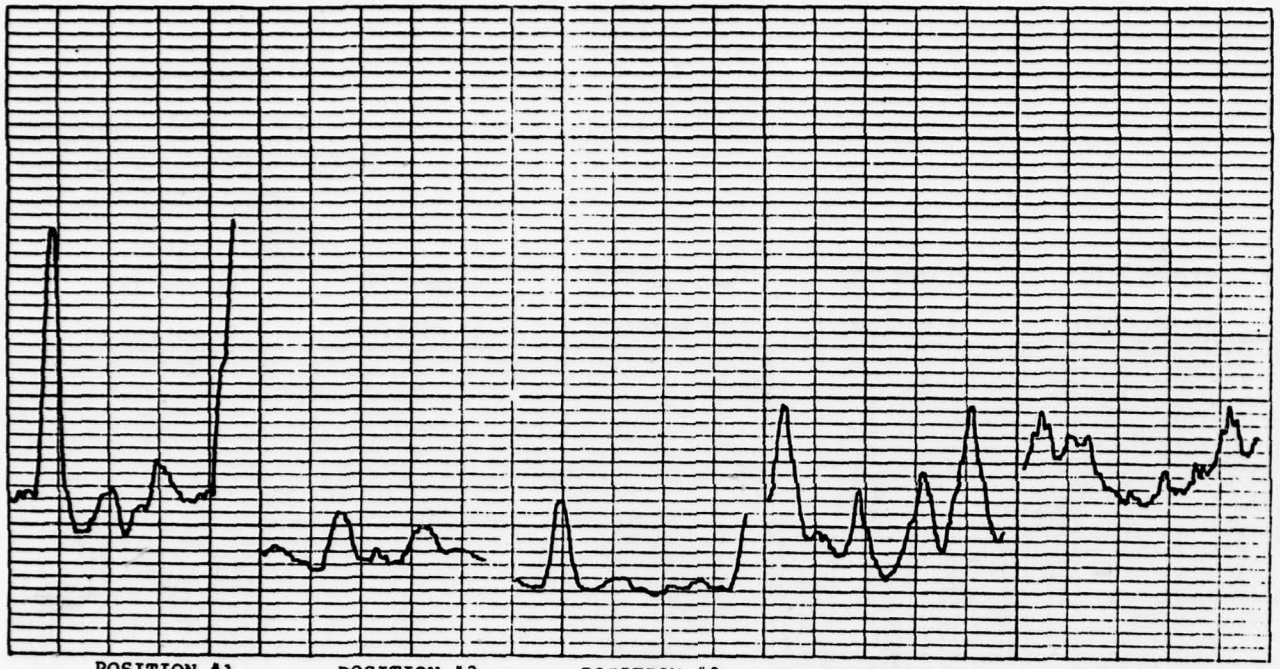

POSITION #1	POSITION #2	POSITION #3	POSITION #4	POSITION #5
100 ppm/in	100 ppm/in	100 ppm/in	100 ppm/in	100 ppm/in
450°				

RUN NO. 1007-233

COATING I ~ 20% @ 30°

SUBSTRATE 26

VENDOR Rockwell

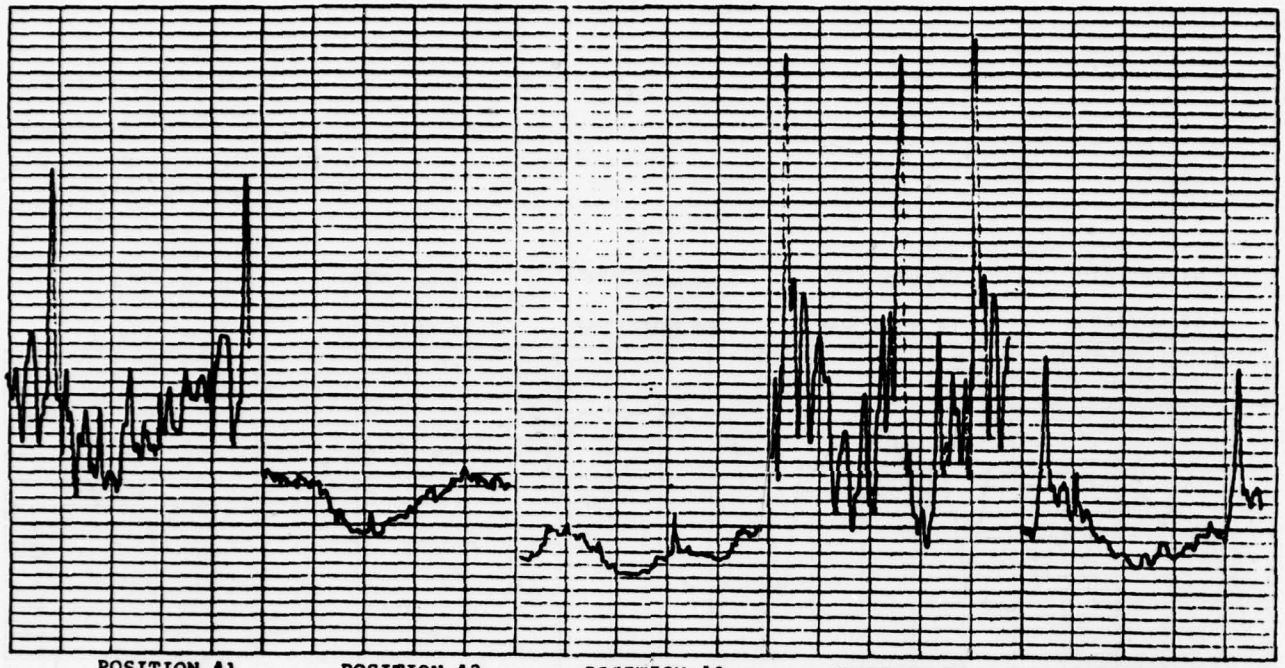

POSITION #1	POSITION #2	POSITION #3	POSITION #4	POSITION #5
100 ppm/in	100 ppm/in	400 ppm/in	100 ppm/in	100 ppm/in
450°				

RUN NO. 1007 - 233

COATING I - Al2O3 @ 30°

SUBSTRATE 3L

VENDOR Rockwell

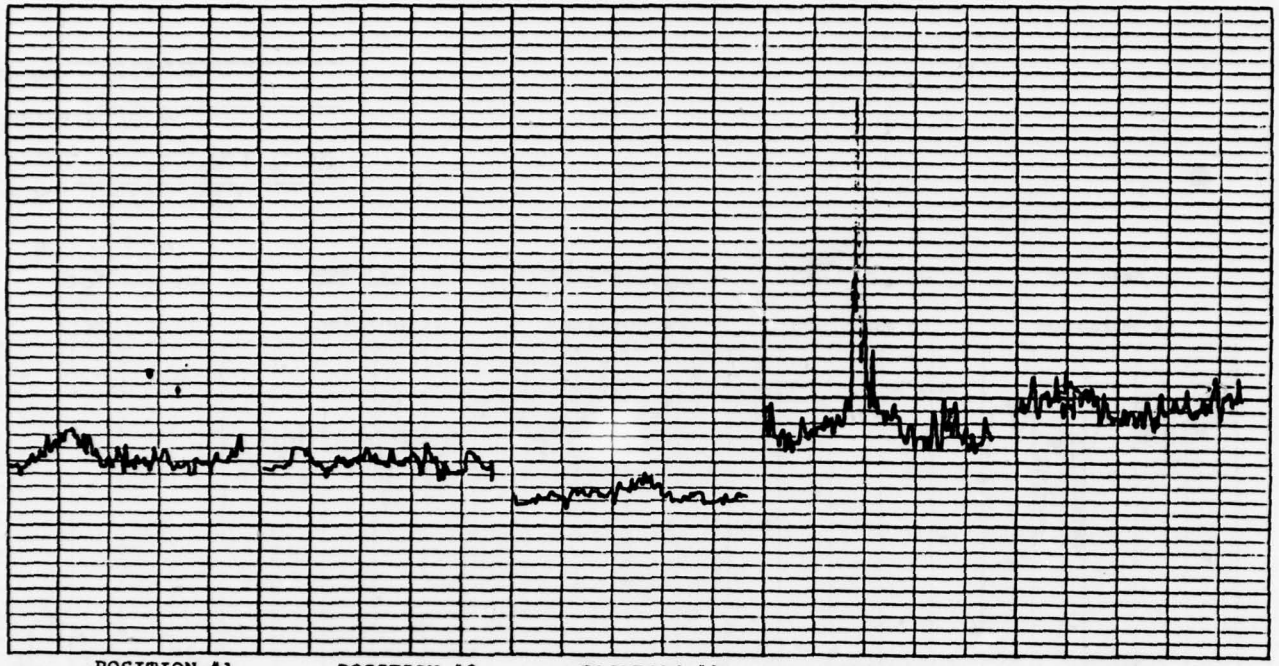

POSITION #1	POSITION #2	POSITION #3	POSITION #4	POSITION #5
1000 ppm/in	1000 ppm/in	1000 ppm/in	1000 ppm/in	1000 ppm/in

450°

RUN NO. 1007-233

COATING T~0.27, @ 30°

SUBSTRATE 4L

VENDOR ROCKWELL

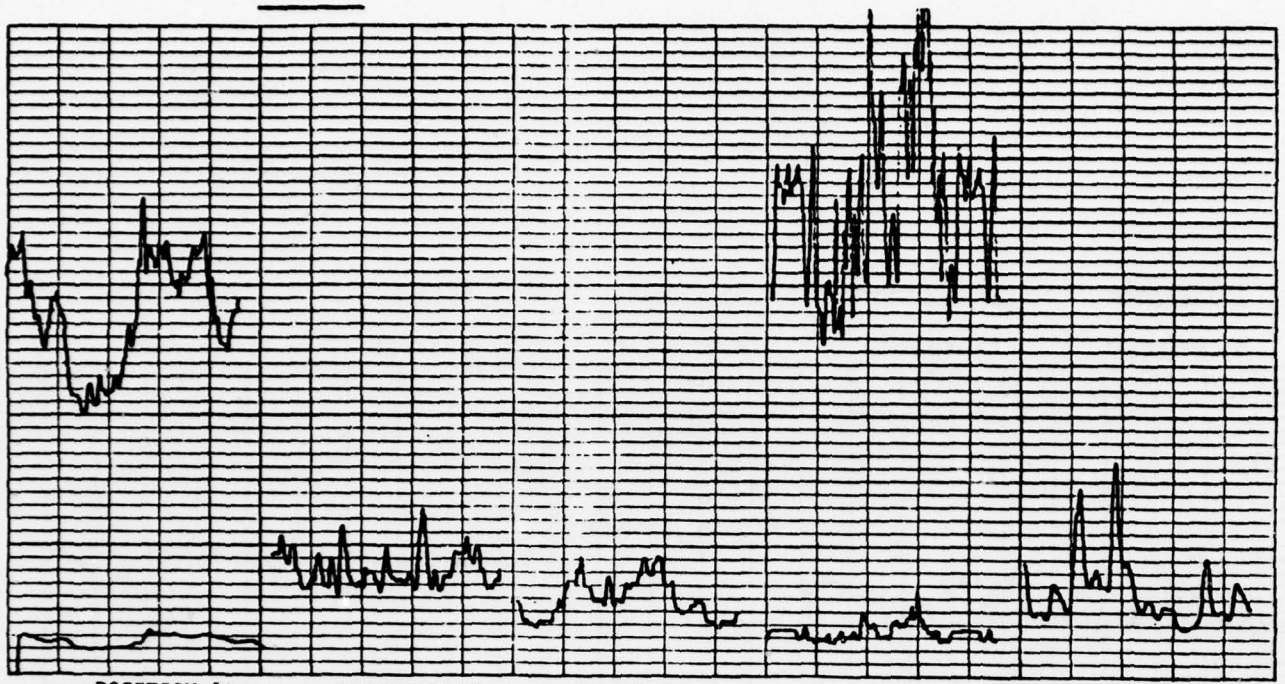

POSITION #1	POSITION #2	POSITION #3	POSITION #4	POSITION #5
100 / 1000 ppm/in	1000 ppm/in	1000 ppm/in	100 (1000) ppm/in	1000 ppm/in

450°

RUN NO. 1007-23

COATING T~0.2% T @ 30°

SUBSTRATE 5 C

VENDOR ROCKWELL

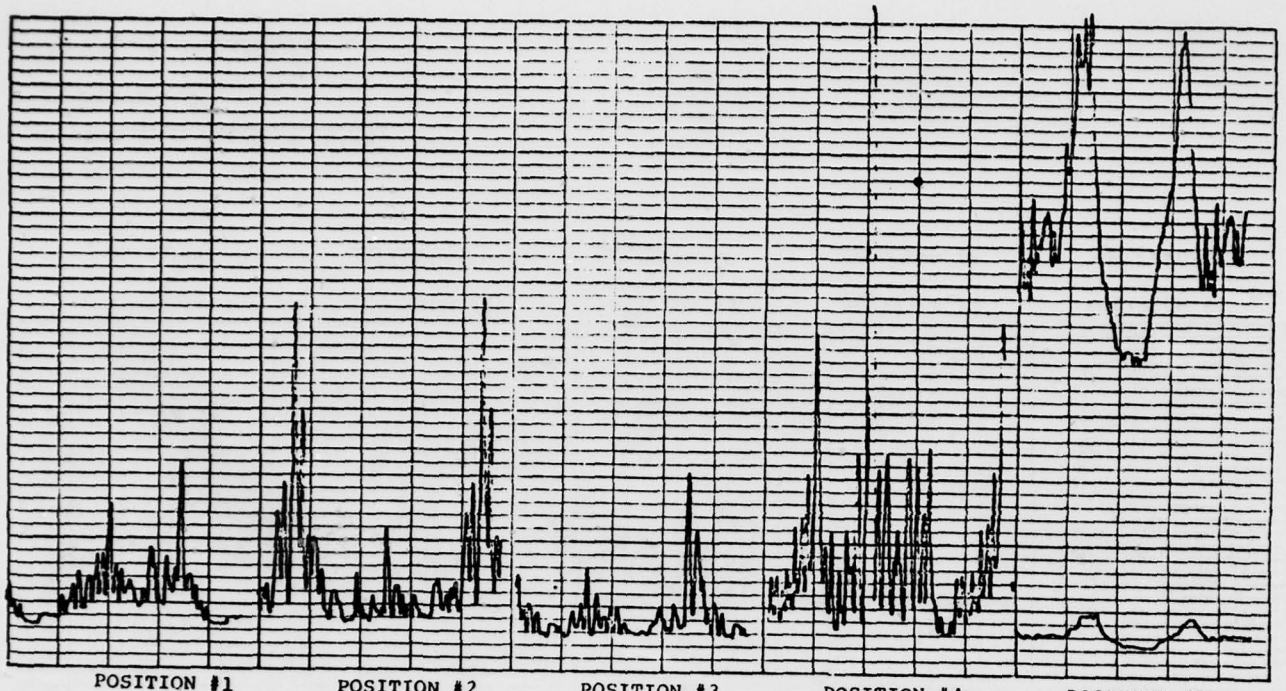

POSITION #1	POSITION #2	POSITION #3	POSITION #4	POSITION #5
1000 ppm/in	1000 ppm/in	1000 ppm/in	1000 ppm/in	100 ppm/in
450°				

RUN NO. 1007-233

COATING T ~ 0.2% T @ 35°

SUBSTRATE GL

VENDOR ROCKWELL

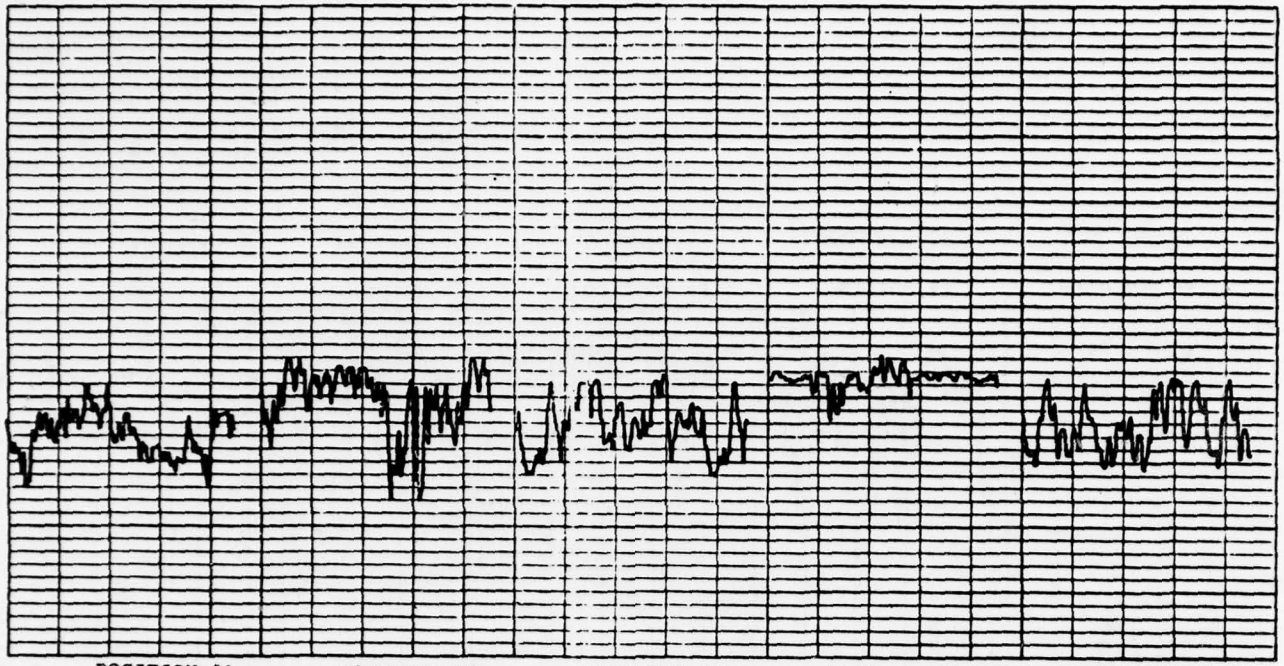

POSITION #1	POSITION #2	POSITION #3	POSITION #4	POSITION #5
10000 ppm/in	10000 ppm/in	10000 ppm/in	10000 ppm/in	10000 ppm/in
450°				

RUN NO. 100>-233

COATING T~0.2%T @30°

SUBSTRATE 2S

VENDOR Rockwell

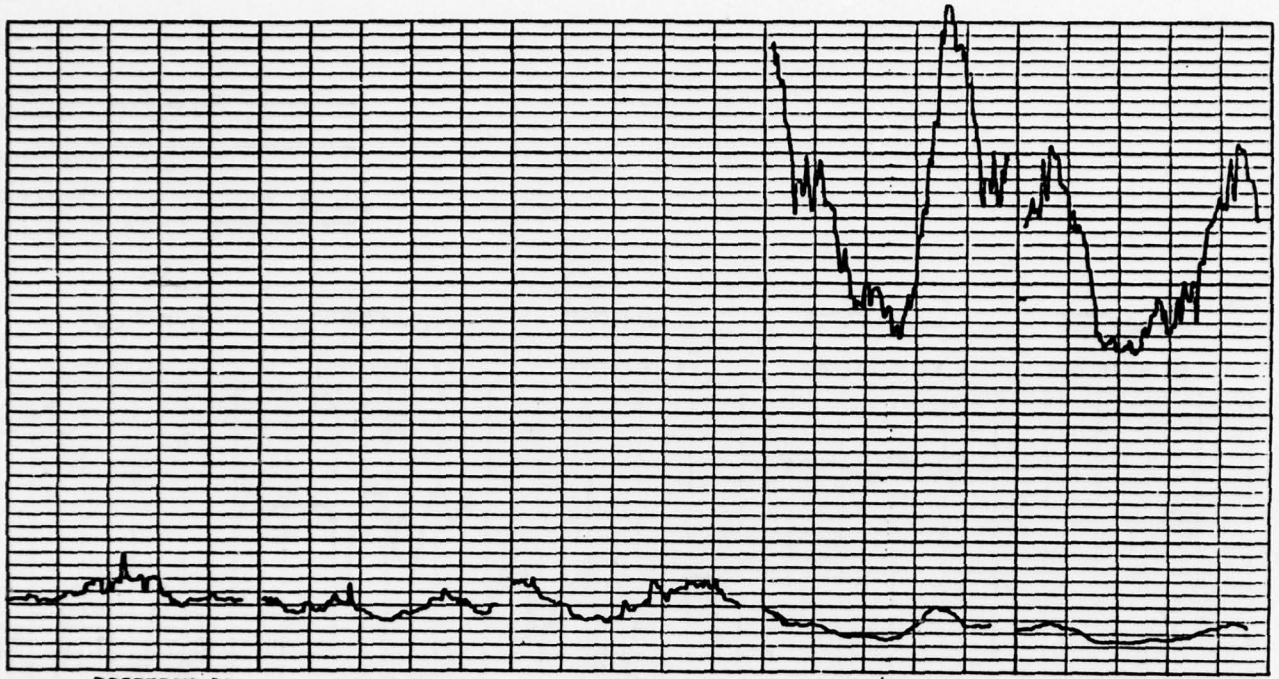

POSITION #1	POSITION #2	POSITION #3	POSITION #4	POSITION #5
1000 ppm/in	1000 ppm/in	100 ppm/in	(100) 100 ppm/in	(100) 100 ppm/in

450°

RUN NO. 1007-733

COATING T-12% @ 30°

SUBSTRATE 35

VENDOR Arcwell

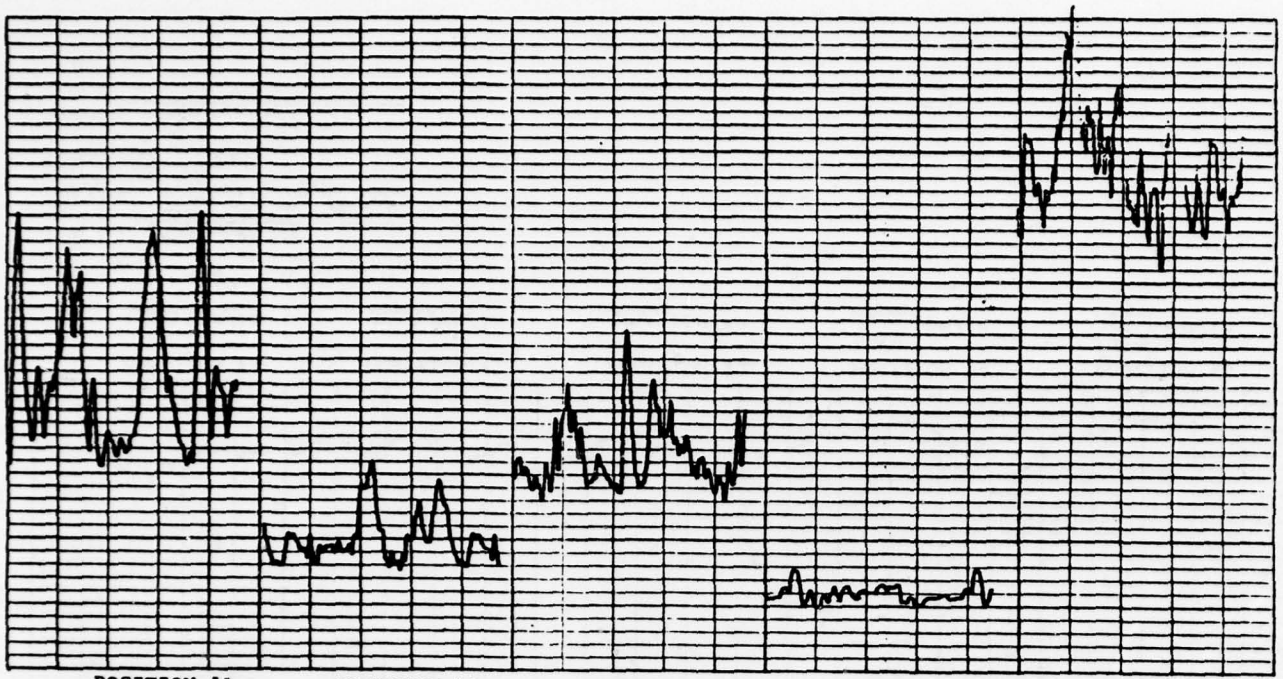

POSITION #1	POSITION #2	POSITION #3	POSITION #4	POSITION #5
1000 ppm/in	1000 ppm/in	1000 ppm/in	10000 ppm/in	1000 ppm/in
450°				

RUN NO. 1007-233

COATING T~ 0.25% @ 30°

SUBSTRATE 4/3

VENDOR Raytheon

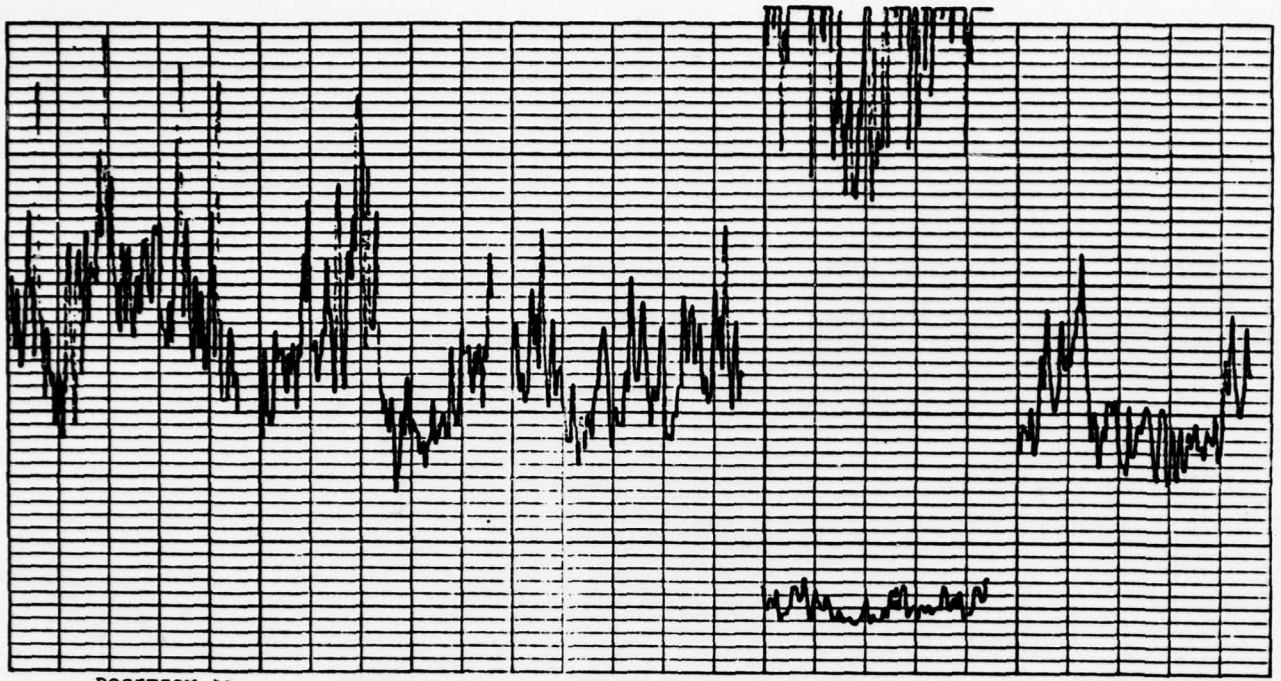

POSITION #1	POSITION #2	POSITION #3	POSITION #4	POSITION #5
1000 ppm/in	1000 ppm/in	1000 ppm/in	1000 ppm/in (1000)	1000 ppm/in
450°				

RUN NO. 1007-233

COATING T~0.2% @ 30°

SUBSTRATE S5

VENDOR Rockwell

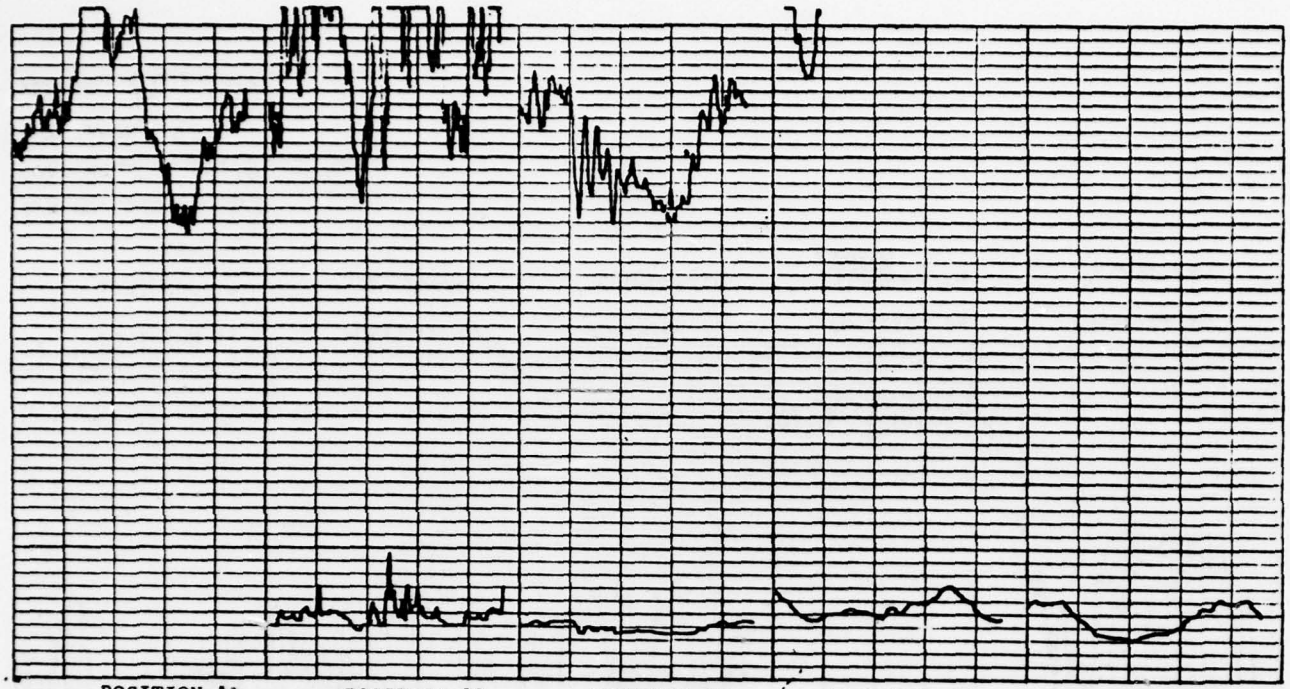

POSITION #1	POSITION #2	POSITION #3	POSITION #4	POSITION #5
100 ppm/in	(,00) 1000 ppm/in	(,00) 1000 ppm/in	1000 ppm/in	____ ppm/in
450°				

RUN NO. 1007-233

COATING T~0.2% @ 30°

SUBSTRATE 65

VENDOR Rockwell

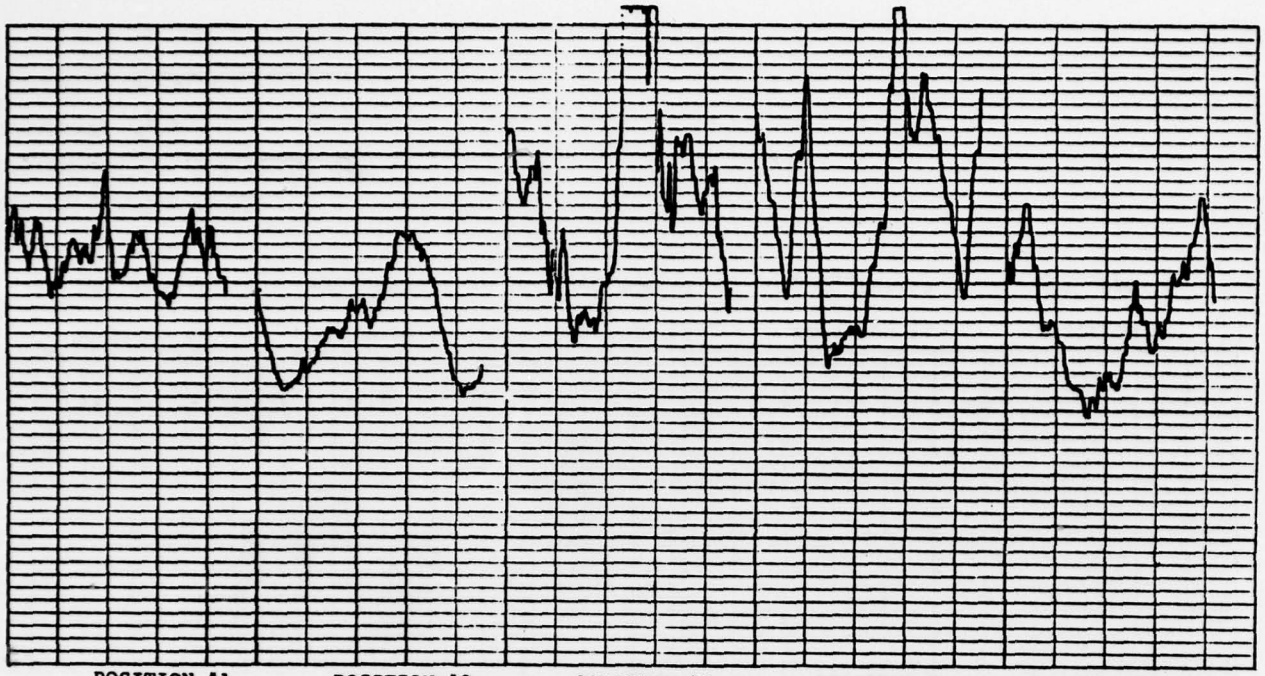

POSITION #1	POSITION #2	POSITION #3	POSITION #4	POSITION #5
100 ppm/in	100 ppm/in	100 ppm/in	100 ppm/in	100 ppm/in

450°

RUN NO. 1007-233

COATING T~0.2%, T @ 30°

SUBSTRATE Ss

VENDOR Rockwell

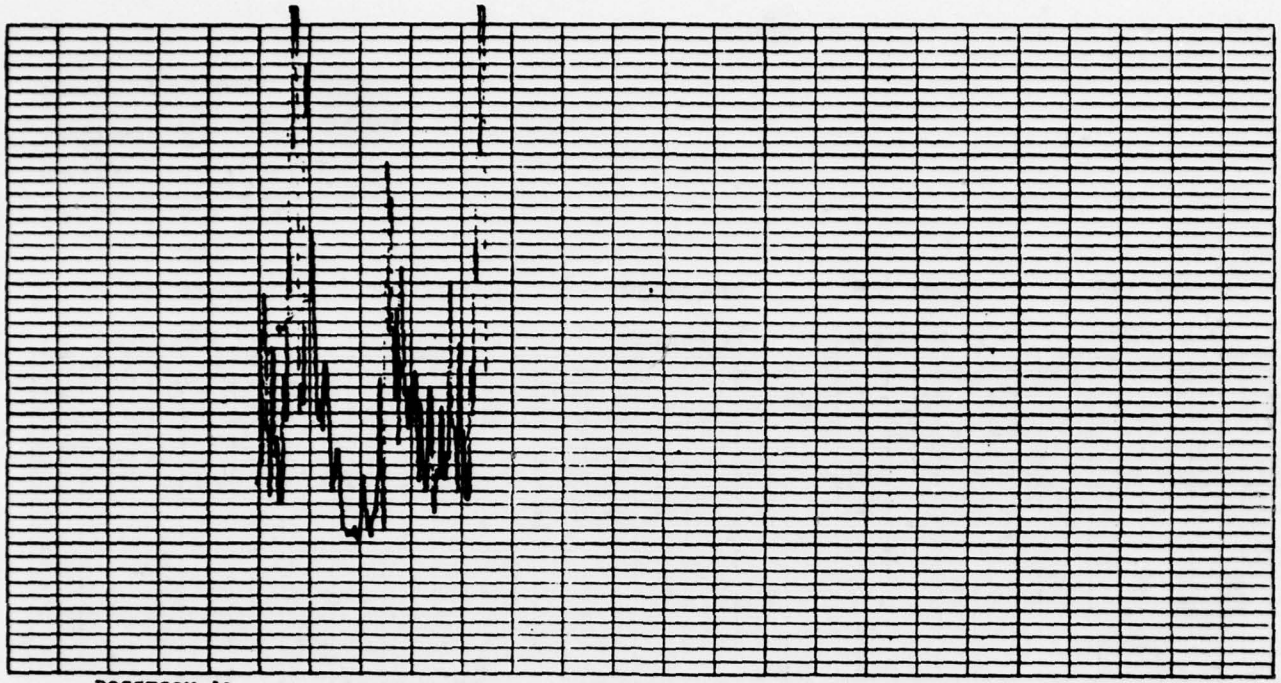

POSITION #1	POSITION #2	POSITION #3	POSITION #4	POSITION #5
~ ppm/in	1000 ppm/in	~ ppm/in	~ ppm/in	~ ppm/in

450°

RUN NO. 1007-233

COATING T ~ 0.2% @ 30°

SUBSTRATE 9s

VENDOR ROCKWELL

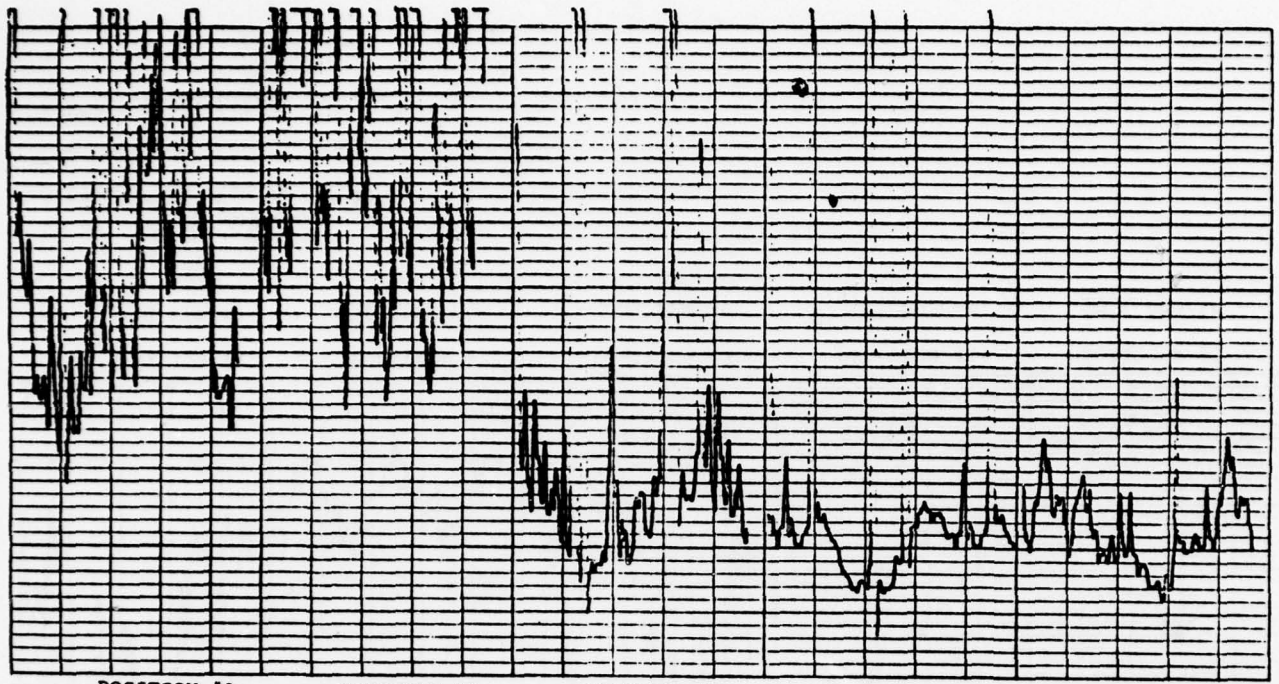

POSITION #1	POSITION #2	POSITION #3	POSITION #4	POSITION #5
1000 ppm/in	1000 ppm/in	1000 ppm/in	1000 ppm/in	1000 ppm/in
450°				

RUN NO. 1007-233

COATING T ~ 0.2% @ 30°

SUBSTRATE 10s

VENDOR Rockwell

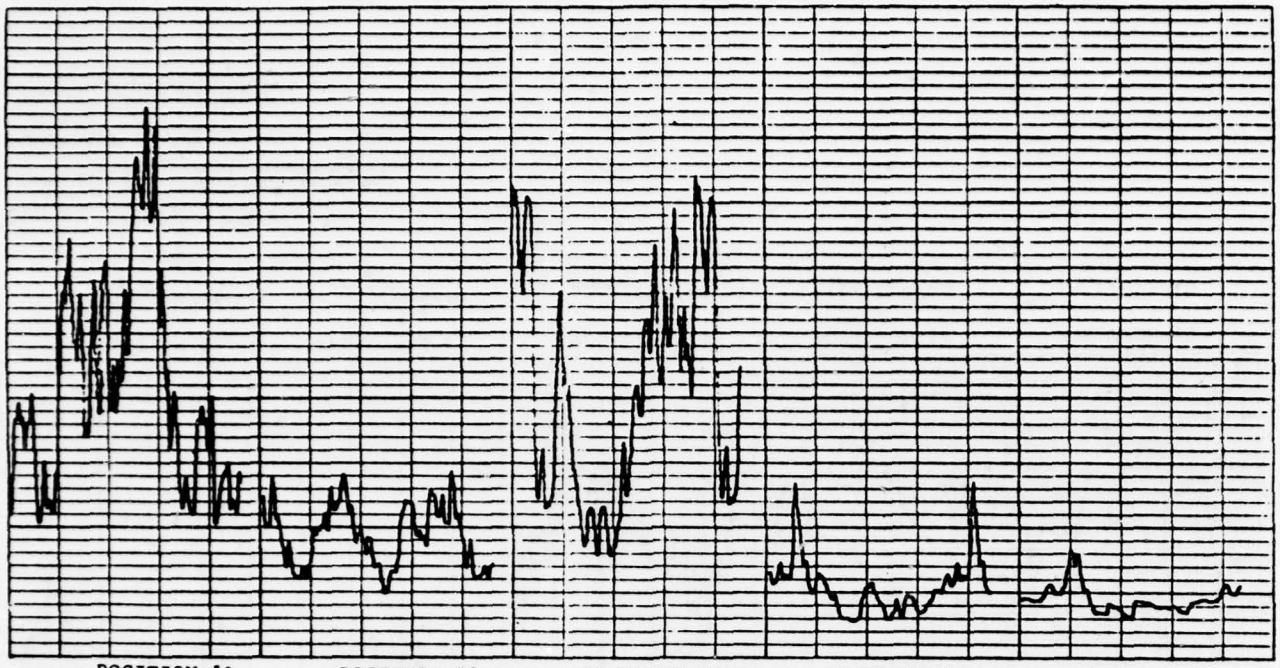

POSITION #1	POSITION #2	POSITION #3	POSITION #4	POSITION #5
1000 ppm/in	1000 ppm/in	1000 ppm/in	1000 ppm/in	1000 ppm/in

450°

RUN NO. 1007-233

COATING T + 0.2% @ 30°

SUBSTRATE 11s

VENDOR Rockwell

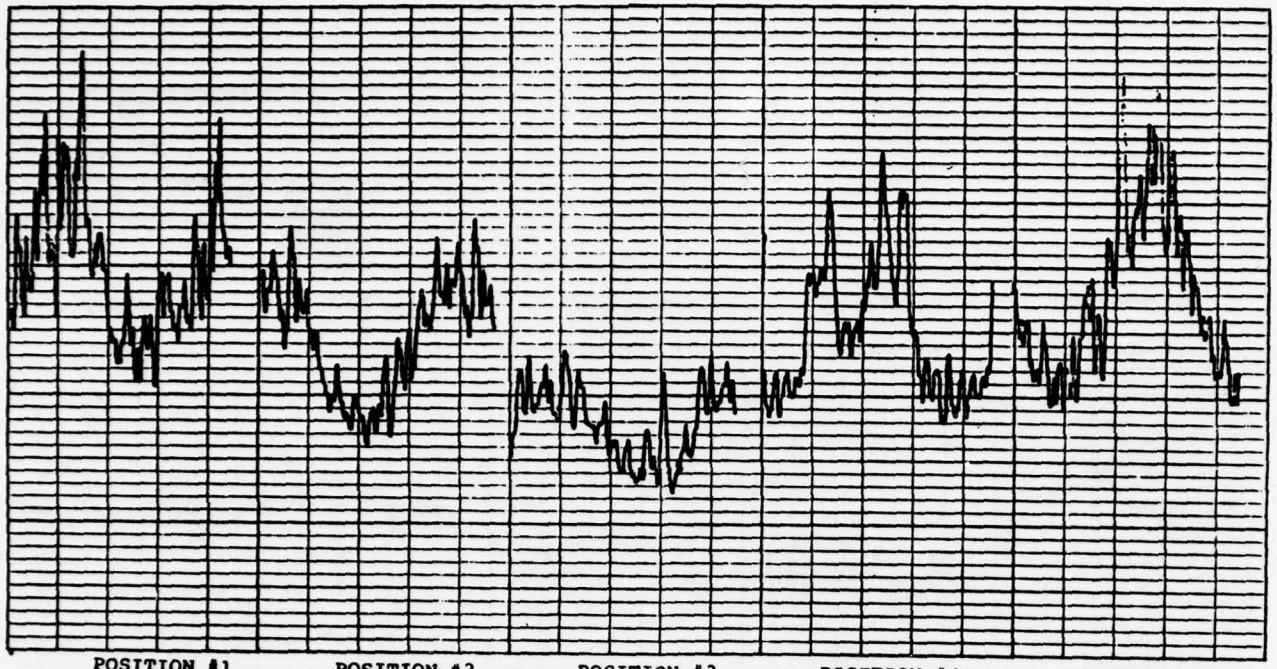

POSITION #1	POSITION #2	POSITION #3	POSITION #4	POSITION #5
1000 ppm/in	1000 ppm/in	1000 ppm/in	1000 ppm/in	1000 ppm/in
450°				

RUN NO. 1007-233

COATING T-Al O_3 @ 30°

SUBSTRATE 1-3

VENDOR Rockwell

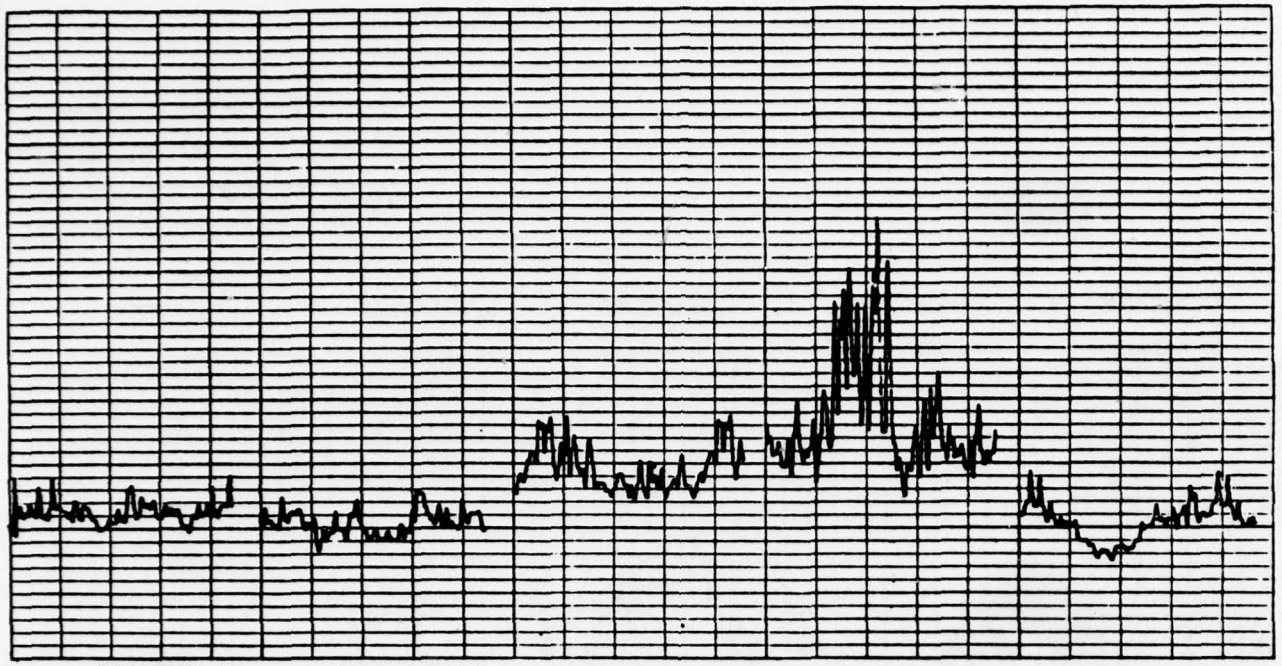

POSITION #1	POSITION #2	POSITION #3	POSITION #4	POSITION #5
1000 ppm/in	1000 ppm/in	1000 ppm/in	1000 ppm/in	1000 ppm/in
450°				

RUN NO. 1007-233

COATING T ~ 0.2% @ 30°

SUBSTRATE 14s

VENDOR Rockwell

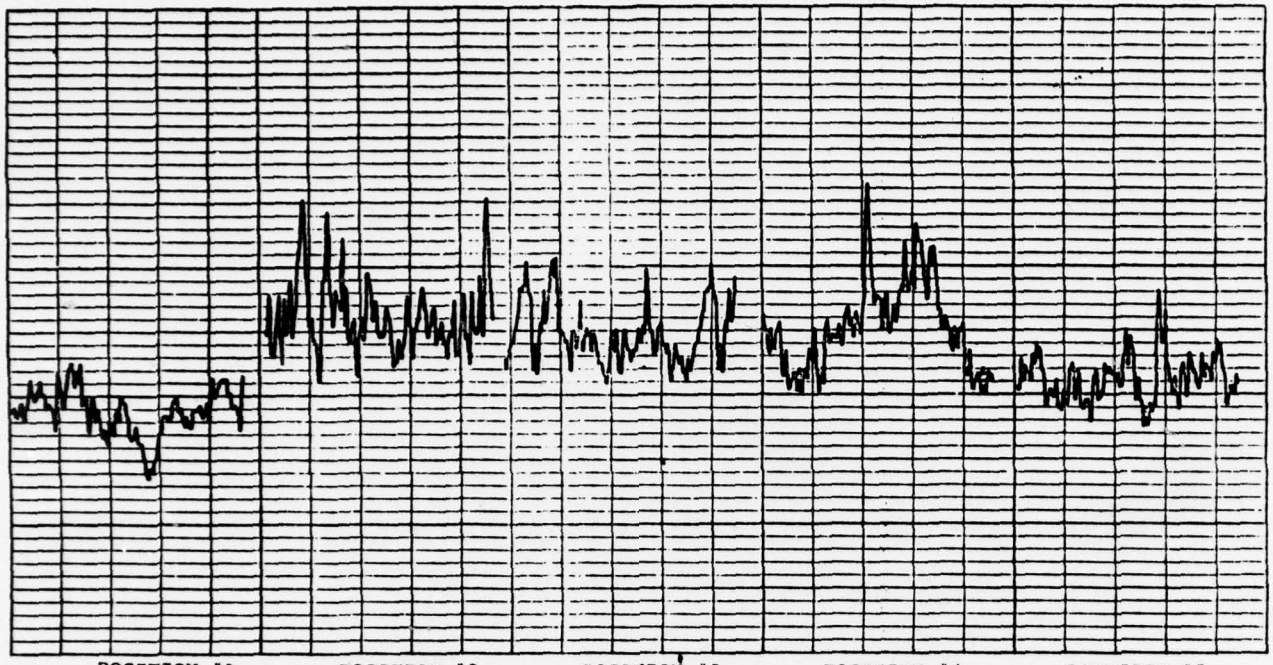

POSITION #1 | POSITION #2 | POSITION #3 | POSITION #4 | POSITION #5

100 ppm/in | 100 ppm/in | 1000 ppm/in | 100 ppm/in | 1000 ppm/in

450°

RUN NO. 1007-233

COATING T~0.2% @ 70°

SUBSTRATE 15

VENDOR Rockwell

*U.S.Government Printing Office: 1979 — 657-002/409


79